

AEDC-TR-80-48

ARCHIVE COPY  
DO NOT LOAN  
ARCHIVE COPY  
DO NOT LOAN

C-1

Performance and Operational Characteristics  
of AEDC/VKF Tunnels A, B, and C



A. H. Boudreau  
ARO, Inc.

July 1981

Final Report for Period February 1980 – September 1980

Approved for public release; distribution unlimited.

TECHNICAL REPORTS  
FILE COPY

ARNOLD ENGINEERING DEVELOPMENT CENTER  
ARNOLD AIR FORCE STATION, TENNESSEE  
AIR FORCE SYSTEMS COMMAND  
UNITED STATES AIR FORCE

## NOTICES

When U. S. Government drawings, specifications, or other data are used for any purpose other than a definitely related Government procurement operation, the Government thereby incurs no responsibility nor any obligation whatsoever, and the fact that the Government may have formulated, furnished, or in any way supplied the said drawings, specifications, or other data, is not to be regarded by implication or otherwise, or in any manner licensing the holder or any other person or corporation, or conveying any rights or permission to manufacture, use, or sell any patented invention that may in any way be related thereto.

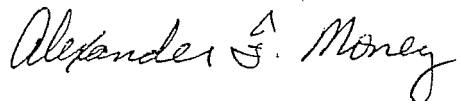
Qualified users may obtain copies of this report from the Defense Technical Information Center.

References to named commercial products in this report are not to be considered in any sense as an indorsement of the product by the United States Air Force or the Government.

This report has been reviewed by the Office of Public Affairs (PA) and is releasable to the National Technical Information Service (NTIS). At NTIS, it will be available to the general public, including foreign nations.

## APPROVAL STATEMENT

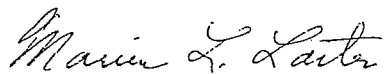
This report has been reviewed and approved.



ALEXANDER F. MONEY  
Project Manager  
Directorate of Technology

Approved for publication:

FOR THE COMMANDER



MARION L. LASTER  
Director of Technology  
Deputy for Operations

**UNCLASSIFIED**

REPORT DOCUMENTATION PAGE		READ INSTRUCTIONS BEFORE COMPLETING FORM
1 REPORT NUMBER AEDC-TR-80-48	2 GOVT ACCESSION NO.	3. RECIPIENT'S CATALOG NUMBER
4 TITLE (and Subtitle) <b>PERFORMANCE AND OPERATIONAL CHARACTERISTICS OF AEDC/VKF TUNNELS A, B, AND C</b>		5 TYPE OF REPORT & PERIOD COVERED Final Report—February 1980—September 1980
7. AUTHOR(s) A. H. Boudreau, ARO, Inc., a Sverdrup Corporation Company		6. PERFORMING ORG. REPORT NUMBER
9. PERFORMING ORGANIZATION NAME AND ADDRESS Arnold Engineering Development Center/DOT Air Force Systems Command Arnold Air Force Station, Tennessee 37389		10. PROGRAM ELEMENT, PROJECT, TASK AREA & WORK UNIT NUMBERS Program Element 65807F
11. CONTROLLING OFFICE NAME AND ADDRESS Arnold Engineering Development Center/DOS Air Force Systems Command Arnold Air Force Station, Tennessee 37389		12. REPORT DATE July 1981
14. MONITORING AGENCY NAME & ADDRESS (if different from Controlling Office)		13. NUMBER OF PAGES 116
		15. SECURITY CLASS. (of this report) <b>UNCLASSIFIED</b>
		15a. DECLASSIFICATION/DOWNGRADING SCHEDULE <b>N/A</b>
16. DISTRIBUTION STATEMENT (of this Report)  Approved for public release; distribution unlimited.		
17. DISTRIBUTION STATEMENT (of the abstract entered in Block 20, if different from Report)		
18. SUPPLEMENTARY NOTES  Available in Defense Technical Information Center (DTIC)		
19. KEY WORDS (Continue on reverse side if necessary and identify by block number) supersonic wind tunnels      Mach number hypersonic wind tunnels wind tunnel tests limitations		
20. ABSTRACT (Continue on reverse side if necessary and identify by block number) Tunnels A, B, and C of the von Kármán Gas Dynamics Facility, Arnold Engineering Development Center, represent state-of-the-art supersonic and hypersonic wind tunnels covering a Mach number range from 1.5 to 10. This report describes their operation and presents detailed performance data for all three tunnels, including practical operational limits.		

**UNCLASSIFIED**

## PREFACE

The work reported herein was conducted by the Arnold Engineering Development Center (AEDC), Air Force Systems Command (AFSC). The results of this study were obtained by ARO, Inc., AEDC Group (a Sverdrup Corporation Company), operating contractor for the AEDC, AFSC, Arnold Air Force Station, Tennessee, under ARO Project No. V32C-01E. Mr. Alex F. Money was the Air Force project manager. The manuscript was submitted for publication on September 16, 1980.

Mr. A. H. Boudreau is currently a member of the faculty of the University of Mississippi.

## CONTENTS

	<u>Page</u>
<b>1.0 INTRODUCTION .....</b>	<b>7</b>
<b>2.0 AIR AND POWER SUPPLY FOR VKF WIND TUNNELS</b>	
<b>2.1 Supersonic and Hypersonic Air Supply Systems-</b>	
<b>General Description .....</b>	<b>9</b>
<b>2.2 Main Compressor System .....</b>	<b>10</b>
<b>2.3 Air Storage System .....</b>	<b>11</b>
<b>2.4 Drier System .....</b>	<b>11</b>
<b>2.5 Heater Systems .....</b>	<b>12</b>
<b>2.6 Cooling System .....</b>	<b>12</b>
<b>3.0 TUNNEL A</b>	
<b>3.1 Description .....</b>	<b>12</b>
<b>3.2 Performance .....</b>	<b>15</b>
<b>3.2.1 Mach 6 Performance (Tunnel A) .....</b>	<b>15</b>
<b>3.2.2 Mach 8 Performance (Tunnel A) .....</b>	<b>16</b>
<b>3.3 Energy and Operational Considerations .....</b>	<b>16</b>
<b>4.0 TUNNEL B</b>	
<b>4.1 Description .....</b>	<b>16</b>
<b>4.2 Performance .....</b>	<b>17</b>
<b>4.2.1 Mach 6 Performance (Tunnel B) .....</b>	<b>17</b>
<b>4.2.2 Mach 8 Performance (Tunnel B) .....</b>	<b>18</b>
<b>4.3 Energy and Operational Considerations .....</b>	<b>19</b>
<b>5.0 TUNNEL C</b>	
<b>5.1 Description .....</b>	<b>19</b>
<b>5.2 Performance .....</b>	<b>19</b>
<b>5.3 Energy and Operational Considerations .....</b>	<b>21</b>
<b>5.4 Tunnel C Real-Gas Corrections .....</b>	<b>21</b>

## ILLUSTRATIONS

### Figure

<b>1.1 VKF Mach Number-Reynolds Number Simulation, Tunnels A, B, C .....</b>	<b>8</b>
<b>2.1 Airflow Circuits for VKF Continuous Tunnels .....</b>	<b>9</b>
<b>2.2 VKF Compressor Plant .....</b>	<b>10</b>
<b>3.1 Tunnel A, Side Wall Removed .....</b>	<b>13</b>

## TABLES

1.1 VKF Wind Tunnels .....	7
3.1 Tunnel A Performance Summary .....	14
3.2 Tunnel A Performance — Open-Circuit Operating Conditions .....	15
4.1 Tunnel B Performance Summary .....	17
4.2 Tunnel B Open-Circuit Operating Conditions .....	18
5.1 Tunnel C Performance Summary .....	20
5.2 Tunnel C Open-Circuit Operating Conditions .....	20

## APPENDIX A — ILLUSTRATIONS

<u>Figure</u>	<u>Page</u>
A-1 Tunnel A .....	25
A-2 Test Section of Tunnel A .....	26
A-3 Trajectories of Disturbance Waves in Aft Test Section .....	28
A-4 Axial Centerline Pitot Pressure Distribution, Tunnel A .....	29
A-5 Vertical Pitot Pressure Profiles, Tunnel A .....	30
A-6 Tunnel A Operating Conditions and Limits .....	31
A-7 Free-Stream Pitot Pressure, Tunnel A .....	45
A-8 Free-Stream Pressure, Tunnel A .....	46
A-9 Simulated Altitude, Tunnel A .....	47
A-10 Electrical Usage for Tunnel A .....	48

## APPENDIX B — ILLUSTRATIONS

B-1 Tunnel B .....	57
B-2 Test Section of Tunnel B .....	60
B-3 Cavity Induced Disturbance Locations at $M = 6.0$ and $P_1 = 30$ .....	62
B-4 Mach Number, Tunnel B — Mach 6 .....	63
B-5 Axial Pitot Pressure Distributions, Tunnel B — Mach 6 .....	64
B-6 Vertical Pitot Pressure Profiles, Tunnel B — Mach 6 .....	65
B-7 Stagnation Conditions, Tunnel B — Mach 6 .....	66
B-8 Free-Stream Pitot, Dynamic, and Static Pressure, Tunnel B — Mach 6 .....	69
B-9 Free-Stream Velocity, Tunnel B — Mach 6 .....	70
B-10 Free-Stream Reynolds Number, Tunnel B — Mach 6 .....	71
B-11 Free-Stream Temperature, Tunnel B — Mach 6 .....	72
B-12 Simulated Altitude, Tunnel B — Mach 6 .....	73

<u>Figure</u>	<u>Page</u>
B-13 Mass Flow, Tunnel B — Mach 6 .....	74
B-14 Mach Number, Tunnel B — Mach 8 .....	75
B-15 Axial Centerline Pitot Pressure Distributions, Tunnel B — Mach 8 .....	76
B-16 Vertical Pitot Pressure Profiles, Tunnel B — Mach 8 .....	77
B-17 Stagnation Conditions, Tunnel B — Mach 8 .....	80
B-18 Free-Stream Pitot, Dynamic, and Static Pressure, Tunnel B — Mach 8 .....	81
B-19 Free-Stream Velocity, Tunnel B — Mach 8 .....	82
B-20 Free-Stream Reynolds Number, Tunnel B — Mach 8 .....	83
B-21 Free-Stream Temperature, Tunnel B — Mach 8 .....	84
B-22 Simulated Altitude, Tunnel B — Mach 8 .....	85
B-23 Mass Flow, Tunnel B — Mach 8 .....	86
B-24 Electrical Usage for Tunnel B .....	87

#### **APPENDIX C — ILLUSTRATIONS**

C-1 Tunnel C .....	93
C-2 Test Section of Tunnel C .....	96
C-3 Tunnel C, Mach 10 .....	98
C-4 Axial Centerline Pitot Pressure Distributions, Tunnel C — Mach 10 .....	99
C-5 Vertical Pitot Pressure Profiles, Tunnel C — Mach 10 .....	100
C-6 Stagnation Conditions, Tunnel C — Mach 10 .....	101
C-7 Free-Stream Pitot, Dynamic, and Static Pressure, Tunnel C — Mach 10 .....	102
C-8 Free-Stream Velocity, Tunnel C — Mach 10 .....	103
C-9 Free-Stream Reynolds Number, Tunnel C — Mach 10 .....	104
C-10 Free-Stream Temperature, Tunnel C — Mach 10 .....	105
C-11 Simulated Altitude, Tunnel C — Mach 10 .....	106
C-12 Mass Flow, Tunnel C — Mach 10 .....	107
C-13 Electrical Usage for Tunnel C .....	108

#### **APPENDIX D**

REAL-GAS CORRECTION FACTORS FOR DETERMINING FREE-STREAM CONDITIONS IN TUNNEL C .....	113
REFERENCES .....	115

**ALL APPENDICES — TABLES**

A-1 Tunnel A Standardized Mach Number .....	50
A-2 Tunnel A Total Mass Flow .....	51
A-3 Tunnel A Operational Time Considerations .....	52
A-4 Tunnel A Standard Test Condition Tolerances .....	53
B-1 Tunnel B Operational Time Considerations .....	88
B-2 Tunnel B Standard Test Condition Tolerances .....	89
C-1 Tunnel C Operational Time Considerations .....	109
C-2 Tunnel C Standard Test Condition Tolerances .....	110
D-1 Typical Correction Factors for Tunnel C .....	114
 NOMENCLATURE .....	116

## 1.0 INTRODUCTION

The Arnold Engineering Development Center (AEDC) von Kármán Gas Dynamics Facility (VKF) wind tunnels provide unique capabilities for supersonic and hypersonic testing. Covering a Mach number range from 1.5 to 10, these modern tunnels provide high-performance, efficient, state-of-the-art simulation. Scaled models of supersonic and hypersonic aircraft, lifting R/V's, projectiles, missiles, plus launch and reentry vehicles are commonly tested. A wide variety of sophisticated test techniques is available including force and moment, heat-transfer rate, pressure, staging, store separation, inlet, materials, dynamic stability, captive trajectory, mass addition, and flow-field diagnostics.

This report provides performance data and operational limits for the VKF continuous Tunnels A, B, and C. A summary of each tunnel's performance is presented in the text. Detailed performance curves are presented for the Tunnels A, B, and C in Appendixes A, B, and C, respectively. Applications of these data are discussed in the text.

Many of the performance diagrams in this report indicate a standard "operating curve." Users are encouraged to plan test programs utilizing these established curves. However, by consulting the VKF staff, other operating points may be defined to suit unusual test requirements.

Mach number-Reynolds number performance curves are shown in Fig. 1.1 for these three tunnels. Their size and Mach range are summarized in Table 1.1.

**Table 1.1. VKF Wind Tunnels**

Tunnel	Test Section Size	Mach Number	Type
A	40 by 40 in.	1.5 through 5.5	Continuous Flow
B	50-in. Diam	6, 8	Continuous Flow
C	50-in. Diam	10	Continuous Flow

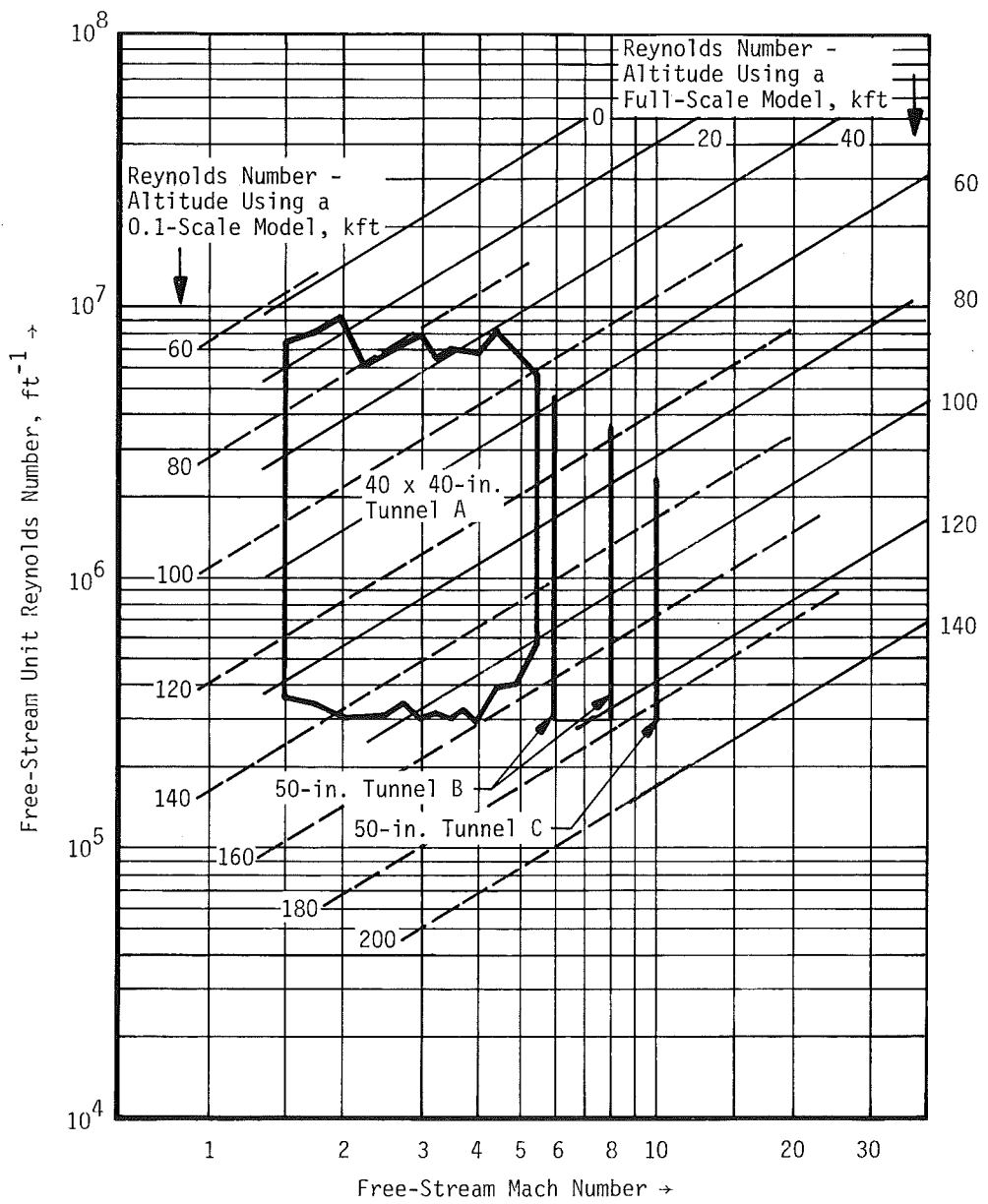


**Figure 1.1. VKF Mach number-Reynolds number simulation,  
Tunnels A, B, C.**

## 2.0 AIR AND POWER SUPPLY FOR VKF WIND TUNNELS

### 2.1 SUPERSONIC AND HYPERSONIC AIR SUPPLY SYSTEMS— GENERAL DESCRIPTION

Air is supplied to the VKF supersonic and hypersonic wind tunnels from the system shown schematically in Fig. 2.1.

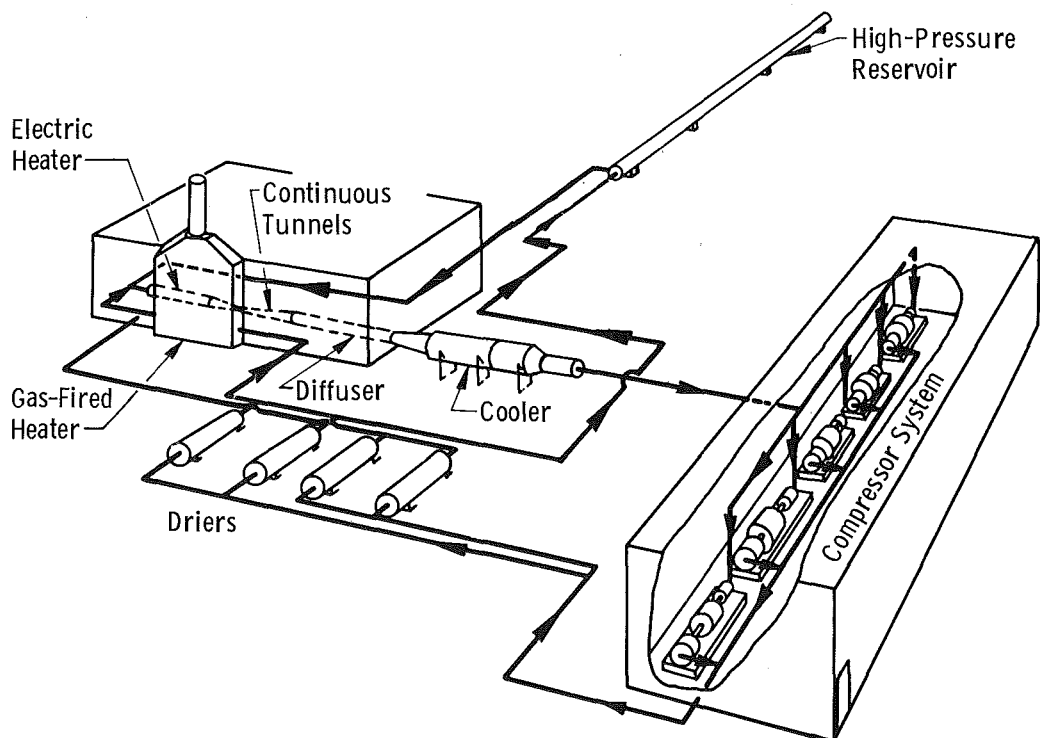
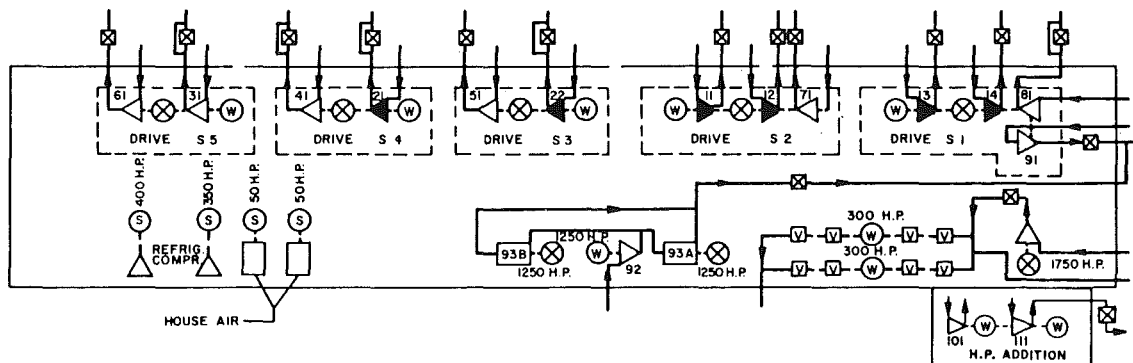
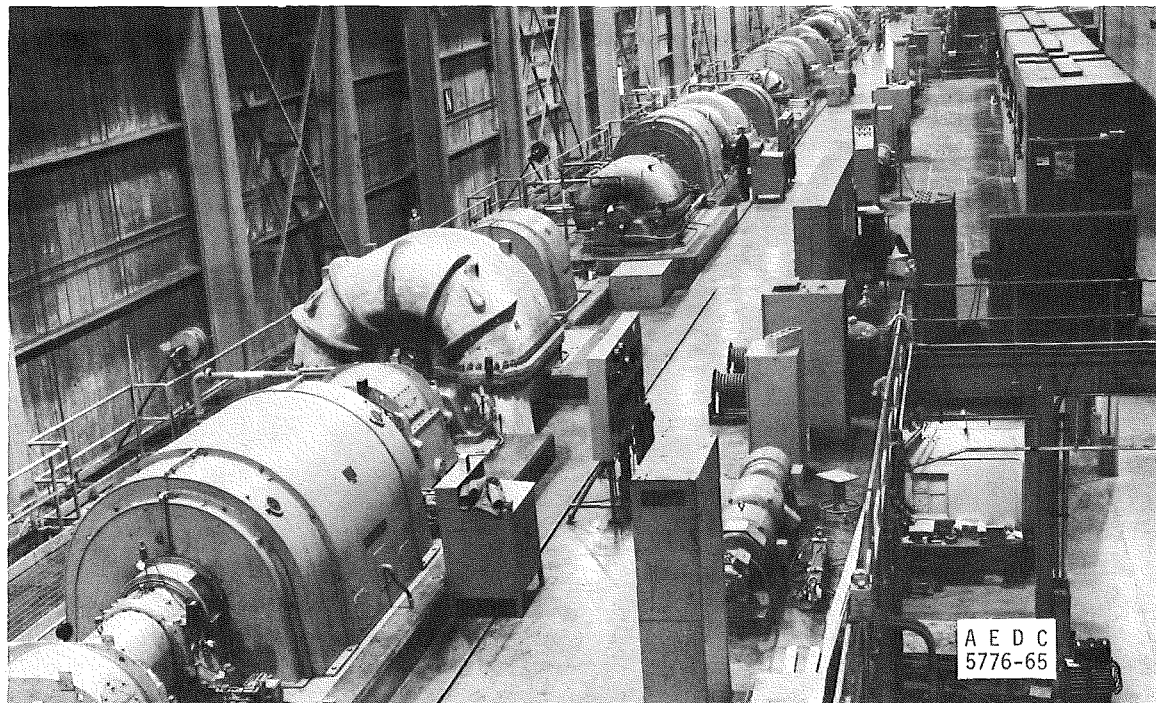


**Figure 2.1. Airflow circuits for VKF continuous tunnels.**

The 40-in. Supersonic Wind Tunnel (A) and the 50-in. Hypersonic Wind Tunnels (B) and (C) are supplied with air at the desired pressures and mass flows from selected stages of the compressor system. From the compressors, air is selectively valved through the driers for Tunnel A and, for the hypersonic tunnels, through the heaters before delivery to the selected wind-tunnel test section. Air then passes through the diffuser for Tunnel A or, for the hypersonic tunnels, through a cooler before reentering the compressor system.

## 2.2 MAIN COMPRESSOR SYSTEM

The main compressor system for continuous operation (Fig. 2.2) is comprised of six axial and seven centrifugal compressors, arranged in nine stages.



- [V] - VACUUM PUMP
- [■] - AXIAL COMPRESSOR
- [△] - CENTRIFUGAL COMP.
- [□] - RECIPROCATING COMP.
- [☒] - COOLER
- SHAFT CONNECTION
- ← AIR LINES
- ⊗ - SYN. MOTOR
- (W) - WOUND ROTOR MOTOR
- (S) - SQUIRREL CAGE MOTOR

NOTE: 1ST NUMERAL IN COMP. NO.  
INDICATES STAGE OF COMPRESSION.  
2ND NUMERAL GIVES COMPRESSOR  
NUMBER IN STAGE.  
IN DRIVE UNITS 1-5, WR MOTORS  
HAVE A H.P. RATING OF 2500;  
SYN. MOTORS HAVE A RATING OF  
16,000 H.P.

Figure 2.2. VKF compressor plant.

These machines are arranged into five groups, each of which is powered by a 16,000-hp synchronous motor and a 2,500-hp wound-rotor motor for a total installed horsepower of 92,500. The first stage is rated at 600,000 cfm inlet with a minimum inlet pressure of 0.25 psia.

The compressors are interconnected by a ducting and piping system which includes intercoolers and valves whereby from one to five stages are used to deliver air to Tunnel A for operation between Mach numbers 1.5 and 5.5. Five stages are used to deliver air to Tunnel B for operation at Mach 6, and seven stages for operation at Mach 8. Nine stages are used to deliver air to Tunnel C for operation at Mach 10.

### 2.3 AIR STORAGE SYSTEM

Air is stored in a 29,770-ft<sup>3</sup> storage system at pressures up to 3,800 psia. This system is composed of the 7,550-ft<sup>3</sup> VKF high-pressure reservoir and the 22,200-ft<sup>3</sup> Aerodynamic and Propulsion Test Unit (APTU) storage tanks. The maximum capacity of the combined storage system is approximately 542,000 lb of air. The stored air is supplied to intermittent wind tunnels, is used to increase pressure levels in the main compressor system and continuous wind tunnels, and is used for the model mass-flow systems in all facilities.

In addition to the main compressor system, a two-compressor system comprising the ninth and tenth stages of the main plant can be used to charge the storage reservoirs at the rate of 84 lb per second. The two-compressor system is powered with a 7,000-hp induction motor.

An auxiliary compressor system is capable of charging the storage system at the rate of 6.3 lb per second.

### 2.4 DRIER SYSTEM

The continuous air supply system is equipped with silica gel driers that reduce the moisture content of the pressurized air to a specific humidity required to produce a wind tunnel flow free from water vapor condensation. The driers, arranged in pairs, are alternately regenerated by natural-gas-fired hot air so as to provide continuous drying.

A drier rated for pressures up to 2,500 psi is located at the discharge of the main compressor plant especially for use with Tunnel C operation. This drier has the capability of an effluent air dewpoint of -80°F, or lower, over the Tunnel C operating range.\*

---

\*Quoted dewpoint temperatures are referenced to atmospheric pressure.

Additional driers rated at 4,000 psia are used to dry the high-pressure air supplied to the storage reservoirs. Typically the storage air dewpoint is -80°F, or lower.

## 2.5 HEATER SYSTEMS

Tunnel A uses heat of compression when required, and maximum temperatures from 100 to 280°F can be obtained (see Table 3.1). Process air heaters prevent air liquefaction in the hypersonic tunnels. Tunnel B is provided with air heated to a maximum of 890°F with a natural-gas-fired heater (HB-1). For Tunnel C, air is heated to 1,800°F by the additional use of an electric heater (HB-3) in series with the natural-gas-fired heater.

## 2.6 COOLING SYSTEM

Tunnel A is not provided with aftercoolers. Tunnels B and C utilize indirect, raw-water coolers to reduce the air temperature to approximately 100°F before it recirculates to the compressor system.

# 3.0 TUNNEL A

## 3.1 DESCRIPTION

Tunnel A (Fig. 3.1) is a 40- by 40-in., continuous, closed-circuit, variable-density, supersonic wind tunnel with a Mach number range of from 1.5 to 5.5. The tunnel is served by the main compressor system, which provides a wide range of mass flows and stagnation pressures up to a maximum of 195 psia. Incorporation of the high-pressure reservoir provides rapid changes of pressure level required for different test points, thus enhancing tunnel capability.

The tunnel is equipped with a model injection system which allows removal of the model from the test section while the tunnel remains in operation. The primary model support is housed in a tank directly underneath the test section (Appendix A, Fig. A-1). The model support is injected into the test section and translated upstream to the test area. Upon concluding the test, the model support is retracted in a similar manner. To allow access to the model and model support, the tank is sealed from the test section and vented to atmosphere while the tunnel is running. After the desired model change or modification, the tank is vented to the test section, the doors separating the tank and test section are opened, and the model is injected into the airstream and translated forward to the test position. The doors are normally closed at this point. The minimum time required for injecting the model is 8 sec, and translating forward requires 8 sec for a total time of 16 sec. Time required for retracting is approximately the same.

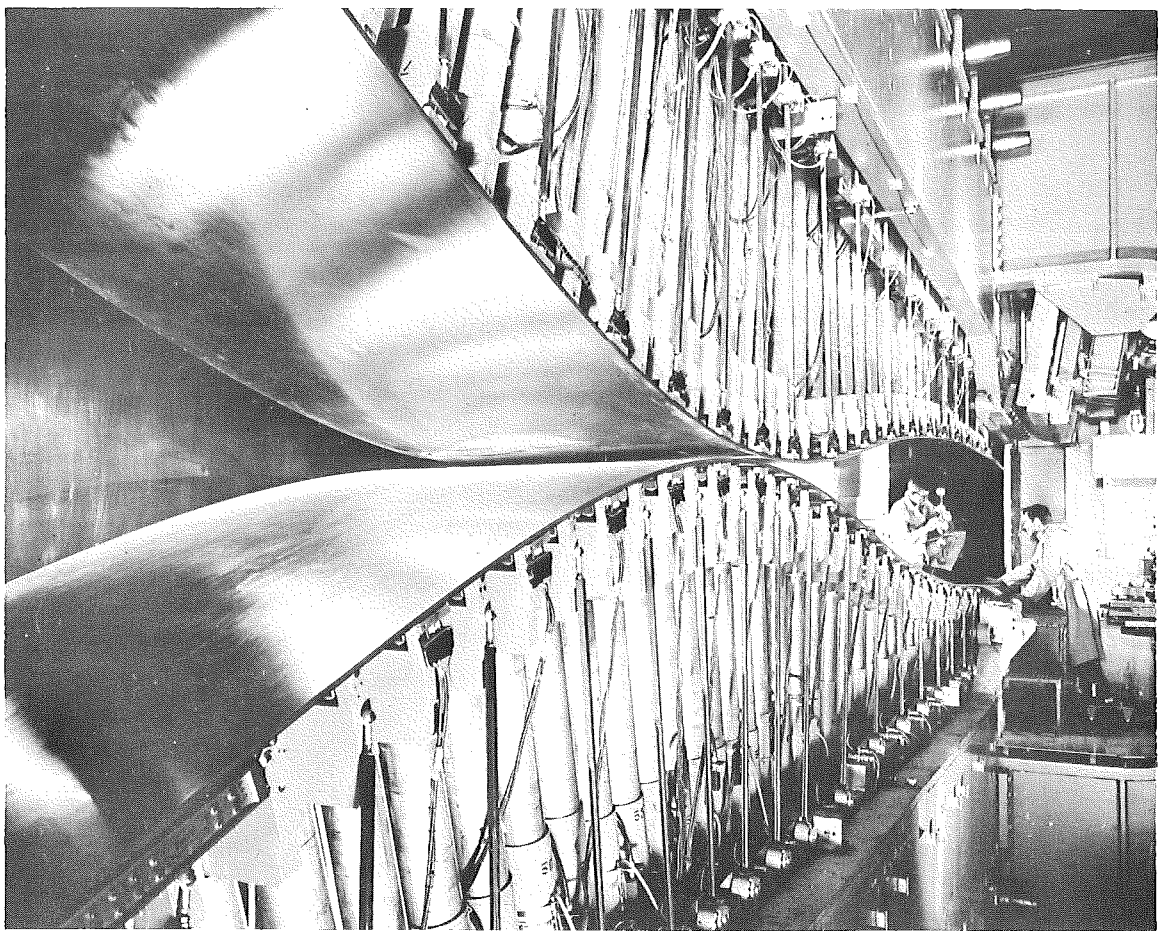


**Figure 3.1. Tunnel A, side wall removed.**

Models are generally supported from the rear by stings that attach to the roll sting hub, or adapter hub, mounted on top of the single-ended support strut. The support system will accommodate a vertical load of 3,500 lb or a horizontal load of 1,500 lb applied at the nominal model center of rotation, with a maximum resultant force of 3,800 lb. The relationship of the model support to the windows is shown in Fig. A-2. In either the retracted or injected position, the model may be rolled  $\pm 180$  deg and pitched  $\pm 15$  deg while the center of rotation is in its most downstream position. At the most forward position of the center of rotation, the model pitch angle is limited to  $\pm 10$  deg. The center of model rotation can be moved within the limits shown in Fig. A-1, which allows pitching the model about any point within the limits. The calibrated test area and boundary-layer thicknesses are shown in Fig. A-2.

Continuous-curvature nozzle contours are obtained by flexible top and bottom walls mounted on electrically driven screw jacks. The side walls of the nozzle are plane and

parallel. Operation of the nozzle-actuating jacks is completely automatic. Mach number changes may be made without stopping the tunnel if two or more stages of compression are used in the air supply system (see Table 3.1).

The test section is 40 by 40 in., with its effective test rhombus approximately centered at the downstream end of the flexible nozzle plates. Figure A-3 shows the aft limits of the test rhombus with the tank doors open. A variable-geometry, five-hinge diffuser is located downstream of the test section.

**Table 3.1. Tunnel A Performance Summary**

Mach No.	Stages of Compression	P <sub>t</sub> , psia		T <sub>t</sub> , °F		q, psia		Re/ft × 10 <sup>-6</sup>	
		Max	Min	Max <sup>(1)</sup>	Min <sup>(3)</sup>	Max	Min	Max <sup>(2)</sup>	Min
1.50	Type B (1 Stage)	24	1.5	100	70	10.3	0.65	7.4	0.35
1.75		28	2.0	100	70	11.2	0.80	8.2	0.50
2.00		34	3.0	100	70	12.1	1.08	9.0	0.70
1.50	2	14	1.5	170	70	6.0	0.65	4.4	0.30
1.75		16	1.5	170	70	6.4	0.60	3.7	0.32
2.00		20	1.5	180	70	7.1	0.54	5.3	0.30
2.25		25	1.7	180	70	7.6	0.50	5.9	0.32
2.50		32	2.0	180	70	8.2	0.50	6.6	0.30
2.75		40	2.5	180	70	8.4	0.51	7.3	0.32
3.00		50	3.2	210	70	8.5	0.51	8.0	0.30
3.00	3	36	2.7	260	70	6.1	0.45	5.8	0.28
3.25		44	3.2	270	70	6.1	0.45	6.2	0.25
3.50		56	3.5	270	70	6.1	0.35	7.0	0.30
3.75		64	4.2	280	70	5.7	0.38	7.0	0.25
4.00		71	4.6	280	70	5.1	0.35	6.7	0.25
4.00	4	49	4.6	170	70	3.5	0.35	4.7	0.32
4.50		114	7.2	190	70	5.5	0.40	8.4	0.40
5.00		148	10.5	220	70	4.6	0.35	6.6	0.40
5.50		148	15.0	240	160	3.3	0.35	3.4	0.45
5.50	5	195	25.0	280	180	3.1	0.50	5.7	0.70

Notes: (1) The maximum temperatures are normally attainable near maximum pressure. A maximum 280°F is available.

(2) (Re/ft)<sub>max</sub> is based on the minimum operating temperature of 70°F or, for Mach Numbers of 4.5, 5.0, and 5.5, the minimum temperature required to prevent air liquefaction.

(3) The minimum operating temperature during the summer months is 90°F instead of 70°F.

### 3.2 PERFORMANCE

Performance data are presented in Tables 3.1 and 3.2 and in Appendix A. In tests where recirculation of the tunnel flow is undesirable because of contaminants from the model, the tunnel may be operated in an open-circuit configuration at the conditions shown in Table 3.2.

**Table 3.2. Tunnel A Performance — Open-Circuit Operating Conditions**

Mach No.	$P_t$ , psia	$Re/ft \times 10^{-6}$	Mach No.	$P_t$ , psia	$Re/ft \times 10^{-6}$
3	25	4.0	4.5	25	1.9
			4.5	63	4.6
	28	3.4	5	34	1.8
	22	2.0	5	97	4.5
4	41	3.8	5.5	46	1.5
			5.5	124	3.8
4	48	4.6			

Standardized Mach numbers derived from calibrations are presented in Table A-1 (p. 50). Actual test Mach numbers are checked with a "Mach probe" which is periodically inserted into the test section from the tunnel sidewall.

Axial and vertical profiles of pitot-pressure ratio are shown in Figs. A-4 and A-5, respectively. Flow-field survey data such as these indicate that the spatial variation of local Mach number is nominally  $\pm 0.015$ . Local flow angularity does not exceed 0.50 deg and over most of the operating range is generally less than 0.30 deg.

The actual Tunnel A performance limits at each calibrated Mach number are shown in Fig. A-6. Reynolds number and dynamic pressure are included for reference. Note that many Mach numbers can be obtained with more than one plant staging arrangement. These plots clearly indicate the tradeoffs for the various configurations. Another consideration is air liquefaction which limits performance at  $M = 4.5$  and above.

The operational envelopes for pitot pressure, static pressure, and pressure altitude are presented in Figs. A-7, A-8, and A-9, respectively. Tunnel mass flow is calculated using the parameters presented in Table A-2 (p. 51).

### 3.3 ENERGY AND OPERATIONAL CONSIDERATIONS

Electrical power usage for various values of Mach and Reynolds numbers is presented in Fig. A-10. Note that some Mach number-Reynolds number combinations can be obtained with two staging arrangements. Using the least number of stages can produce substantial power savings.

The operational time limits for various staging configurations are presented in Table A-3. These criteria, along with aerodynamic requirements and cost, should be considered when selecting tunnel conditions.

Table A-4 presents the allowable tolerances for normal testing in Tunnel A. Tighter tolerances should be specified only when absolutely necessary since setting the tighter tolerances is time consuming. Conversely, if test objectives permit, the standard tolerances should be relaxed to save time.

As in all supersonic wind tunnels, the concentration of water vapor in the test air must be kept below some minimum value to ensure that condensation does not significantly alter the test section conditions. In Tunnel A, water vapor concentration is monitored by passing an air sample through a hygrometer which measures the dew/frost point temperature at atmospheric pressure. Frost point temperatures of 0°F or lower are normally regarded as acceptable for testing in Tunnel A. The corresponding water vapor concentration is small enough to ensure that the test section Mach number will be within one percent of the desired value. For most test conditions the capacity of the air driers is sufficient to keep the air frost point below 0°F; however, in-leakage of atmospheric air and/or cooling water may produce higher frost points when the tunnel is operated at low pressure in the Mach number range from 1.5 to 3.0. The test section Mach number is, therefore, monitored with a Mach probe which is periodically inserted into the test section from the tunnel sidewall. The Mach number computed from the probe data reflects the strength of the condensation process in the nozzle and is used as a basis for accepting or rejecting the test condition. If the Mach number is within one percent of the calibrated Mach number, the condition is normally accepted.

## 4.0 TUNNEL B

### 4.1 DESCRIPTION

Tunnel B (Appendix B, Fig. B-1) is a closed-circuit, hypersonic wind tunnel with a 50-in.-diam test section. Two axisymmetric, contoured nozzles are available to provide

Mach numbers of 6 and 8, and the tunnel may be operated continuously over a range of pressure levels from 20 to 300 psia at Mach number 6, and from 50 to 900 psia at Mach number 8, with air supplied by the VKF main compressor plant. Stagnation temperatures sufficient to avoid air liquefaction in the test section (up to 890°F) are obtained with use of a natural-gas-fired combustion heater. The entire tunnel (throat, nozzle, test section, and diffuser) is cooled by integral, external water jackets. The tunnel is equipped with a model injection system, which allows removal of the model from the test section while the tunnel remains in operation. The calibrated test section area is shown in Fig. B-2, along with the boundary-layer thickness and displacement thickness.

## 4.2 PERFORMANCE

The performance of Tunnel B is summarized in Table 4.1 below and is detailed in Appendix B. During tests requiring injection of foreign gases into the airstream, the tunnel is operated in an open-circuit mode. In this mode, atmospheric pressure must be attained at some stage of plant compression resulting in the test conditions being limited to those listed in Table 4.2.

**Table 4.1. Tunnel B Performance Summary**

Nominal Mach Number	$P_t$ , psia		$T_t$ , °F	$q$ , psia		$Re/ft \times 10^{-6}$	
	Min.	Max.	Max.	Min.	Max.	Min.	Max.
6	20	270 (1)	390 (3)	0.3	4.1	0.3	4.7
8	50	850 (2)	890	0.3	3.8	0.3	3.7

Notes:

- (1) Maximum for short duration 300 psia
- (2) Maximum for short duration 900 psia
- (3) Up to 890°F can be supplied at low stagnation pressures.

The performance at Mach 6 differs markedly from that at Mach 8. Therefore, each Mach number will be discussed separately.

### 4.2.1 Mach 6 Performance (Tunnel B)

In addition to the limits of test area shown in Fig. B-2, cavity induced disturbances limit testing at Mach 6 whenever the injection tank doors are open. The location of these weak disturbances is shown in Fig. B-3.

**Table 4.2. Tunnel B Open-Circuit Operating Conditions**

Mach Number	P <sub>t</sub> , psia	Re/ft $\times 10^{-6}$
6	25	0.5
	60	1.1
	175	3.1
8	125	0.7
	250	1.2
	850	3.7

The calibrated-Mach number relationship to total pressure is presented in Fig. B-4 for the Mach 6 nozzle. Note that this relationship is based upon pitot rake measurements, whereas the Mach number relationships for Tunnel B at Mach 8 and Tunnel C at Mach 10 are based on cone pressure measurements. The difference between pitot and cone derived Mach numbers is considered negligible at Mach 6.

Typical longitudinal and vertical pitot profiles are shown in Figs. B-5 and B-6 for the Mach 6 nozzle. Small disturbances along the tunnel centerline extend  $\pm 4$  in. vertically and  $\pm 2$  in. horizontally. Beyond this region the flow is uniform.

Operational limits in terms of stagnation pressure and temperature are shown in Fig. B-7 for Tunnel B at Mach 6. Note that the calibrated operating curve does not follow the liquefaction curve. The stagnation temperature is normally held constant ( $T_t \approx 390^{\circ}\text{F}$ ) at all values of  $P_t$ . Figures B-8 through B-13 present various free-stream parameters versus  $P_t$  for the Mach 6 nozzle.

#### 4.2.2 Mach 8 Performance (Tunnel B)

The calibrated-Mach number relationship to total pressure is presented in Fig. B-14 for the Mach 8 nozzle. This relationship is derived from cone pressure measurements in the test section. Note that there is an average difference of 0.05 in Mach number between the pitot and cone derived curves. Cone derived values are used since experience has shown that these values indicate a more exact Mach number. The differences between the 1978 blunt and sharp cone results are within the accuracy of measurement.

Longitudinal and vertical pitot profiles are shown in Figs. B-15 and B-16 for the Mach 8 nozzle. The flow is reasonably uniform at all locations for all pressure levels.

Operational limits in terms of stagnation pressure and temperature are shown in Fig. B-17 for Tunnel B at Mach 8. The calibrated operating curve is above the air liquefaction line at all pressures. Figures B-18 through B-23 present various free-stream parameters versus  $P_t$  for the Mach 8 nozzle.

#### **4.3 ENERGY AND OPERATIONAL CONSIDERATIONS**

Tunnel B electrical power usage for Mach 6 and 8 at Reynolds numbers is presented in Fig. B-24. These curves are based on  $T_t = 390^{\circ}\text{F}$  at Mach 6 and  $T_t = 890^{\circ}\text{F}$  at Mach 8.

A summary of operational time limits for various tunnel configurations is presented in Table B-1. These criteria, along with aerodynamic requirements and cost, should be used in selecting tunnel conditions. The allowable tolerances for normal testing in Tunnel B are presented in Table B-2. Tighter tolerances should be specified only when absolutely necessary since setting tighter tolerances is time consuming. The standard tolerances should be relaxed to save time whenever test objectives permit.

### **5.0 TUNNEL C**

#### **5.1 DESCRIPTION**

Tunnel C (Fig. C-1) is a closed-circuit, hypersonic wind tunnel with a Mach number 10 axisymmetric, contoured nozzle and a 50-in.-diam test section. The tunnel can be operated continuously over a range of pressure levels from 200 to 2,000 psia with air supplied by the VKF main compressor plant. Stagnation temperatures sufficient to avoid air liquefaction in the test section (up to  $1,800^{\circ}\text{F}$ ) are obtained utilizing the resistance heater. The entire tunnel (throat, nozzle, test section, and diffuser) is cooled by integral, external water jackets. The tunnel is equipped with a model injection system, which allows removal of the model from the test section while the tunnel remains in operation. The calibrated test section area is shown in Fig. C-2, along with the boundary-layer thickness and displacement thickness.

#### **5.2 PERFORMANCE**

The performance of Tunnel C is summarized in Table 5.1 below and is detailed in Appendix C. During tests requiring injection of foreign gases into the airstream, the tunnel is operated in an open-circuit mode. In this mode, atmospheric pressure must be attained at some stage of plant compression that results in the test conditions being limited to those listed in Table 5.2.

**Table 5.1. Tunnel C Performance Summary**

Nominal Mach Number	$P_t$ , psia		$T_t$ , °F	$q$ , psia		$Re/ft \times 10^{-6}$	
	Min.	Max.	Max. (1)	Min.	Max.	Min.	Max..
10	200	2,000	1,450	0.3	3.0	0.3	2.7

Note: (1) Up to 1,800°F can be supplied at pressure levels up to 1,300 psia.

**Table 5.2. Tunnel C Open-Circuit Operating Conditions**

Mach Number	$P_t$ , psia	$Re/ft$ $\times 10^{-6}$
10	300	0.5
10	500	0.8
10	700	1.1
10	875	1.3
10	1,700	2.3

The calibrated-Mach number relationship to total pressure is presented in Fig. C-3 for nominal Mach 10 operation. This relationship is derived from cone pressure measurements in the test section. Note that there is an average difference of 0.10 in Mach number between the pitot and cone derived values. The cone derived values are used since experience has shown that these values indicate a more exact Mach number.

Typical longitudinal and vertical pitot profiles are shown in Figs. C-4 and C-5. The flow is reasonably uniform except for a slight dip at  $Z_T = -4$  (see Fig. C-5), particularly noticeable at  $Y_T = \pm 4$  in.

Operational limits in terms of stagnation pressure and temperature are shown in Fig. C-6 for Tunnel C at Mach 10. The calibrated operating curve is above the air liquefaction line at all pressures. Figures C-7 through C-12 present various free-stream parameters versus  $P_t$  for the Mach 10 nozzle.

### 5.3 ENERGY AND OPERATIONAL CONSIDERATIONS

Tunnel C electrical power usage for various values of Mach and Reynolds numbers is presented in Fig. C-13. This curve is based on  $T_t = 1,440^{\circ}\text{F}$ .

Operational time considerations are included in Table C-1. These criteria, along with aerodynamic requirements and cost, should be used in selecting tunnel conditions.

The allowable tolerances for normal testing in Tunnel C are presented in Table C-2. Tighter tolerances should be specified only when absolutely necessary since setting tighter tolerances is time consuming and will result in higher test costs. Conversely, the standard tolerances should be relaxed to save time if test objectives permit more latitude.

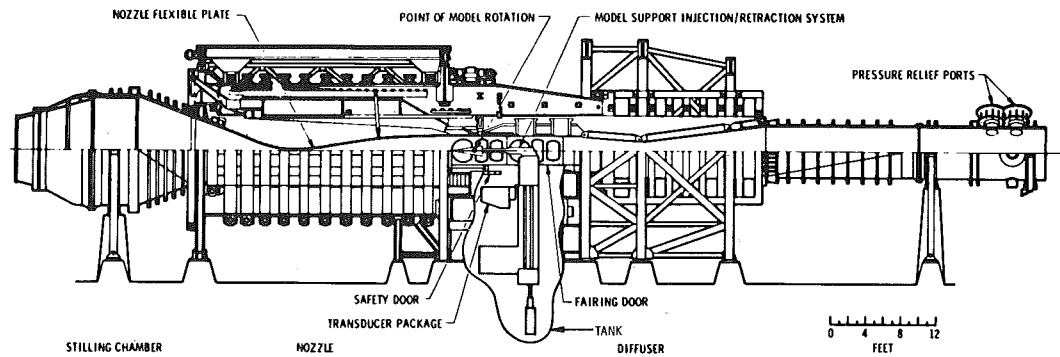
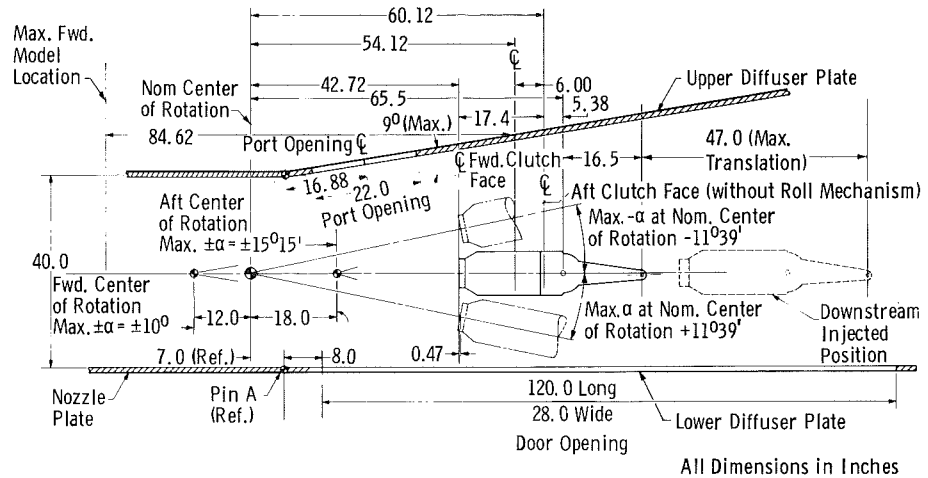
### 5.4 TUNNEL C REAL-GAS CORRECTIONS

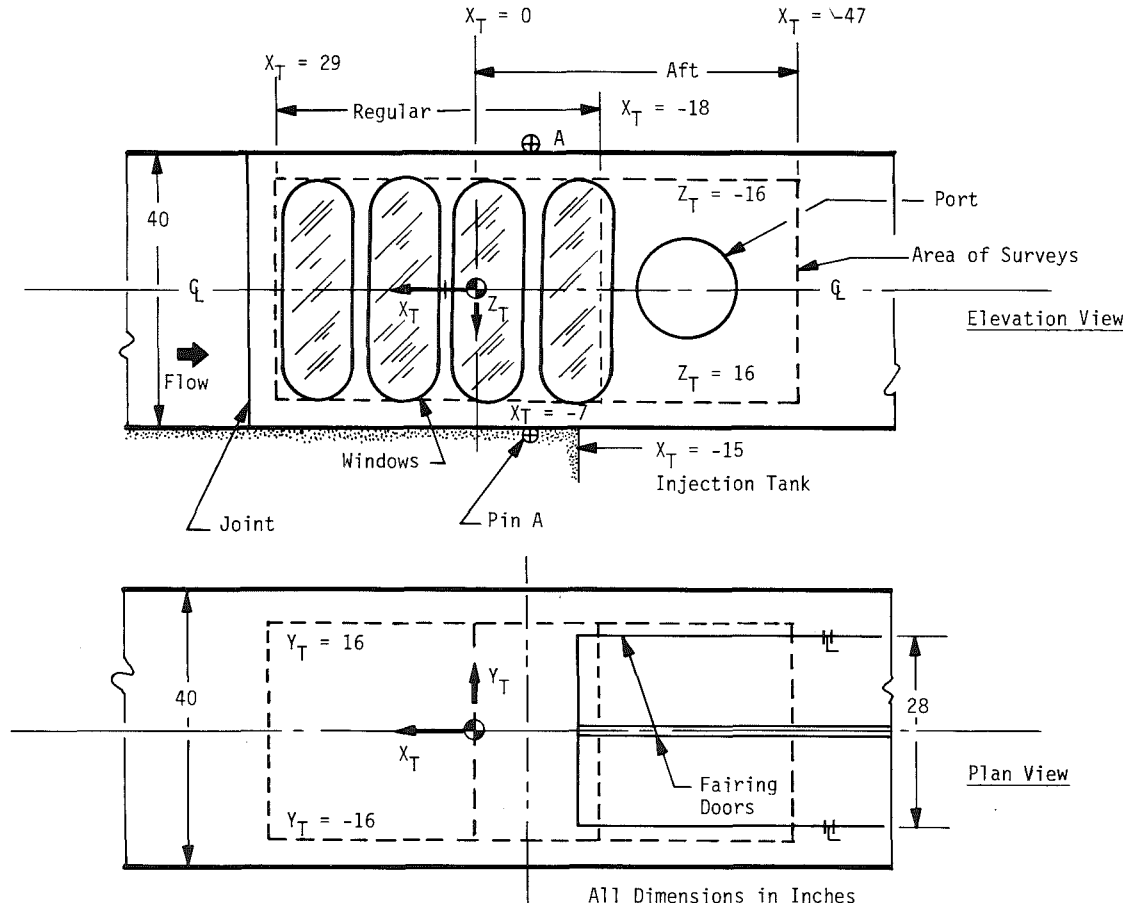
Measurements in Tunnel C must be corrected for real-gas effects. Appendix D presents a discussion and summary of these correction factors for free-stream static and dynamic pressure, free-stream static temperature, and free-stream pitot pressure.



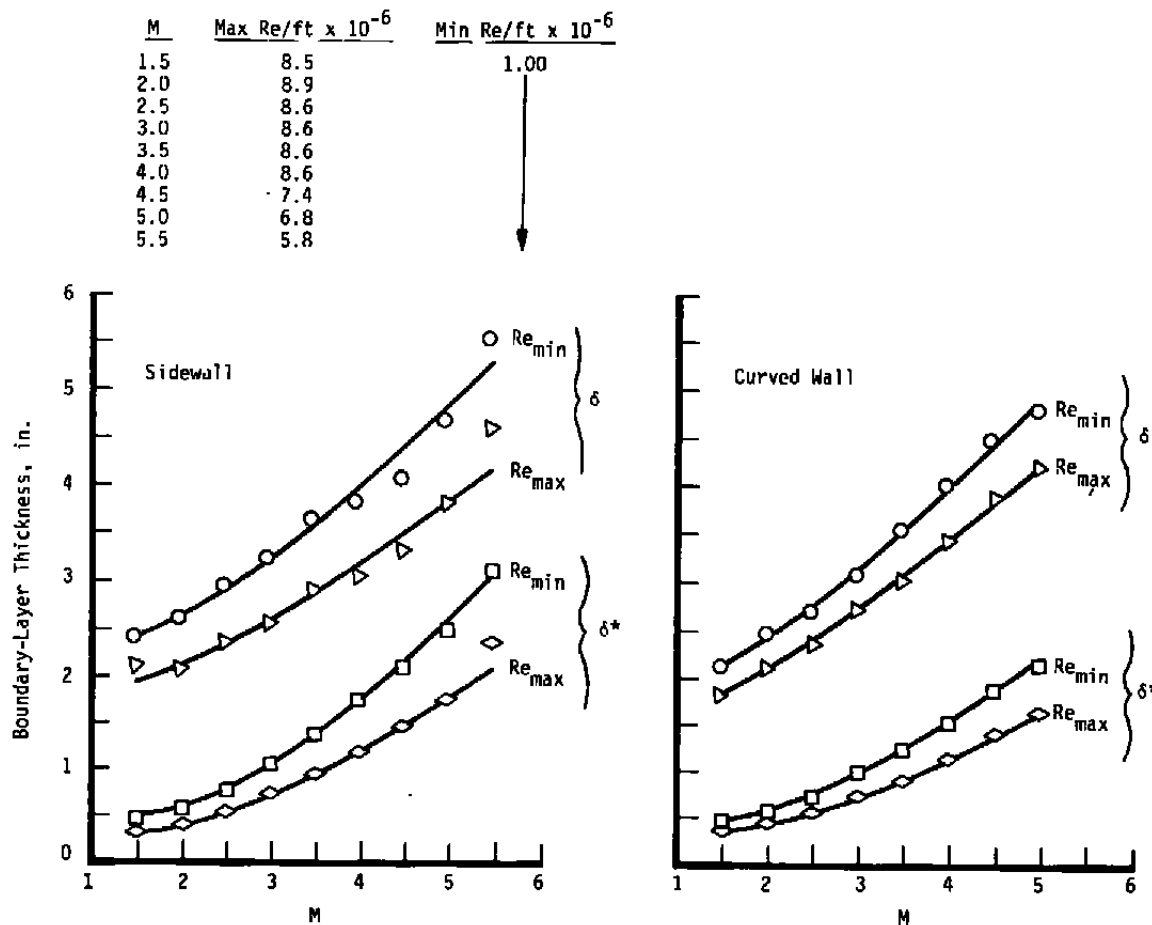
**APPENDIX A  
TUNNEL A**



**a. Tunnel A assembly****b. Test section (elevation), Tunnel A****Figure A-1. Tunnel A.**



a. Surveyed area  
Figure A-2. Test section of Tunnel A.



b. Tunnel A boundary-layer and displacement thickness  
Figure A-2. Concluded.

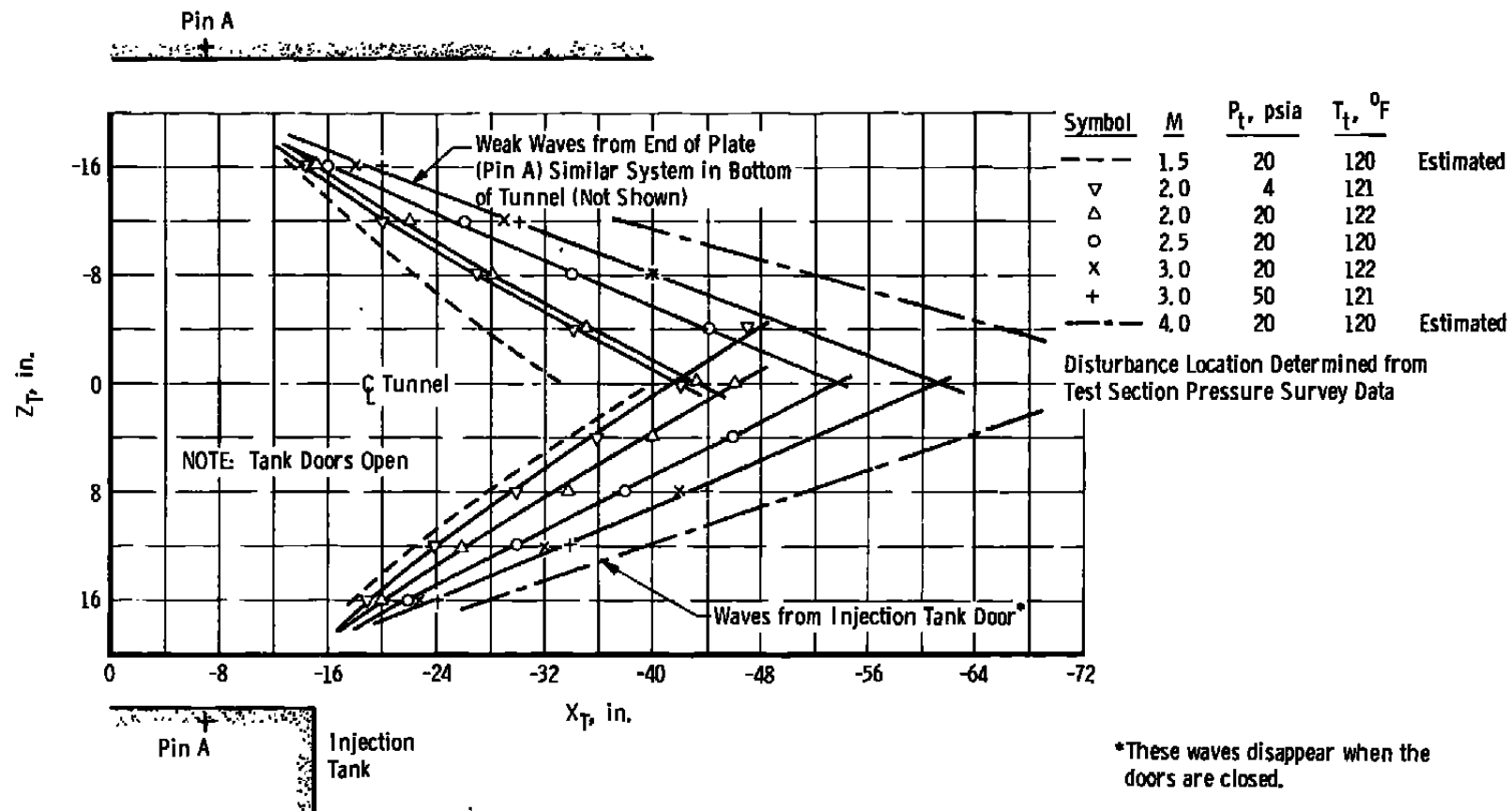


Figure A-3. Trajectories of disturbance waves in aft test section.

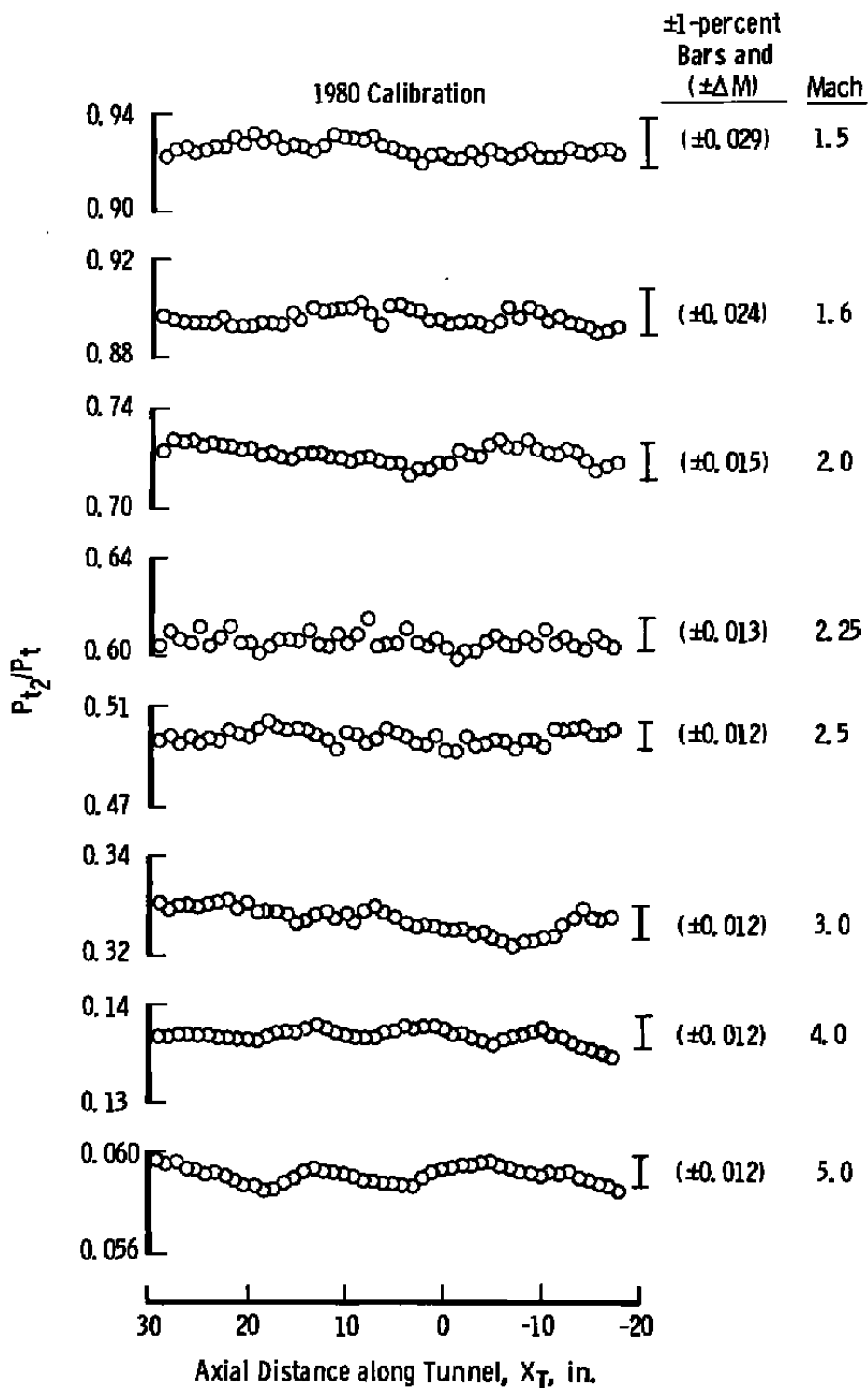


Figure A-4. Axial centerline pitot pressure distributions, Tunnel A.

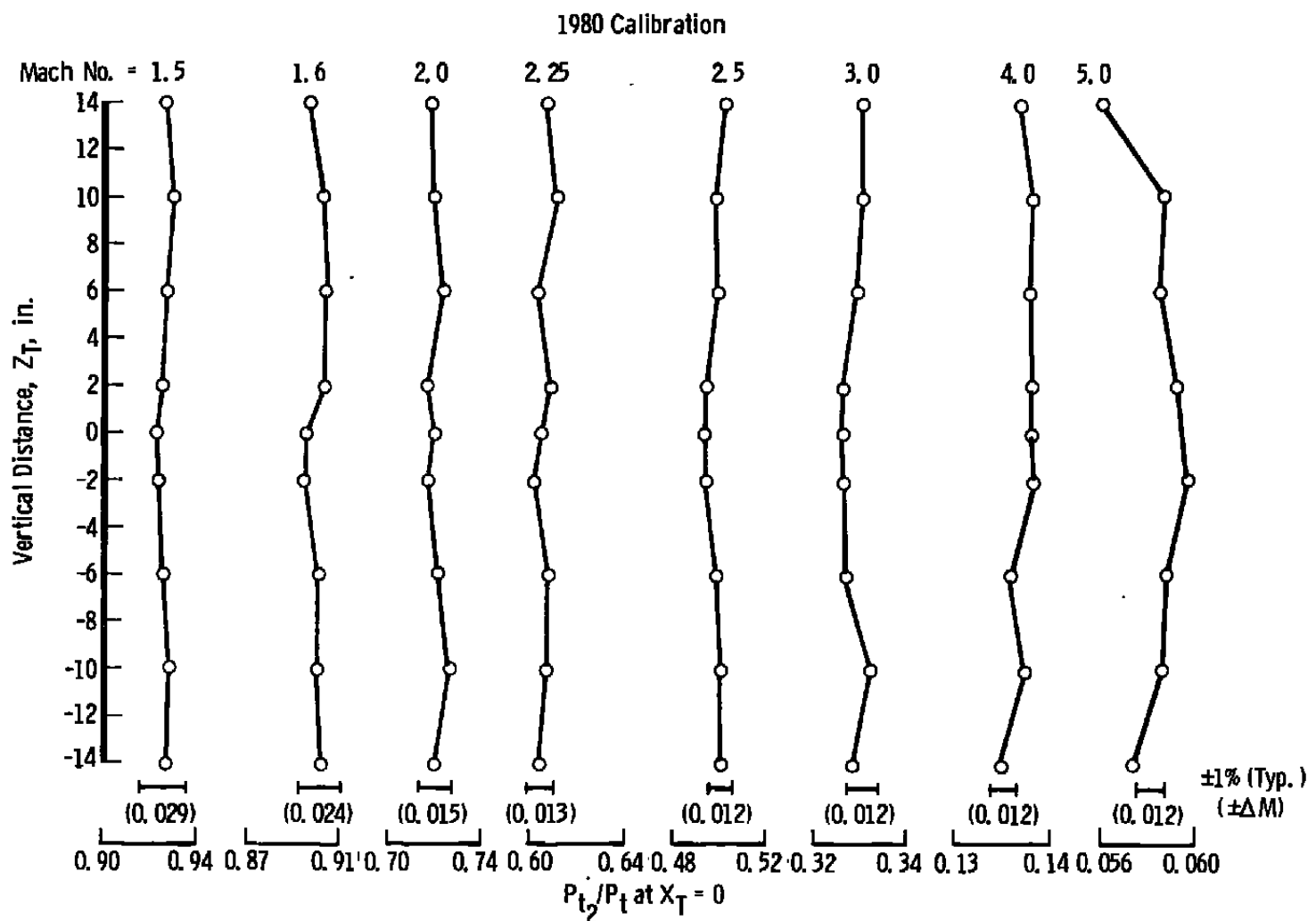
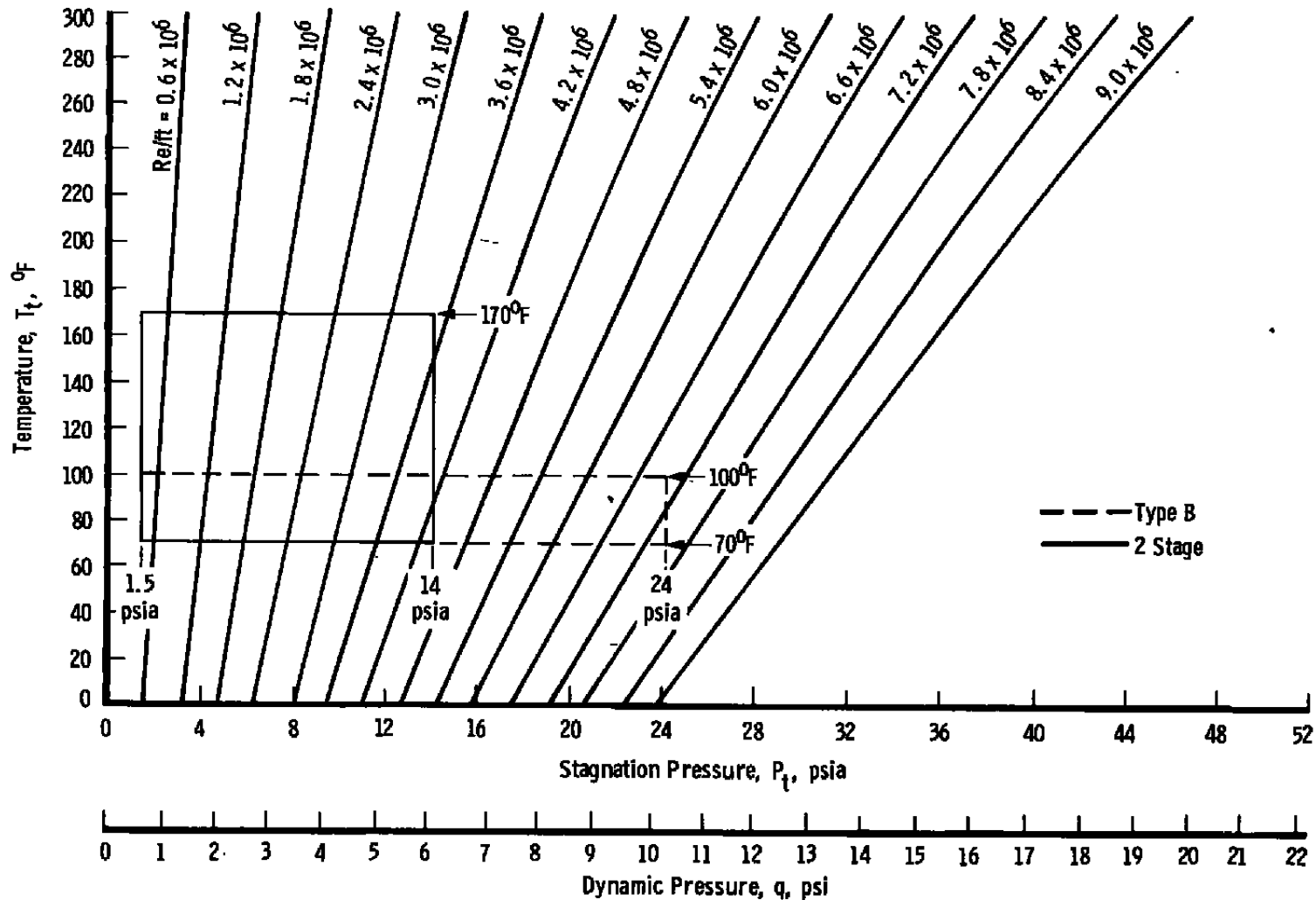
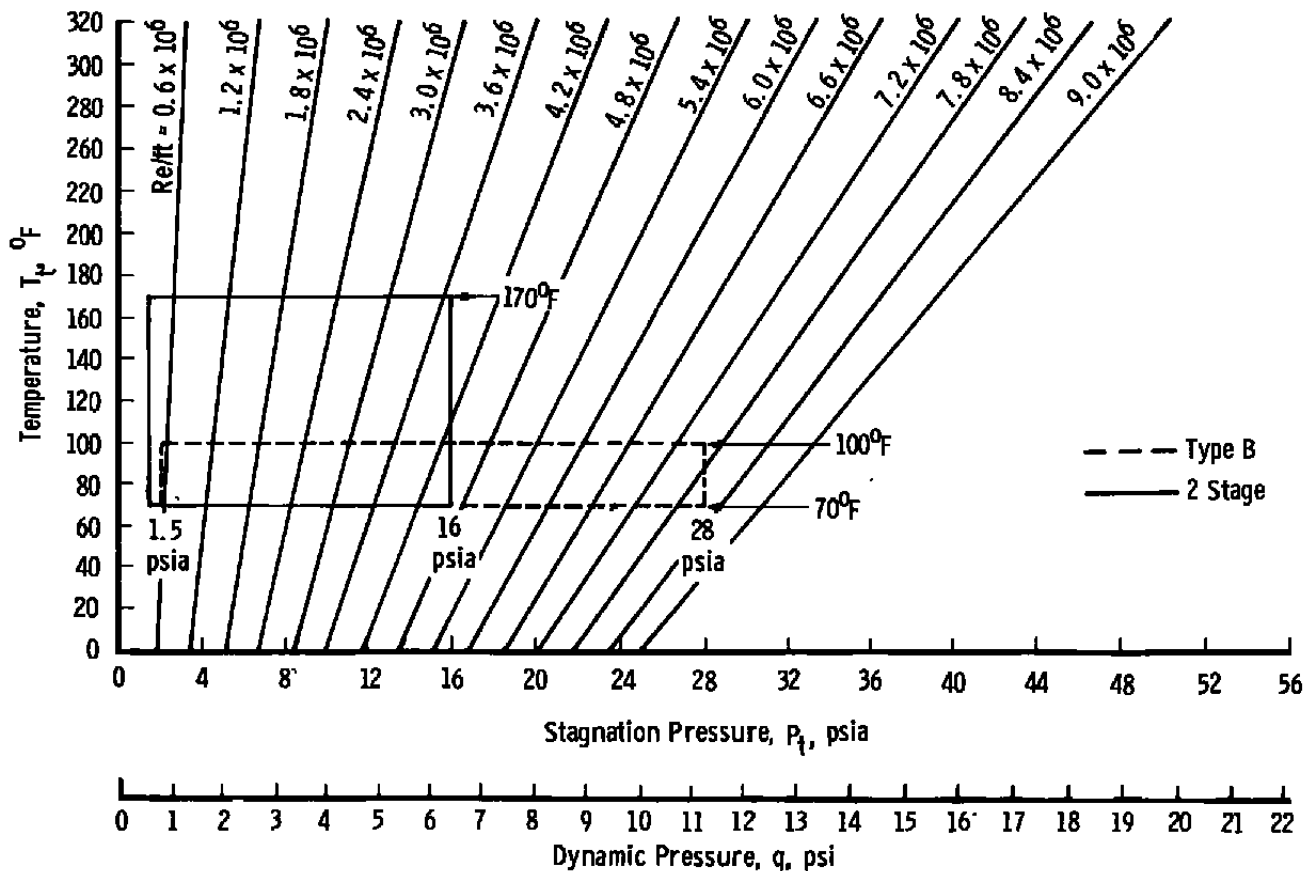


Figure A-5. Vertical pitot pressure profiles, Tunnel A.

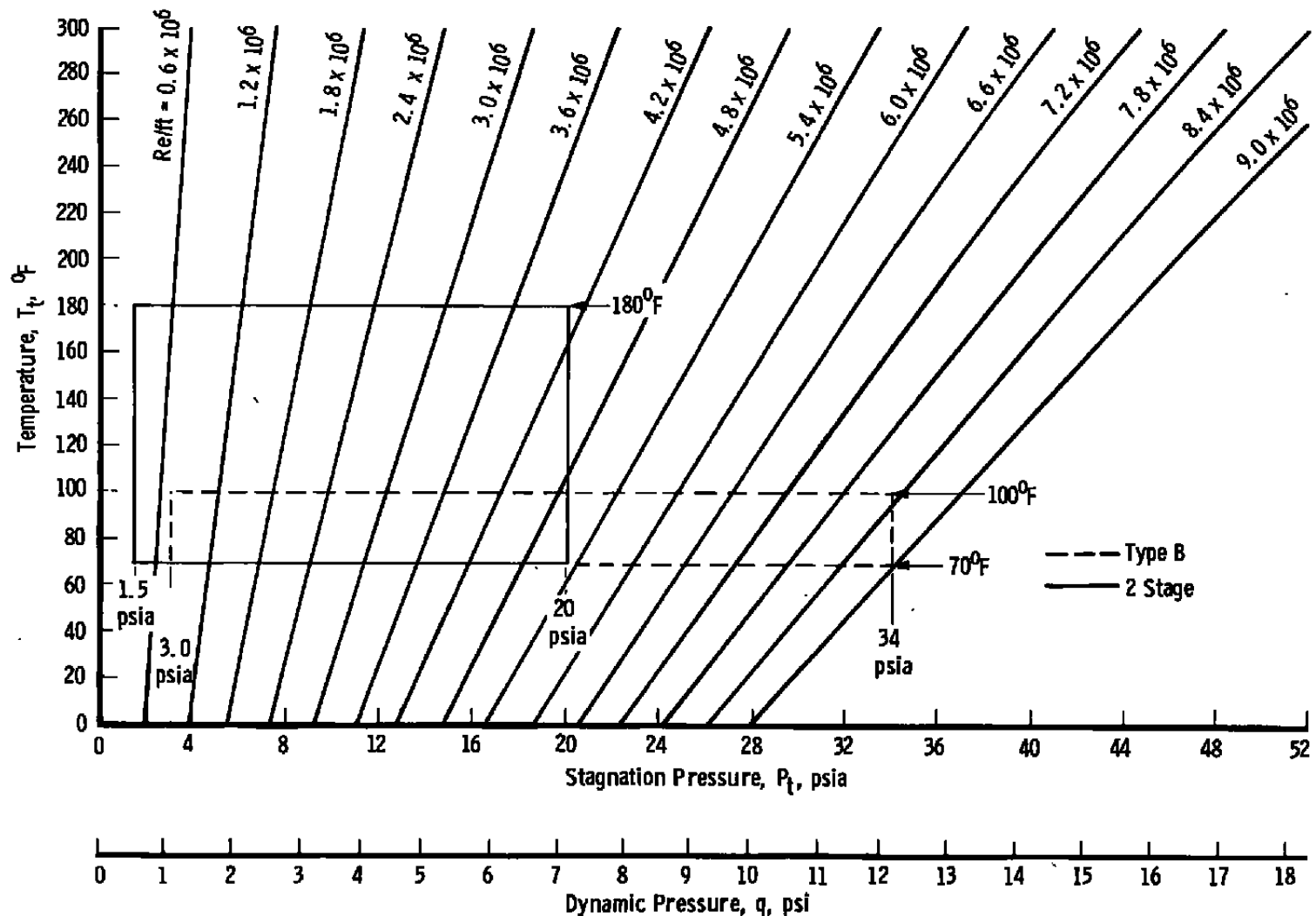


a.  $M = 1.50$

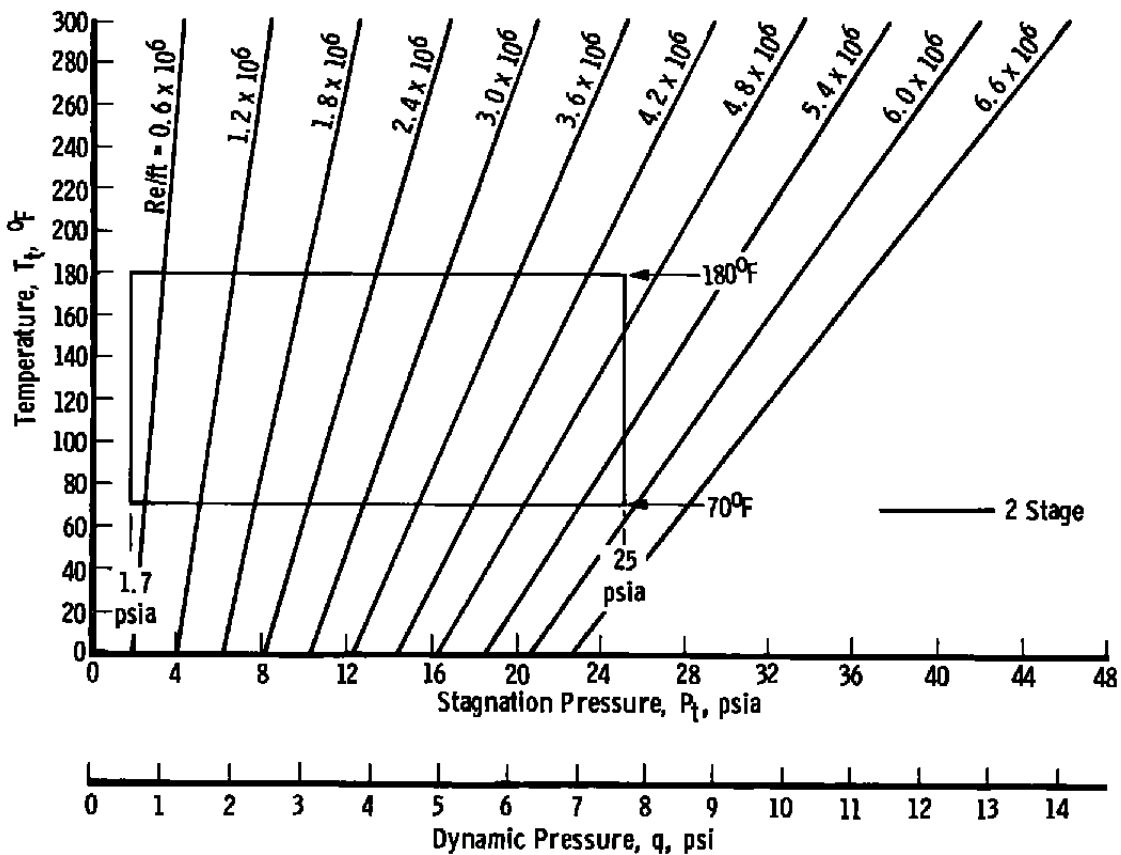
Figure A-6. Tunnel A operating conditions and limits.



b.  $M = 1.75$   
Figure A-6. Continued.

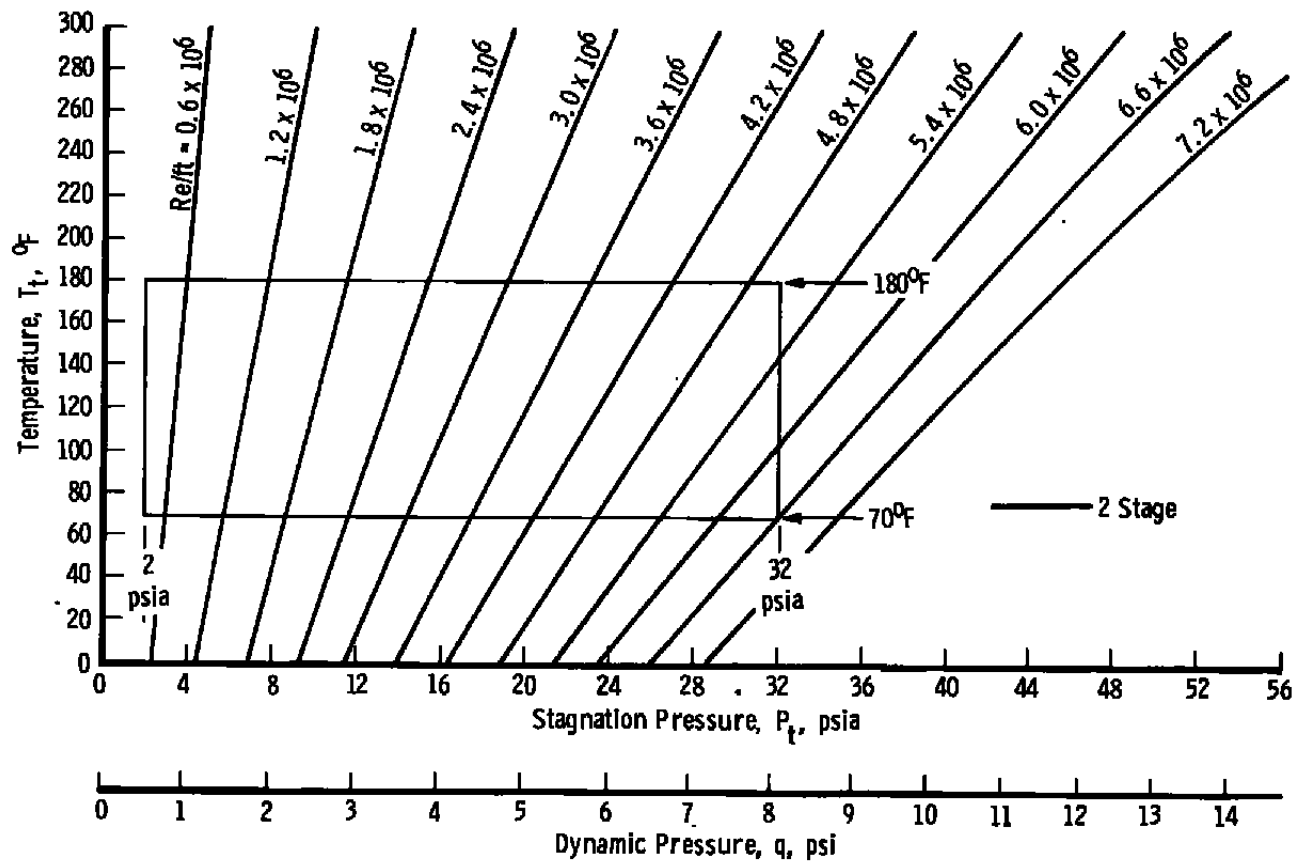


c.  $M = 2.00$   
Figure A-6. Continued.

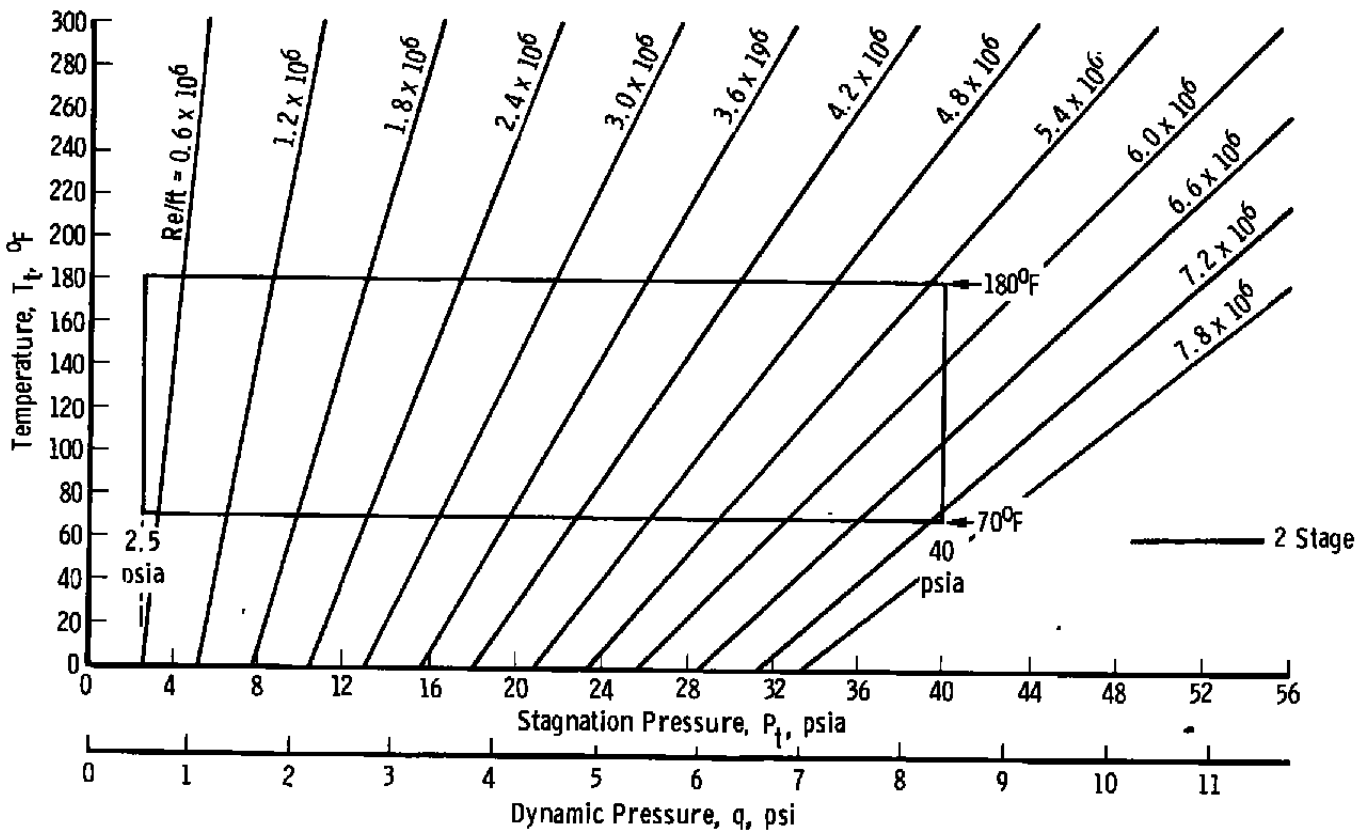


d.  $M = 2.25$

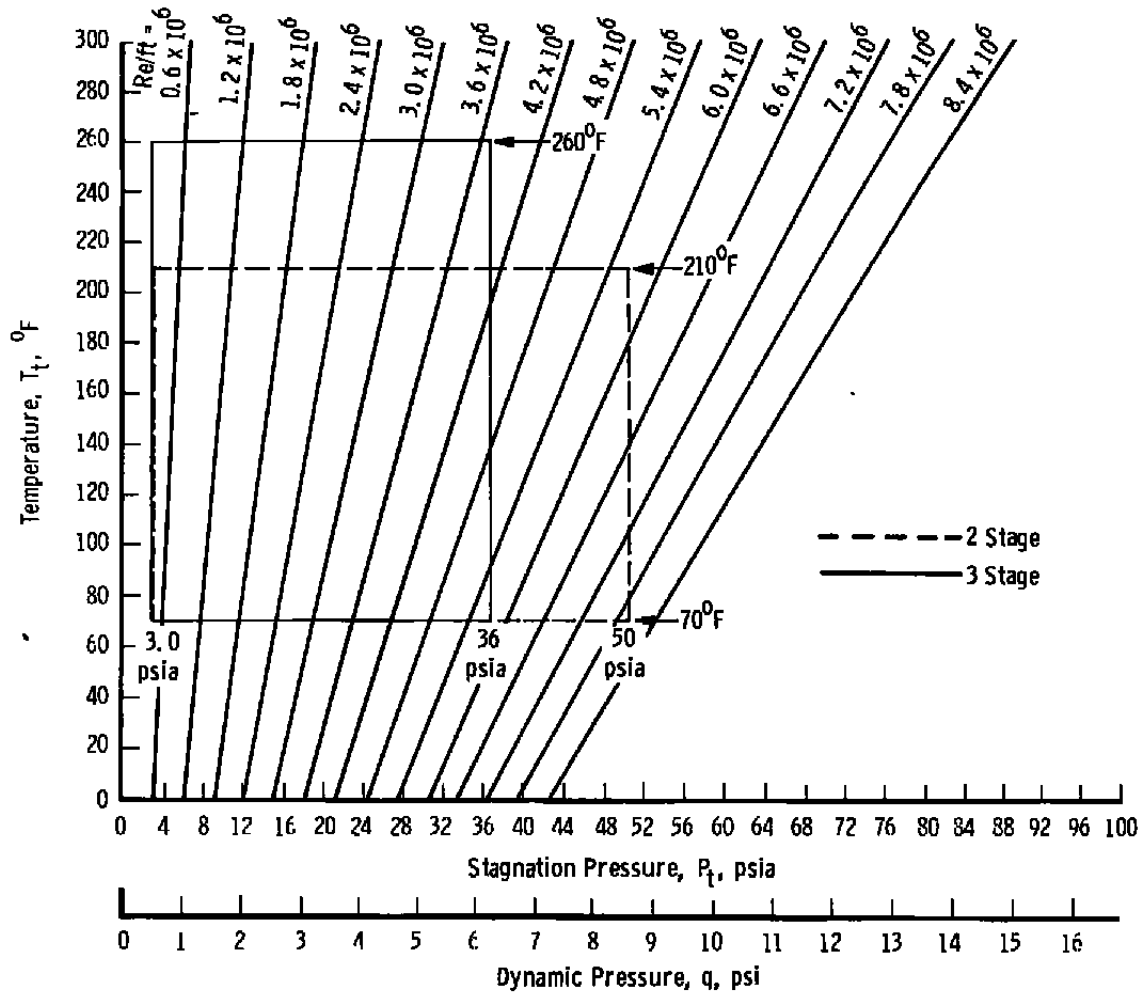
Figure A-6. Continued.



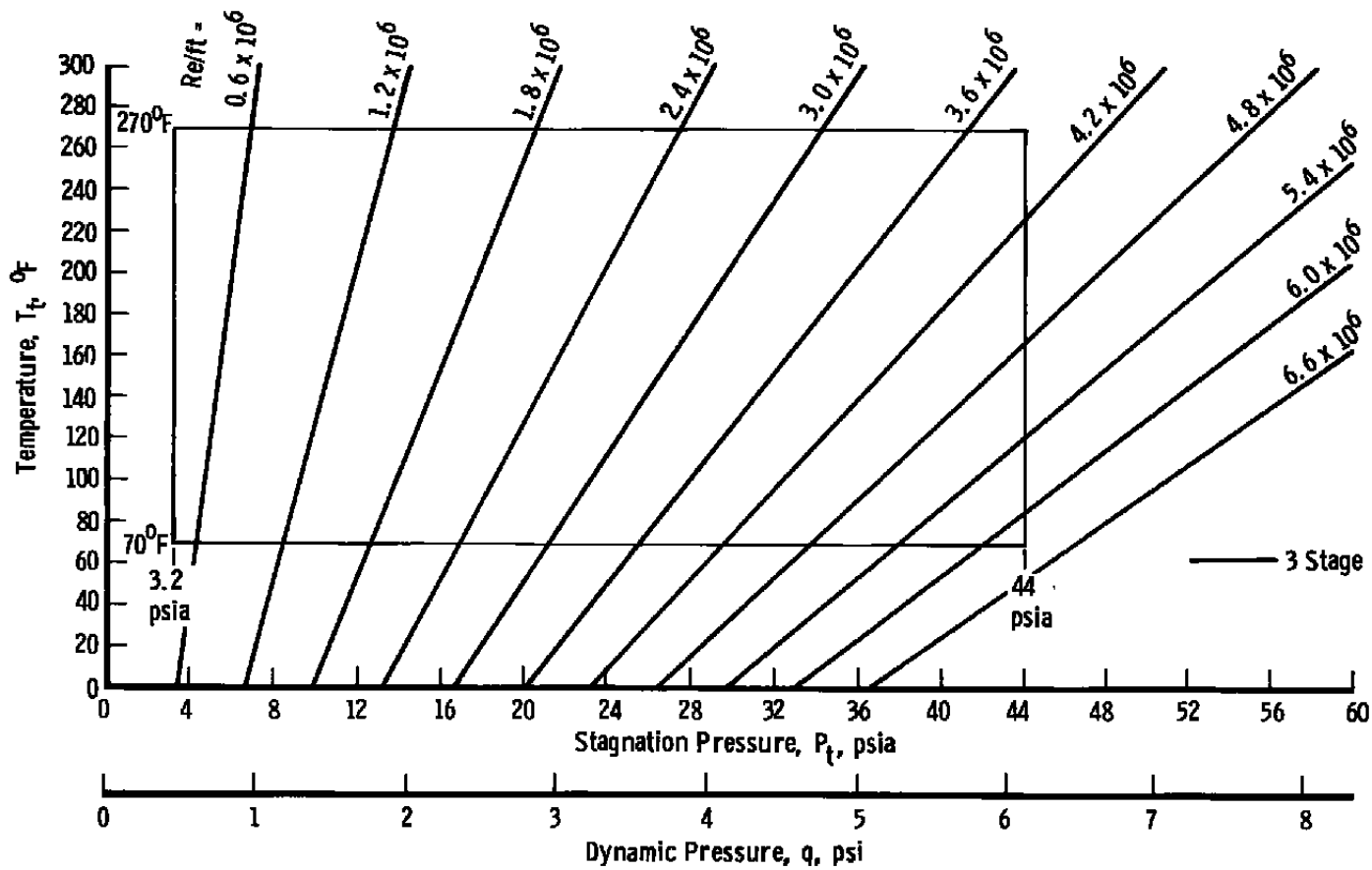
e.  $M = 2.50$   
Figure A-6. Continued.



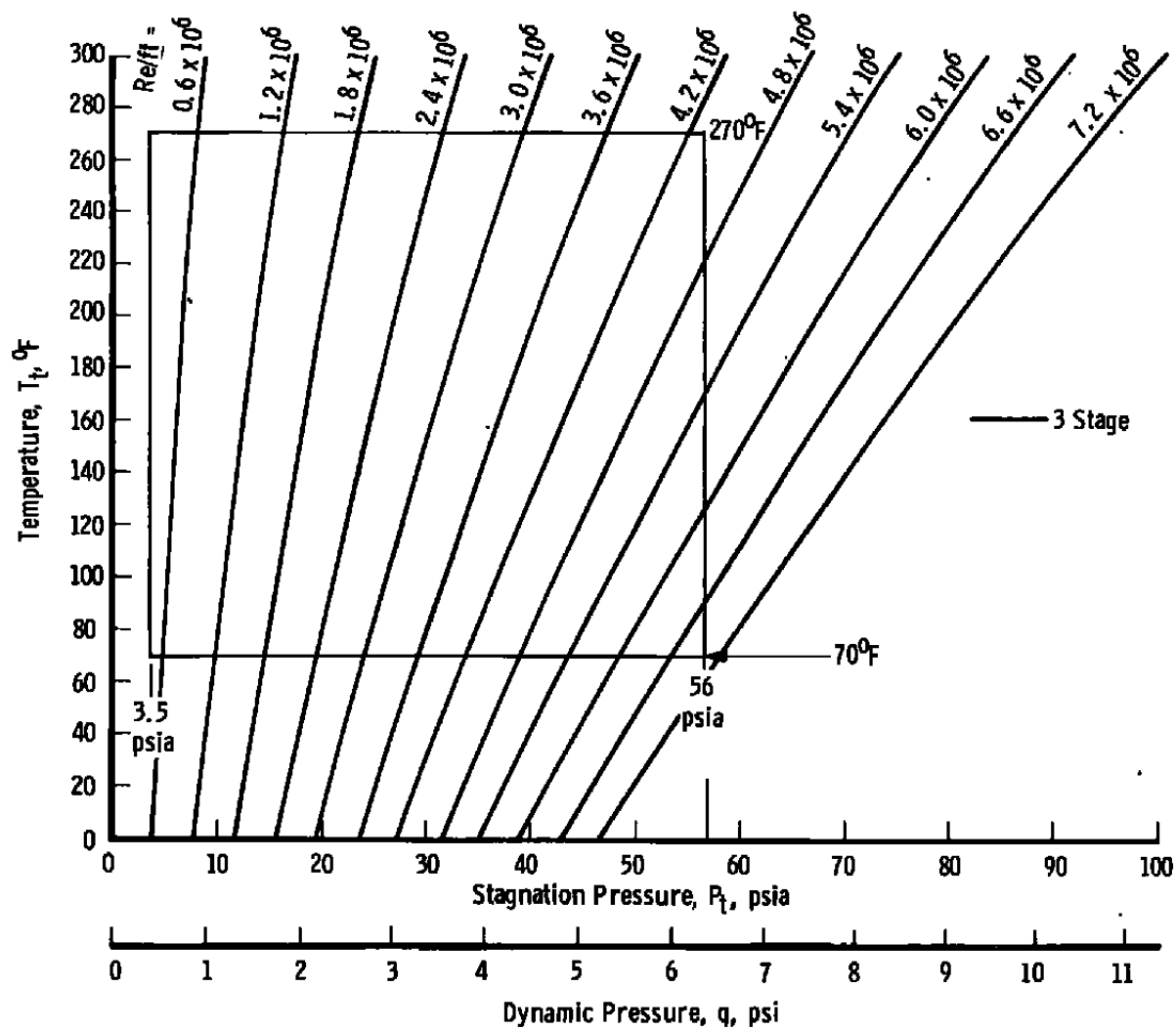
f.  $M = 2.75$   
Figure A-6. Continued.



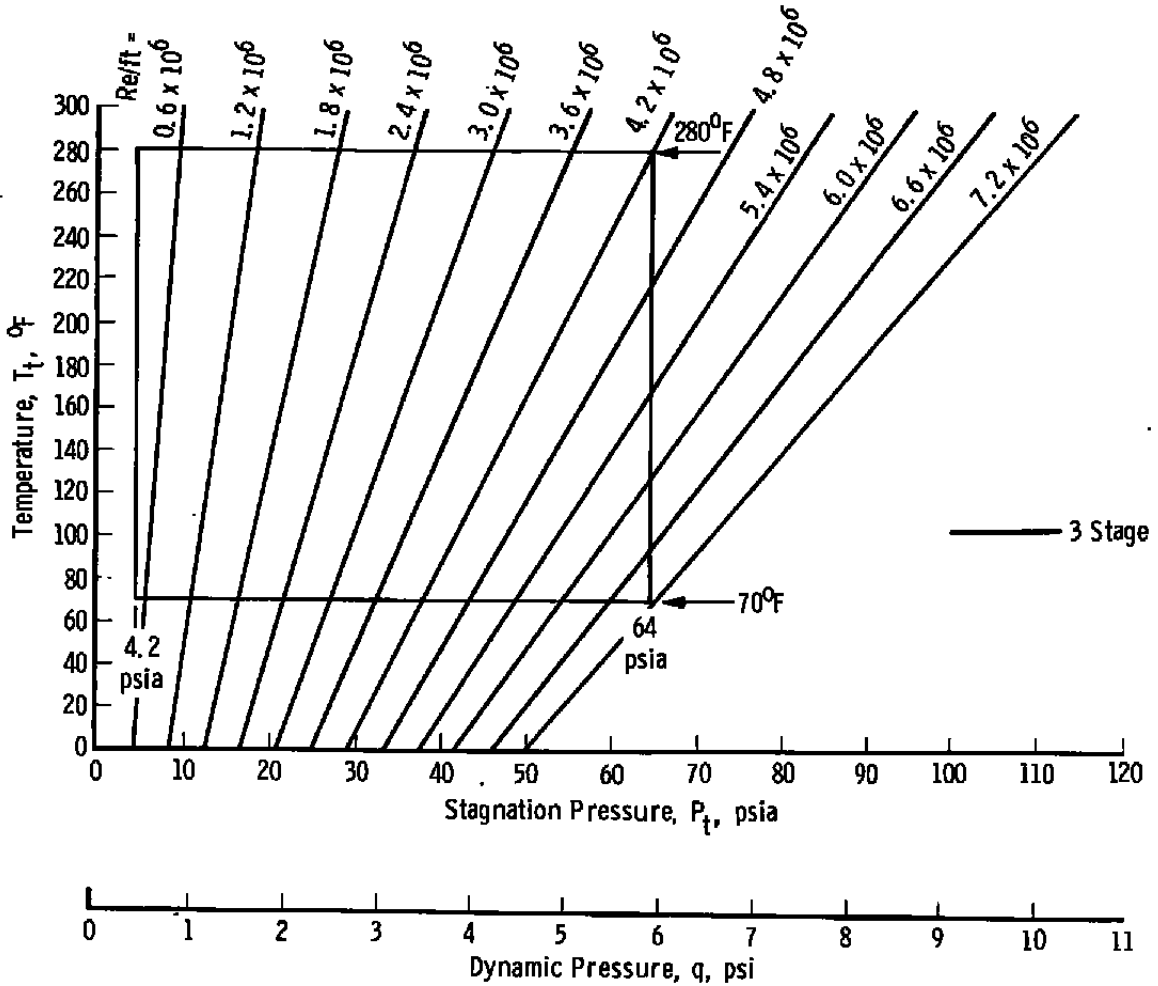
g.  $M = 3.00$   
Figure A-6. Continued.



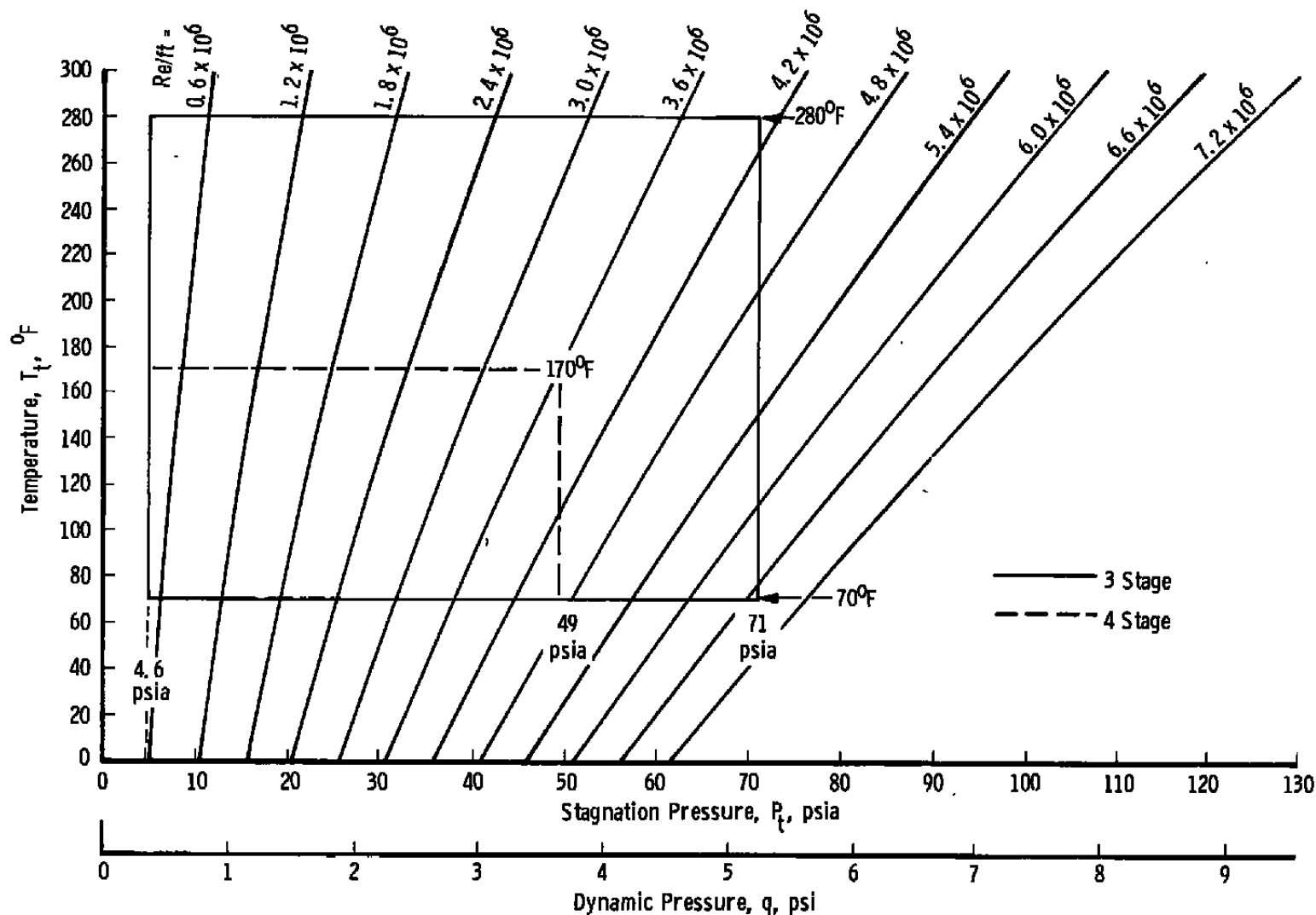
h.  $M = 3.25$   
Figure A-6. Continued.



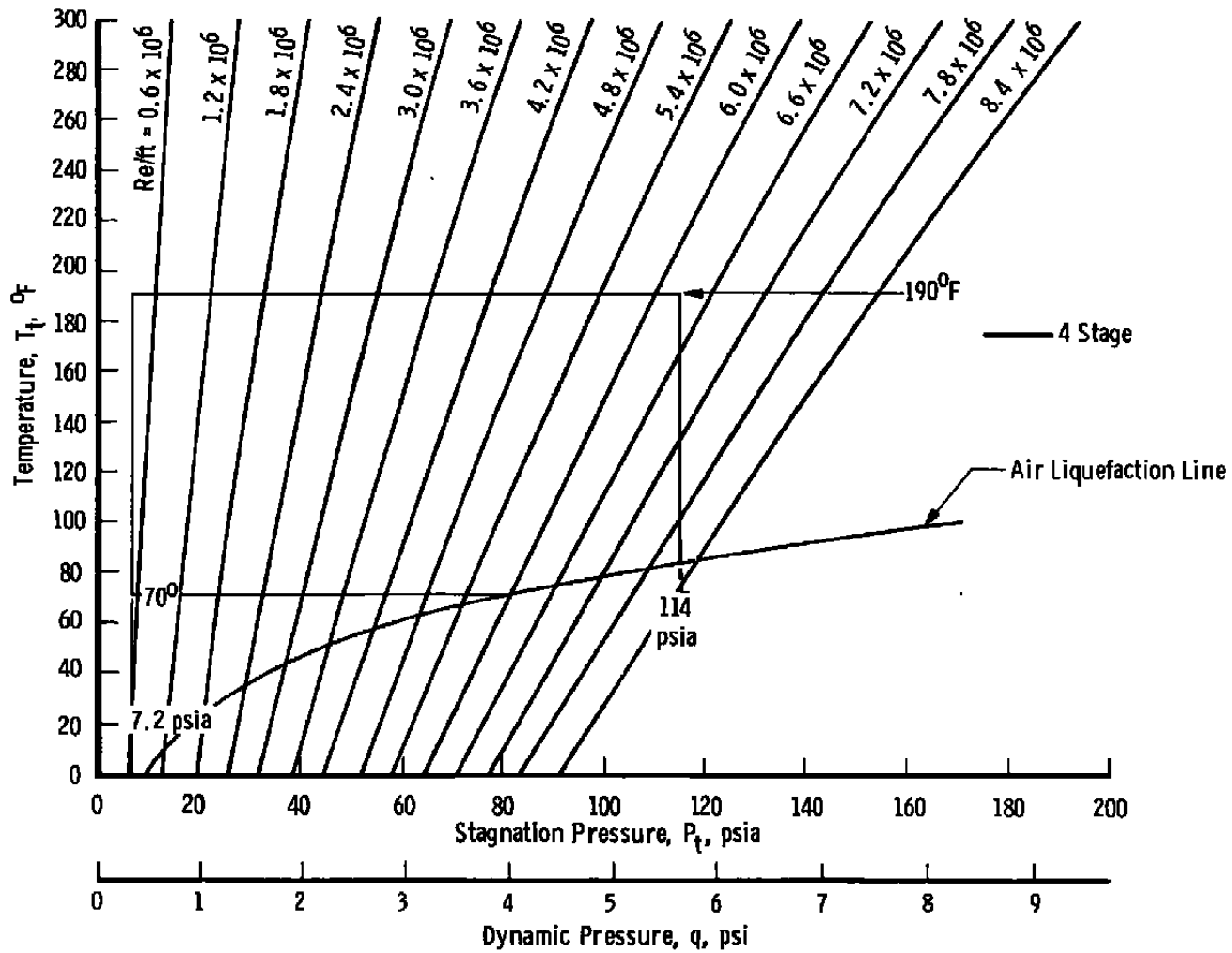
i.  $M = 3.50$   
Figure A-6. Continued.



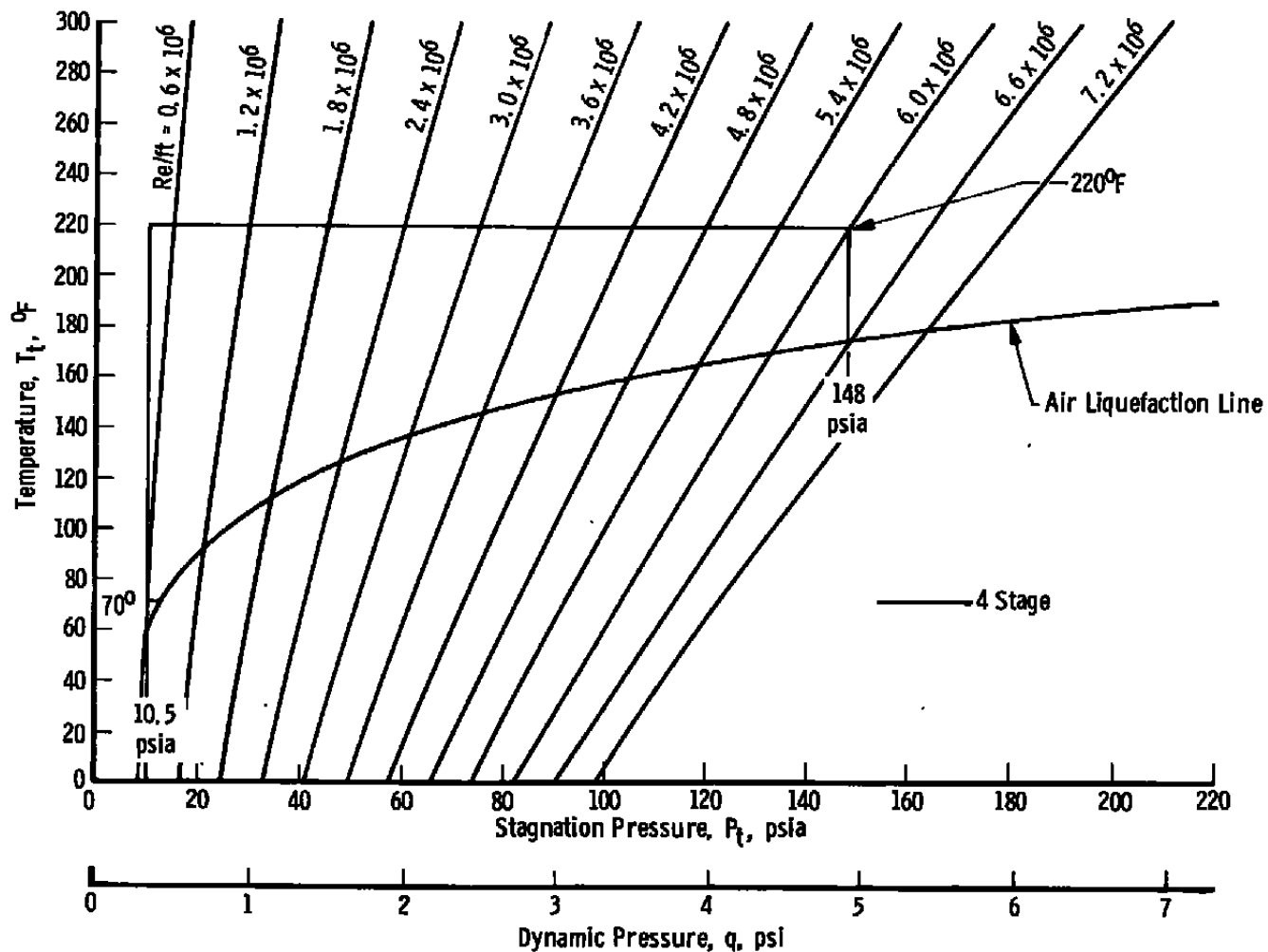
j.  $M = 3.75$   
Figure A-6. Continued.



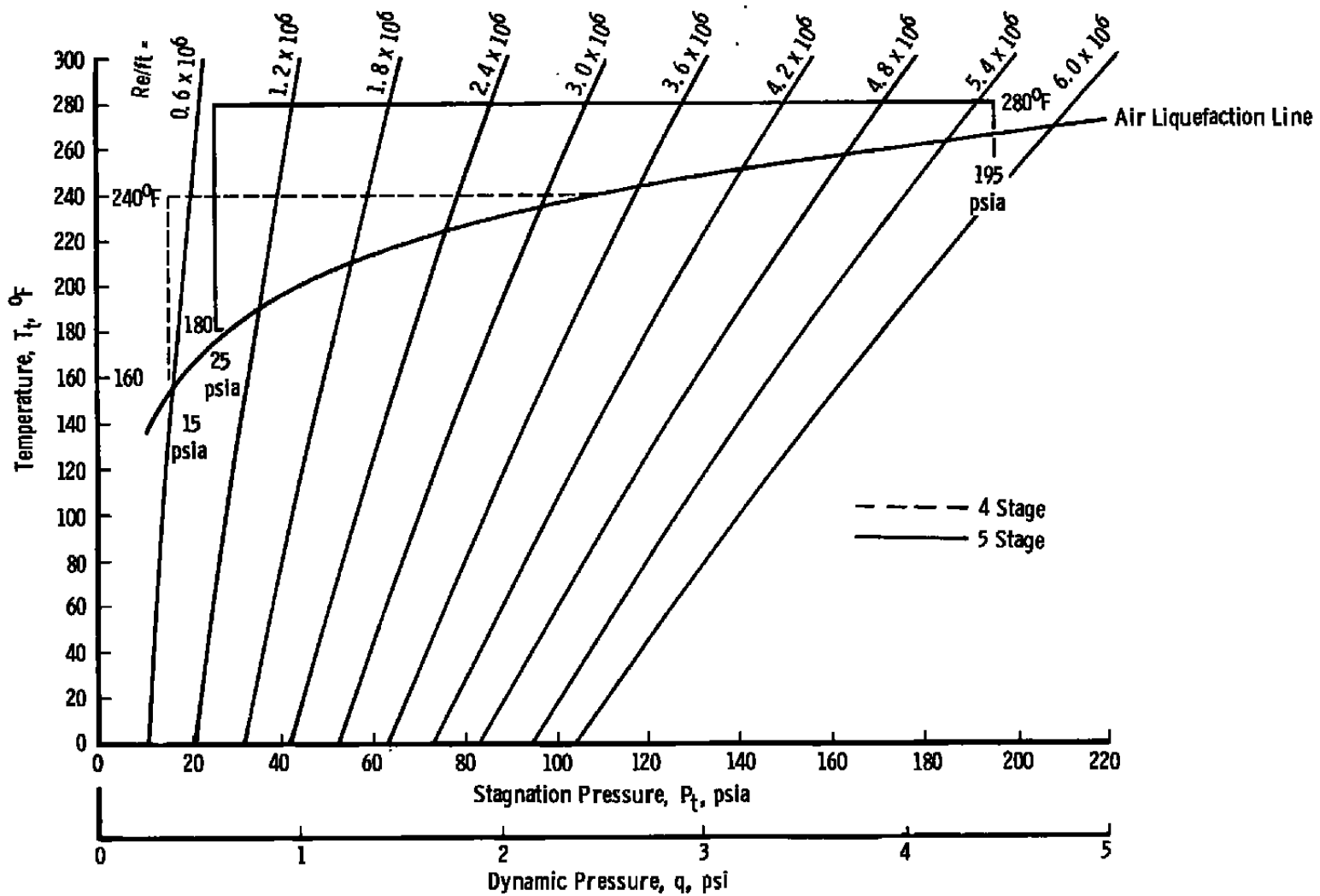
$k$ .  $M = 4.00$   
 Figure A-6. Continued.



I.  $M = 4.50$   
Figure A-6. Continued.



m.  $M = 5.00$   
Figure A-6. Continued.



n.  $M = 5.50$   
**Figure A-6. Concluded.**

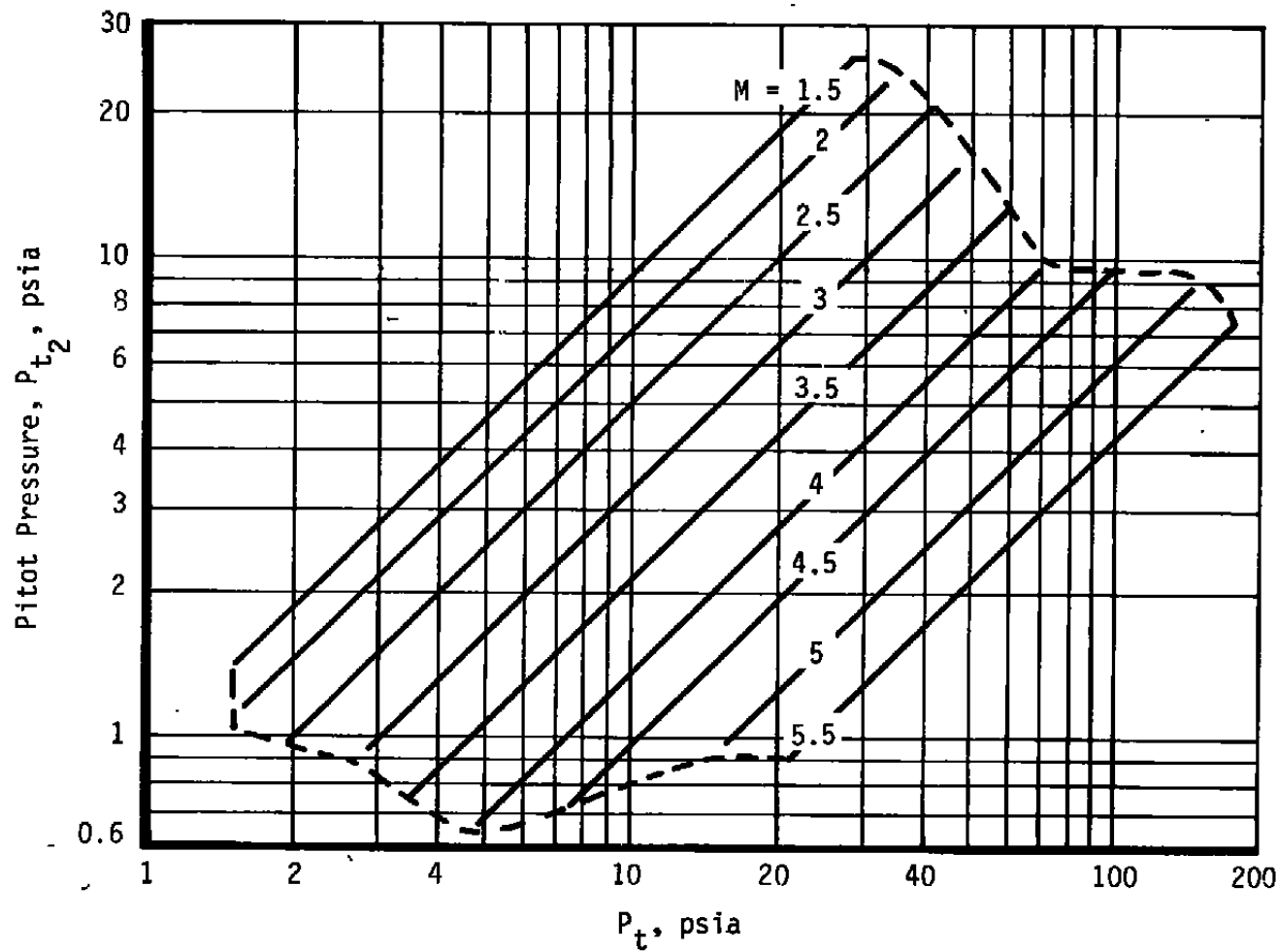


Figure A-7. Free-stream pitot pressure, Tunnel A.

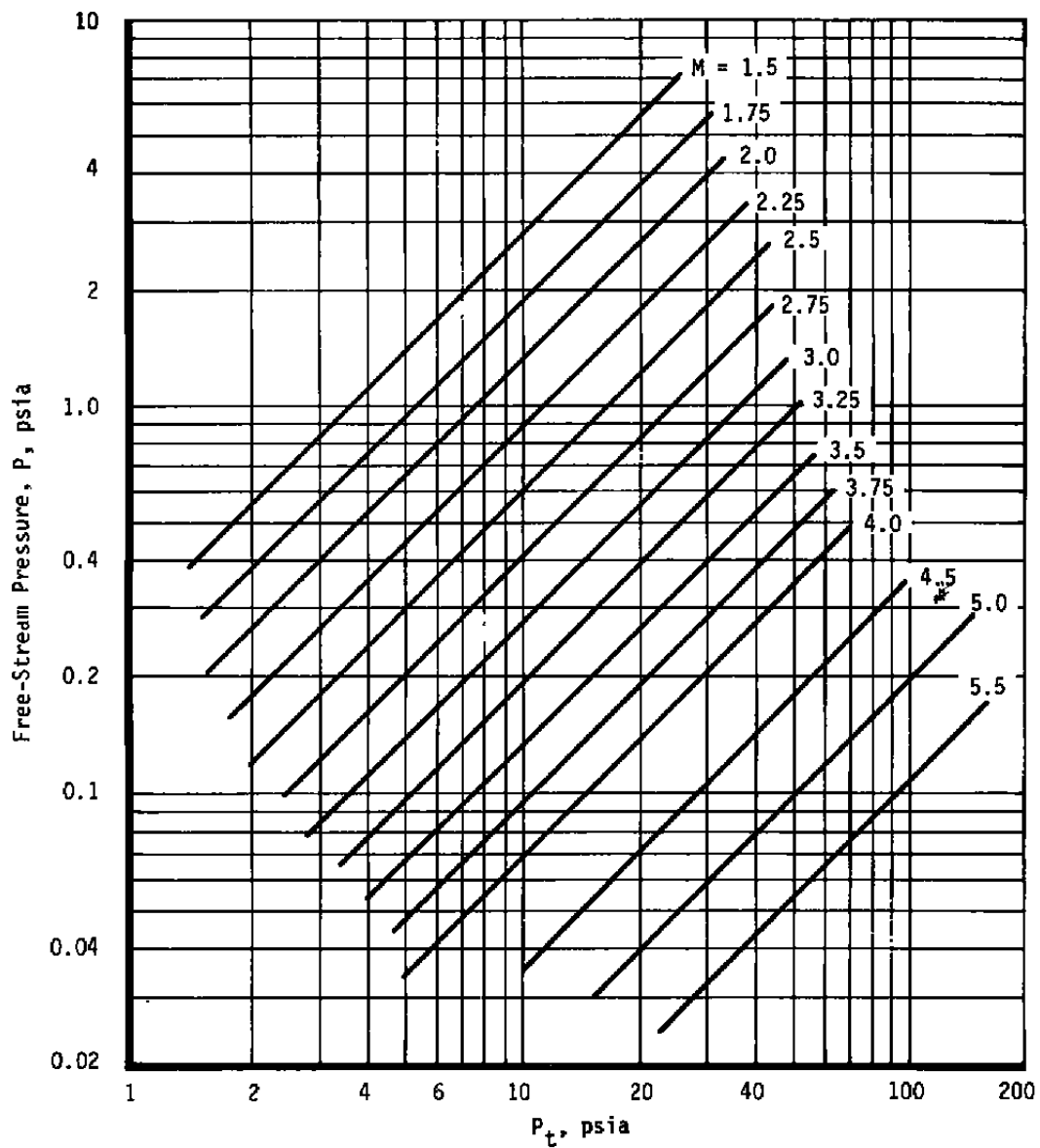


Figure A-8. Free-stream pressure, Tunnel A.

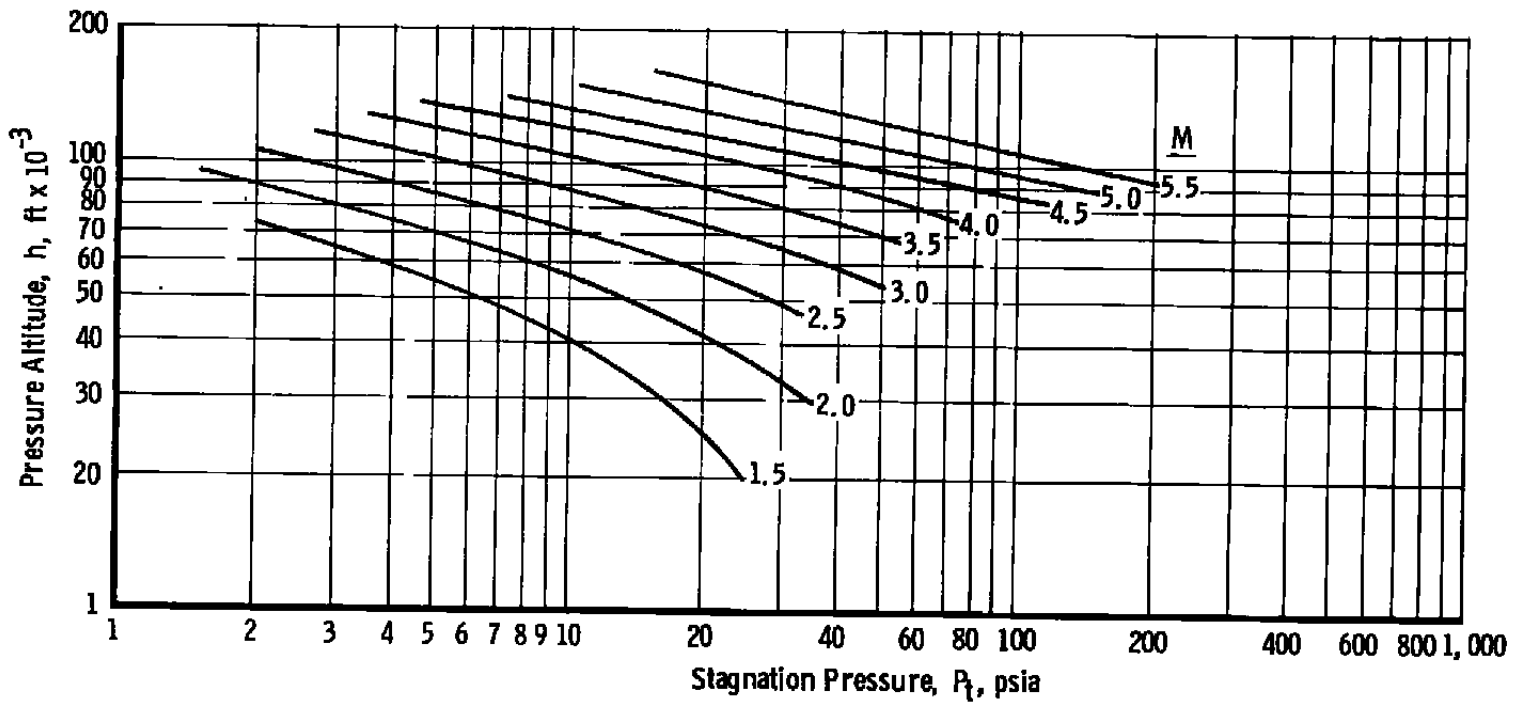


Figure A-9. Simulated altitude, Tunnel A.

NOTE: Compressor Usage Only

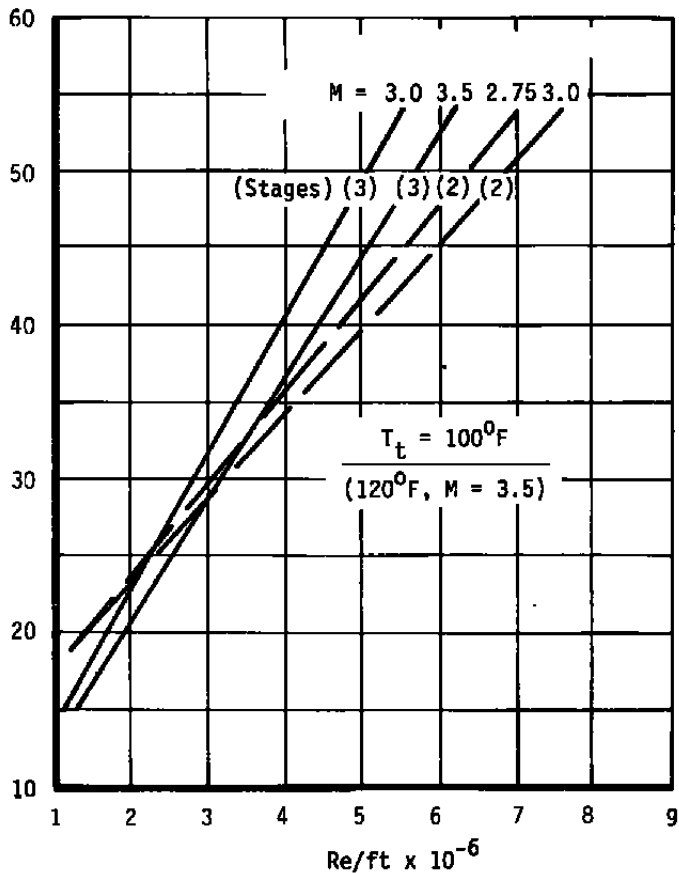
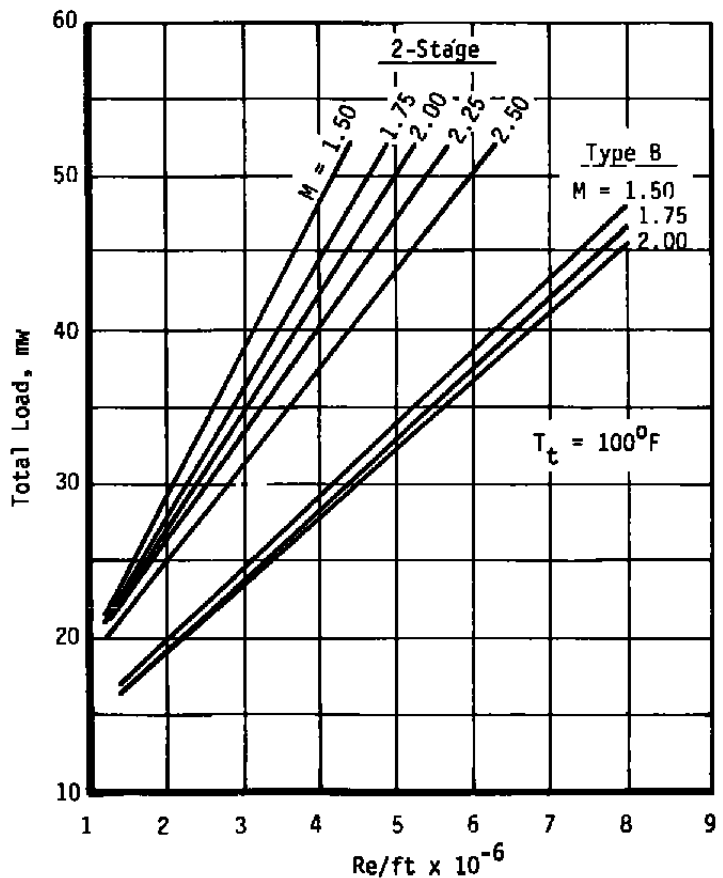


Figure A-10. Electrical usage for Tunnel A.

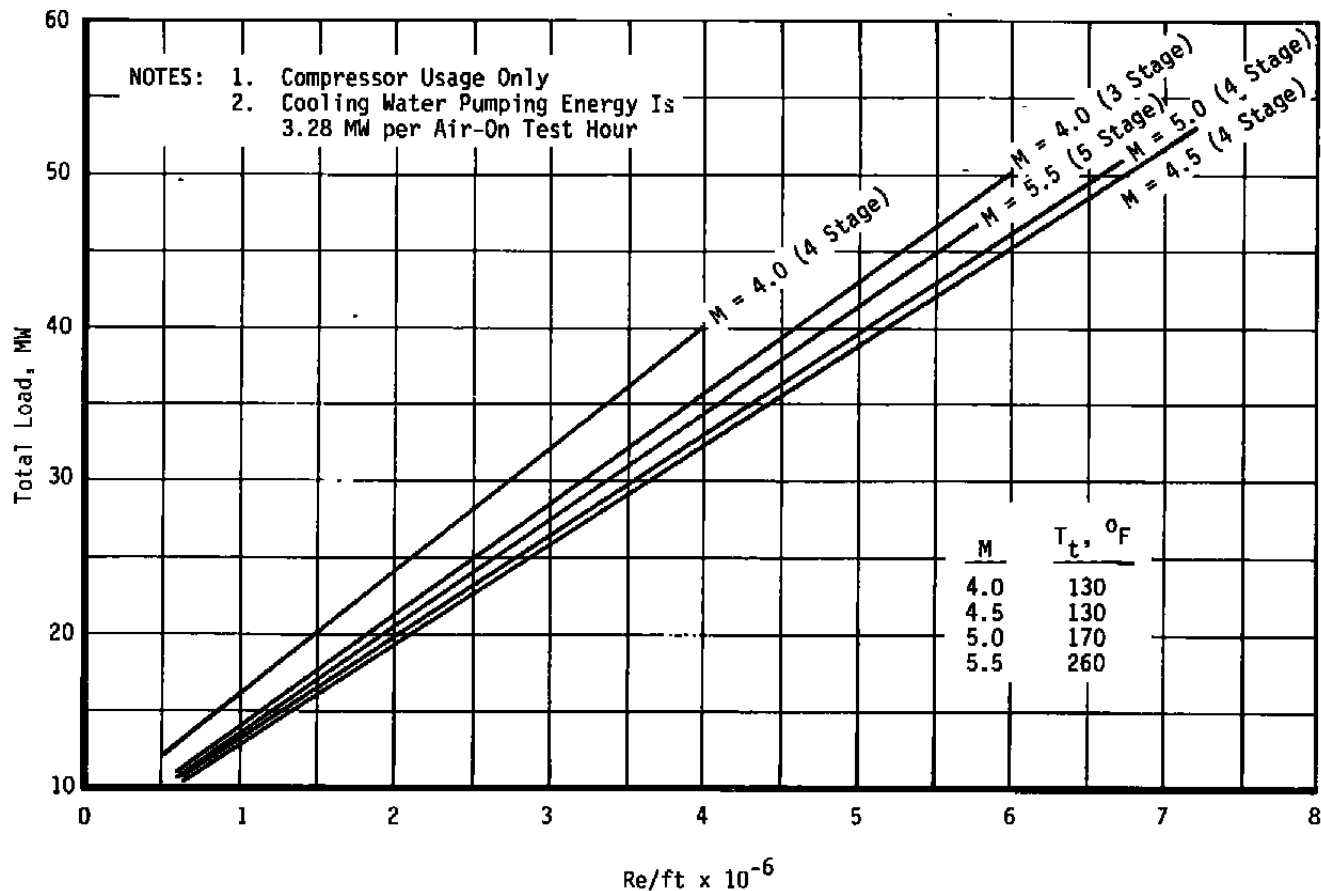


Figure A-10. Concluded.

**Table A-1. Tunnel A Standardized Mach Number**

Nozzle Contour	M	$P_t$ Range
1.50	1.51	Atm to Max.
1.75	1.76	
2.00	2.00	
2.25	2.26	
2.50	2.50	
2.75	2.75	
3.00	3.01	
3.25	3.25	
3.50	3.51	
3.75	3.76	
4.00	4.02	22 to Max.
4.00	4.01	14 to 22
4.50	4.52	50 to Max.
	4.51	30 to 50
	4.50	18 to 30
	4.49	14 to 18
	5.06	130 to 170
	5.05	90 to 130
	5.04	60 to 90
	5.03	30 to 60
	5.02	11 to 30

Note: For  $M > 5$ , Mach - probe data are used.

**Table A-2. Tunnel A Total Mass Flow**

Total mass flow through the throat is given by\*

$$\dot{m} = 0.532 \frac{P_t A^*}{\sqrt{T_t}}$$

$A^*$  is as follows:

M	Z*	A*
1.50	16.428	1314.2
1.75	13.900	1112.0
2.00	11.377	910.2
2.25	9.103	728.2
2.50	7.183	574.6
2.75	5.643	451.4
3.00	4.383	350.6
3.25	3.450	276.0
3.50	2.663	213.0
3.75	2.095	167.6
4.00	1.635	130.8
4.50	1.027	82.2
5.00	0.658	52.6
5.50	0.431	34.5

\* Units of measurement:

$P_t$  - psia

$A^*$  - sq. in.

$T_t$  - °R

$\dot{m}$  - lbm/sec

$Z^*$  - (throat half-height) in.

**Table A-3. Tunnel A Operational Time Considerations**

Operation	Time Increments, min	Notes
Tunnel Start ( $T_t = 180^{\circ}\text{F}$ )	30	
( $T_t = 240$ to $280^{\circ}\text{F}$ )	60	
All Stage Changes	30	
Stagnation Pressure Changes	15	90 percent of Range
Change Mach Number*		
1/2 Mach No. Increments (Mach No. 1.5 to 3.0)	10	
All Online Changes (Mach No. 3.0 to 5.5)	20	
Mach Probe Check	5	Add to Mach-Change Time
Diffuser Cool-Down ( $T_t \geq 180^{\circ}\text{F}$ )	30 to 60	Not Always Necessary
Change Reynolds Number	15	
Cool Model	5 to 10	
Model Change**	5	
Tunnel Shutdown	20	

\* Mach number changes can be effected concurrently with stage changes.

\*\* Time increment for actual operation on model must also be added.

† Last operational shift of the week requires an additional 20 min.

**Table A-4. Tunnel A Standard Test Condition Tolerances**

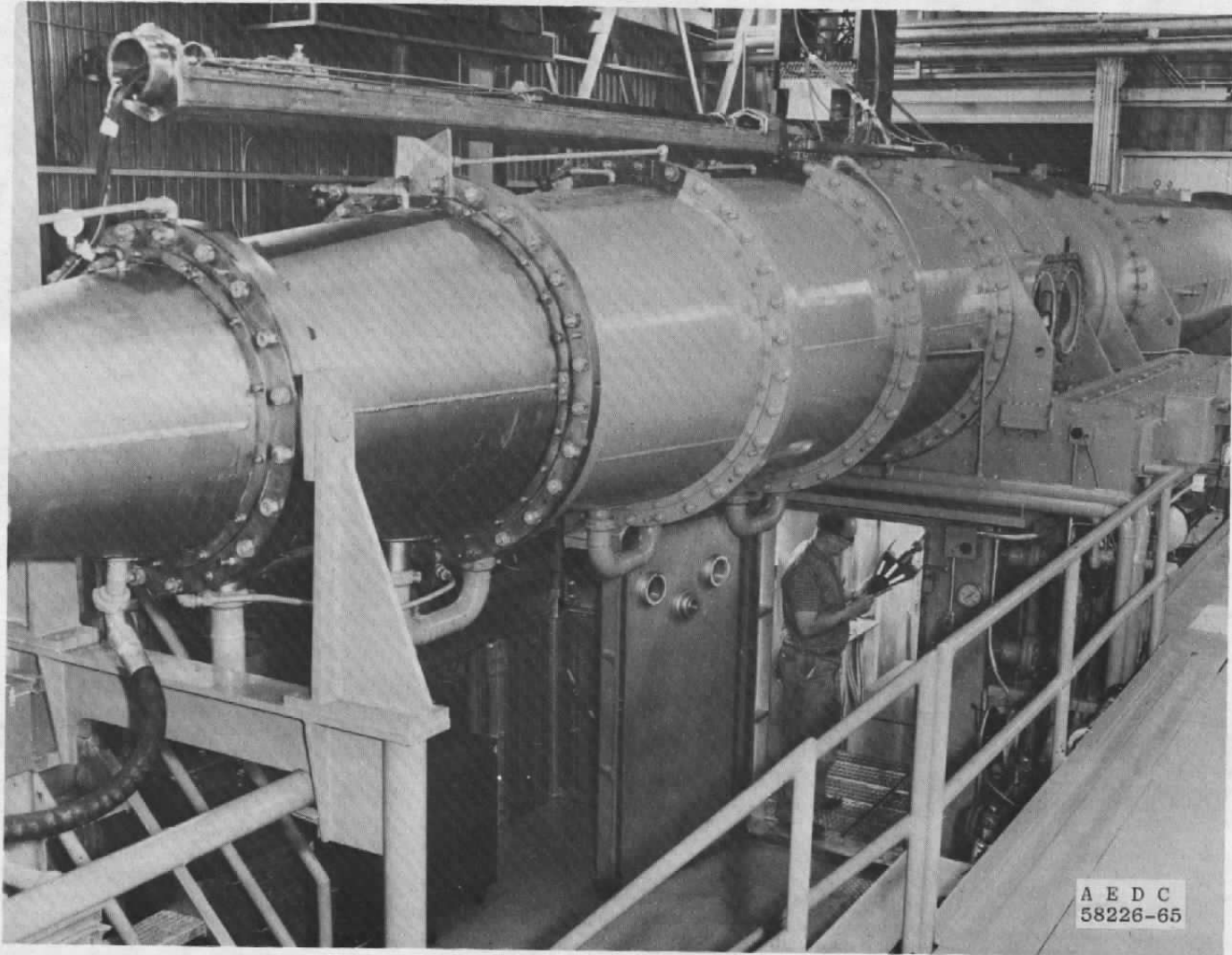
Operational procedures for VKF wind tunnels emphasize efficiency. As part of this effort, standard tolerances are set which allow the tunnel operator some latitude in setting test conditions. The following tolerances on stilling chamber pressure and temperature and limits on humidity are recommended.

$P_t$ , psia	$\pm \Delta P_t$ , psia	$T_t$	$\pm \Delta T_t$	$T_{DP}^1$
1.5 to 2.9	0.10	All	5°F	0°F
3.0 to 9.0	0.15			
10 to 19	0.20			
20 to 29	0.20			
30 to 39	0.30			
40 to 49	0.40			
50 to 59	0.50			
60 to 69	0.60			
70 to 79	0.70			
80 to 89	0.80			
90 to 99	0.90			
100 to 119	1.0			
120 to 139	1.2			
140 to 159	1.4			
160 to 179	1.6			
180 to 200	1.8			

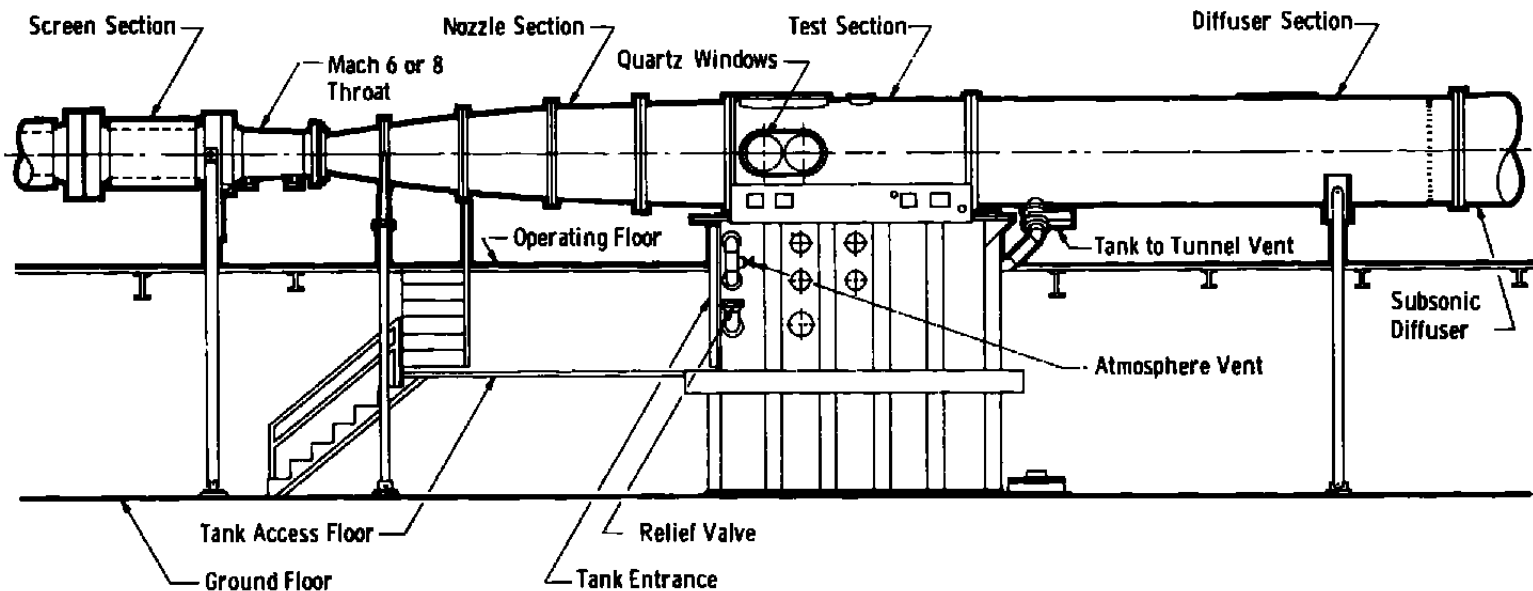
Operation within these tolerances ensures that the requested Reynolds number will be set to within  $\pm 8$  percent.

<sup>1</sup> $T_{DP} \leq 0°F$  is a nominal guideline. The Mach probe is used to check the Mach number at each test condition. Higher  $T_{DP}$  is acceptable at some conditions when the drop in Mach number associated with water vapor is less than one percent of the calibrated Mach number. (See Section 3.3.)

**APPENDIX B  
TUNNEL B**

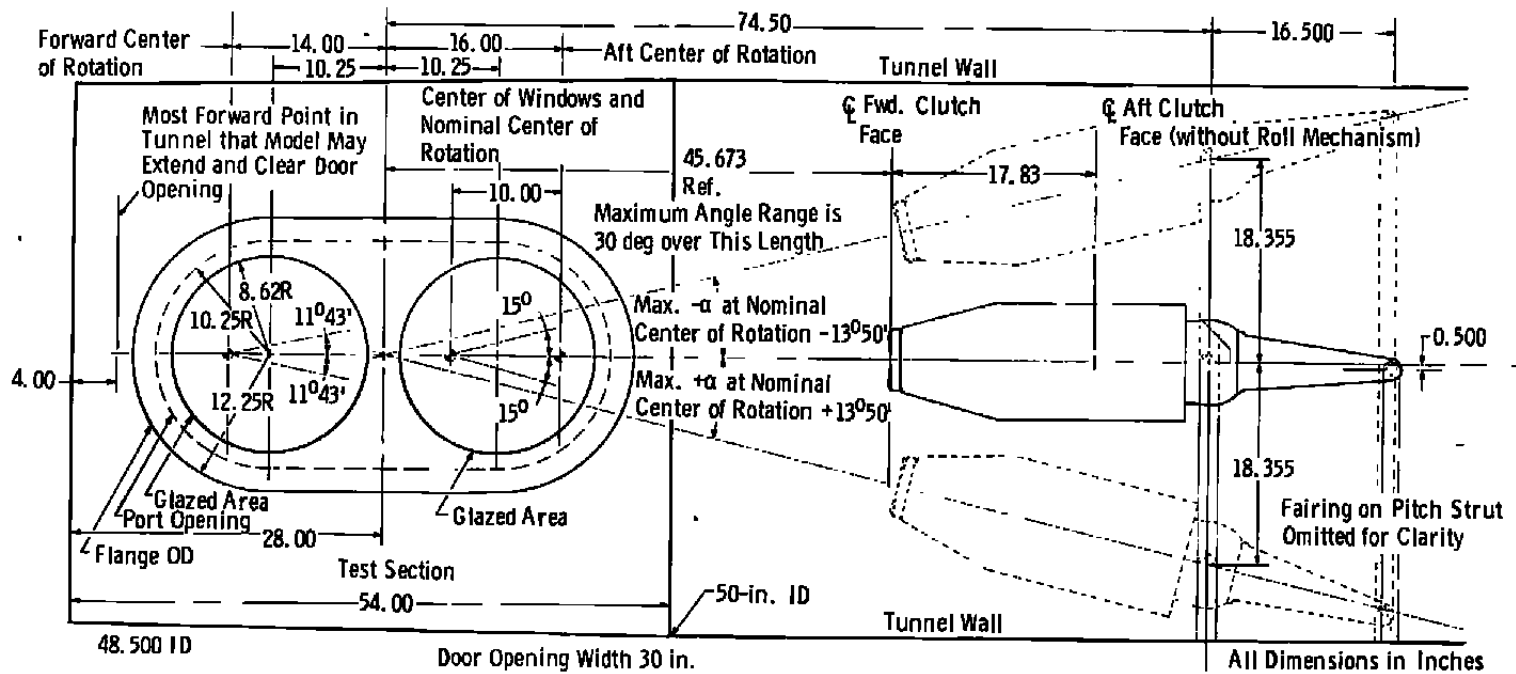


a. Tunnel B  
Figure B-1. Tunnel B.



b. General assembly, Tunnel B

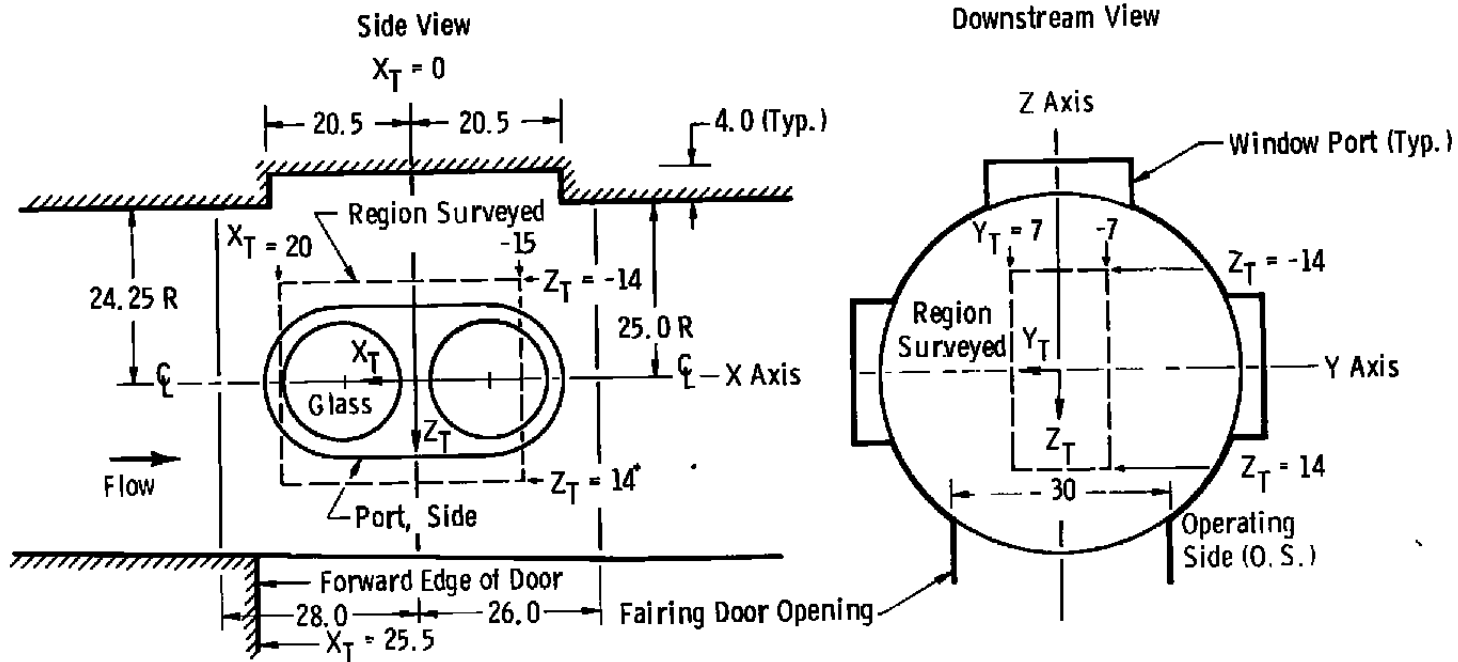
Figure B-1. Continued.



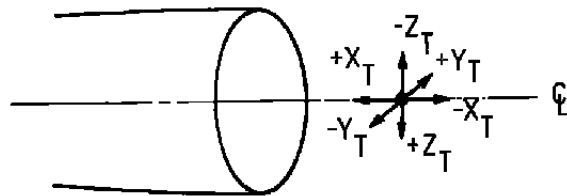
c. Test section (elevation), Tunnel B

Figure B-1. Concluded.

60



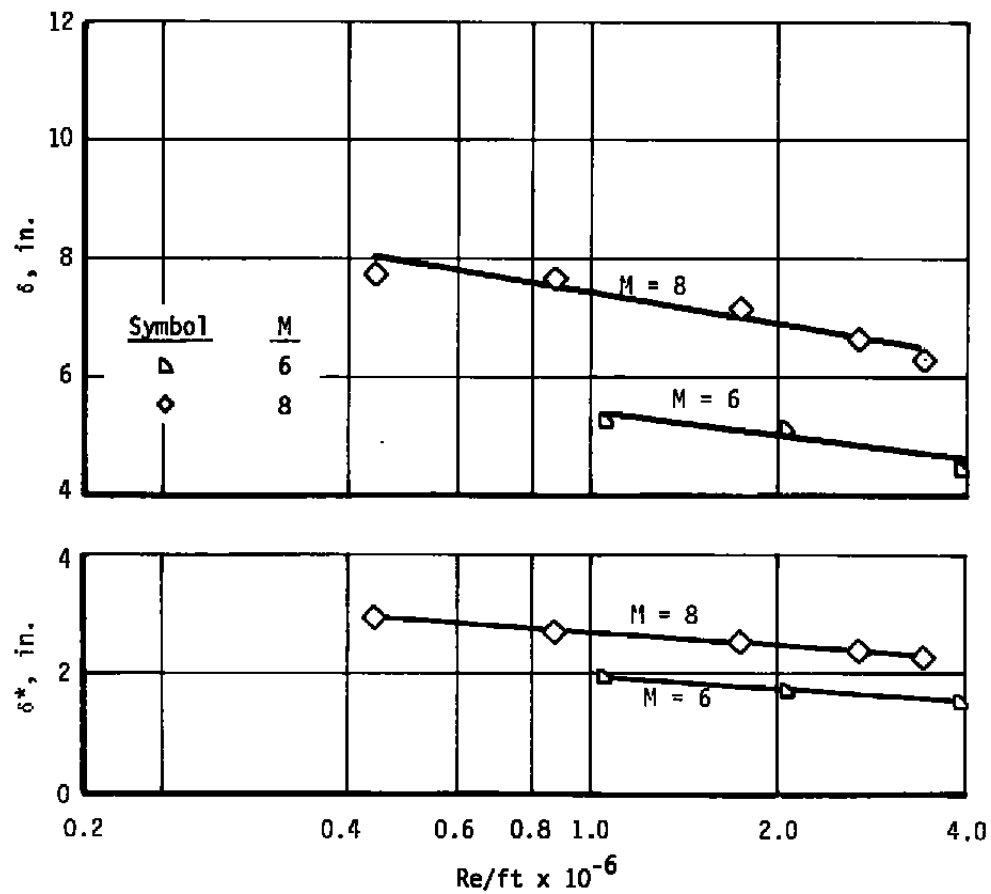
All Dimensions in Inches



Sta  
45, 673

a. Surveyed area

Figure B-2. Test section of Tunnel B.



b. Tunnel B boundary-layer and displacement thickness  
Figure B-2. Concluded.

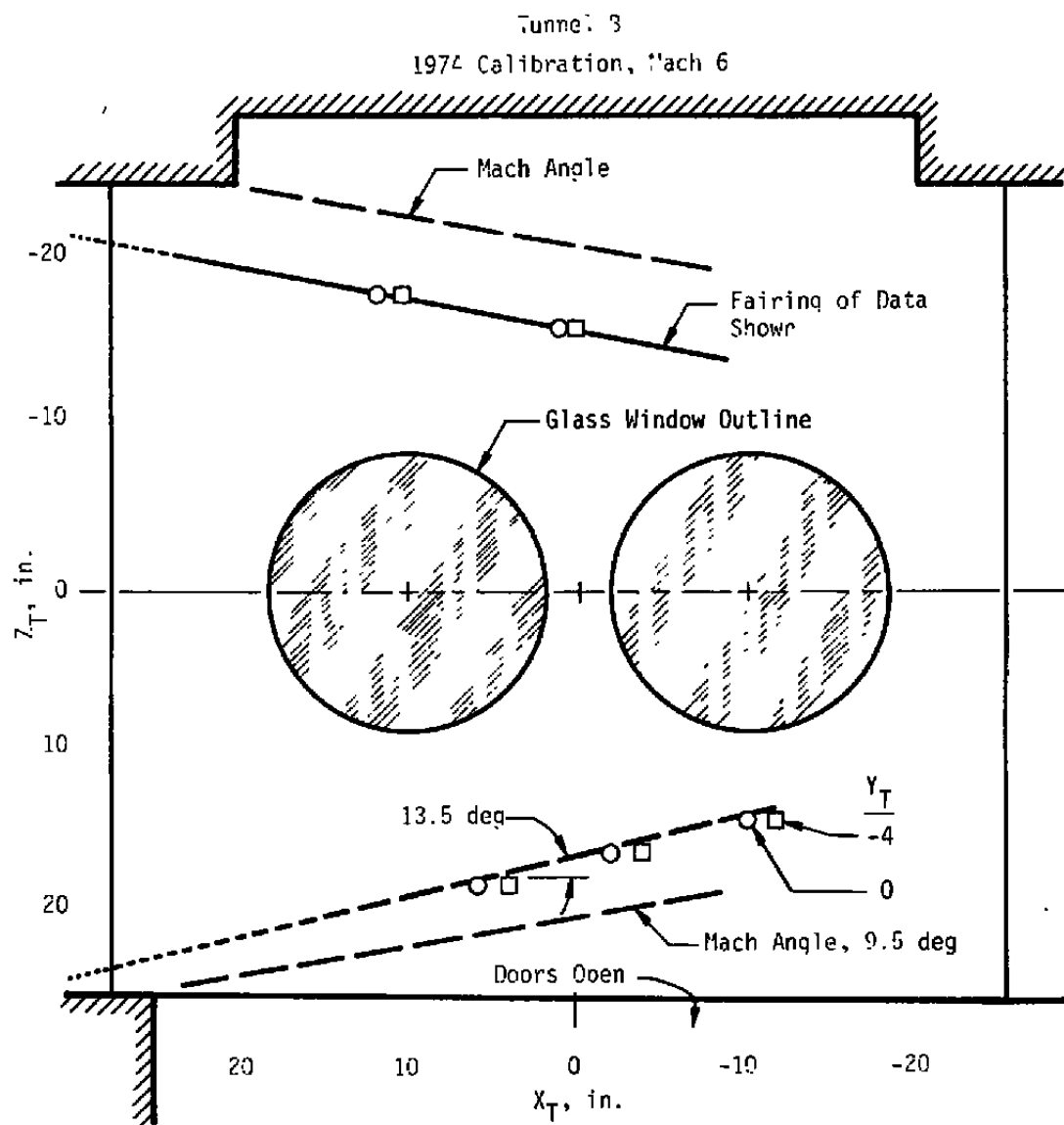


**Figure B-3. Cavity induced disturbance locations at  $M = 6.0$  and  $P_1 = 30$ .**

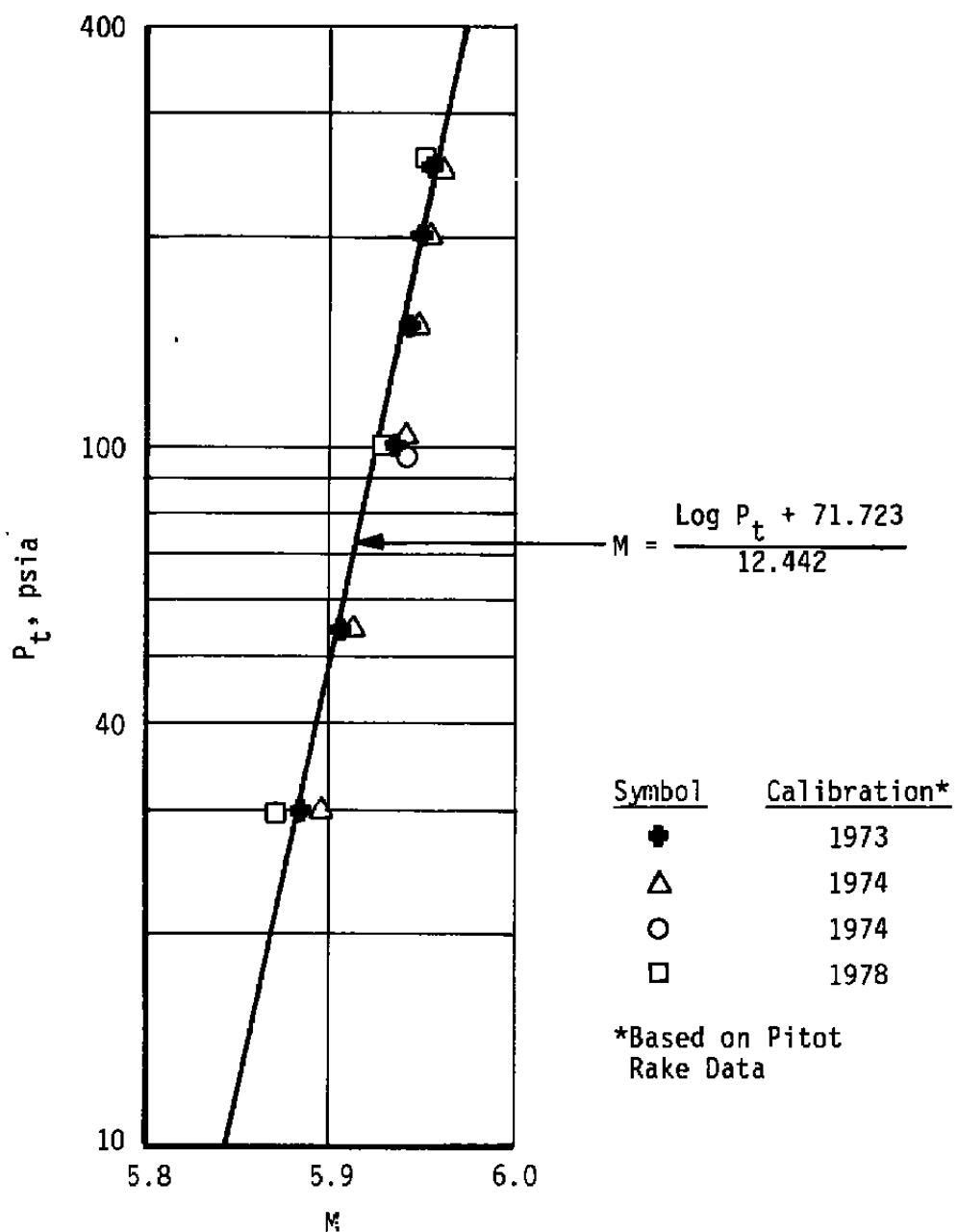
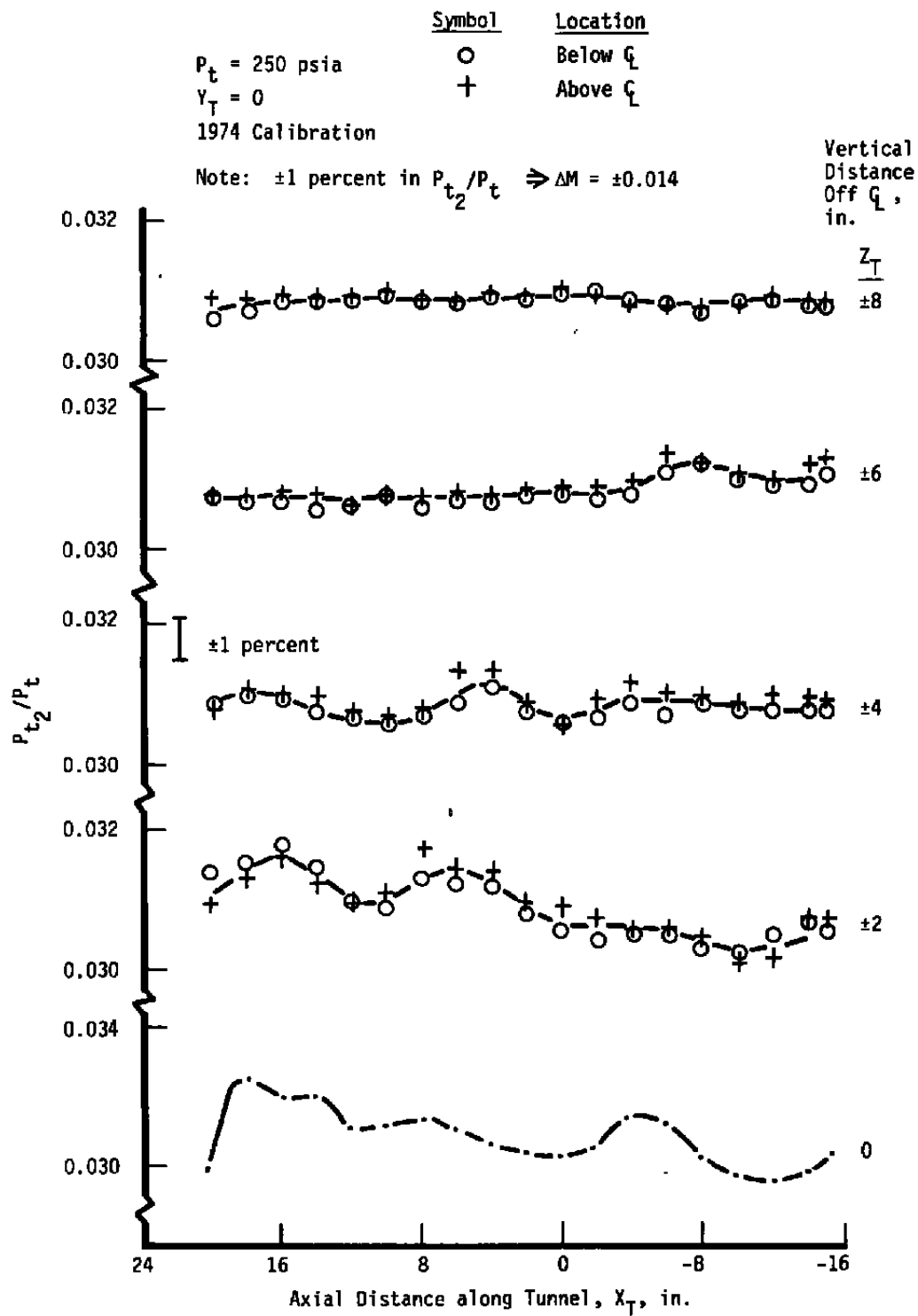
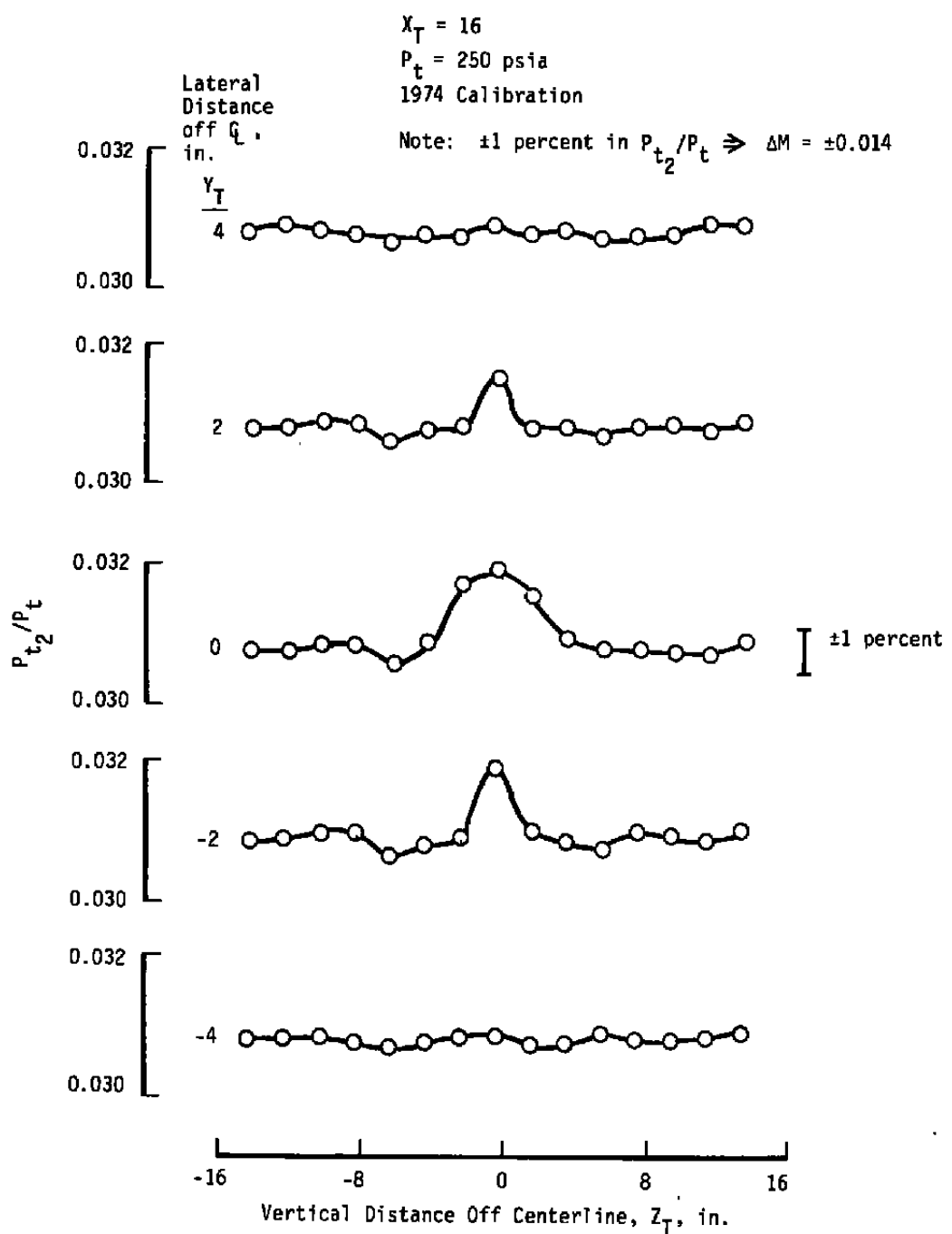


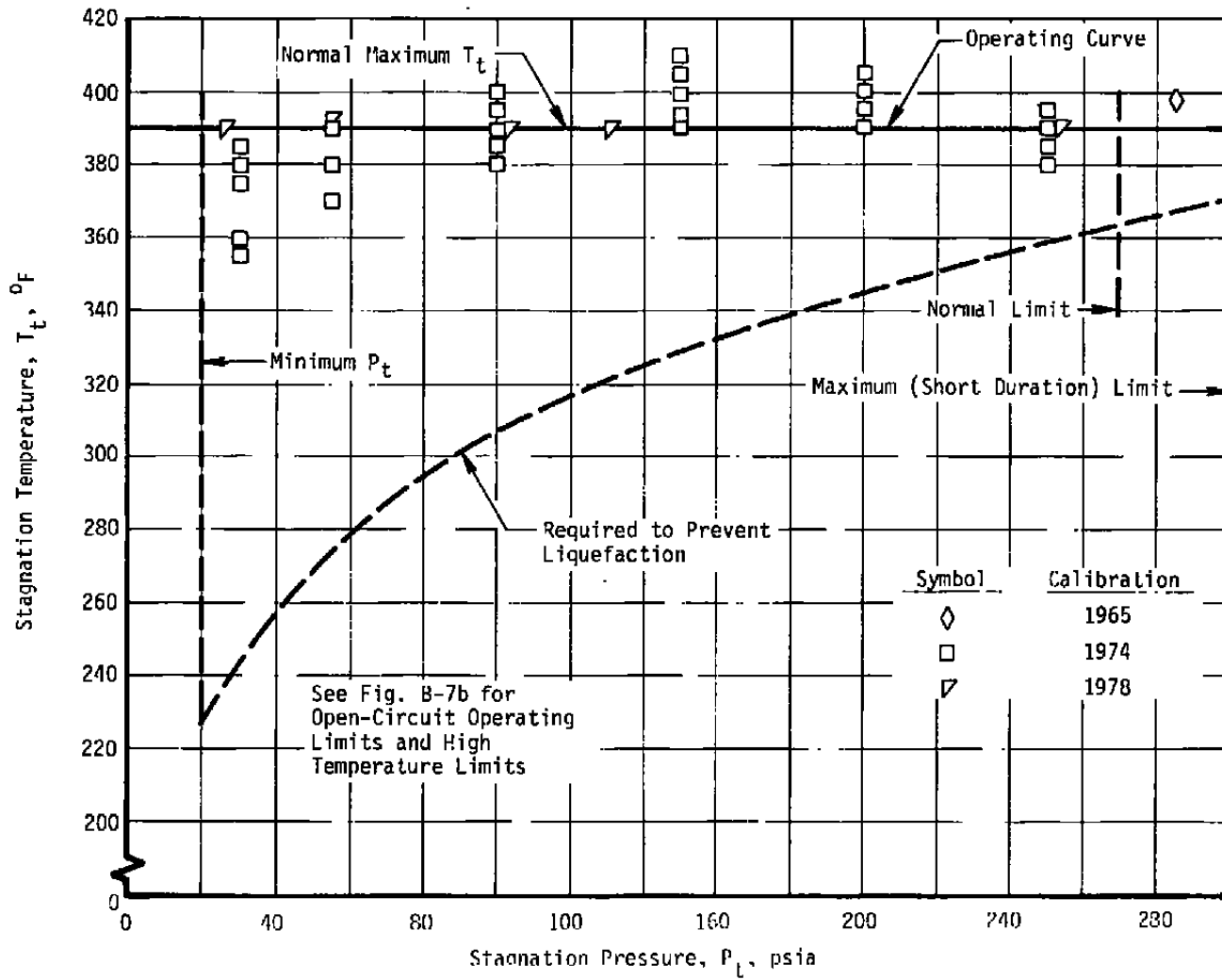
Figure B-4. Mach number, Tunnel B — Mach 6.



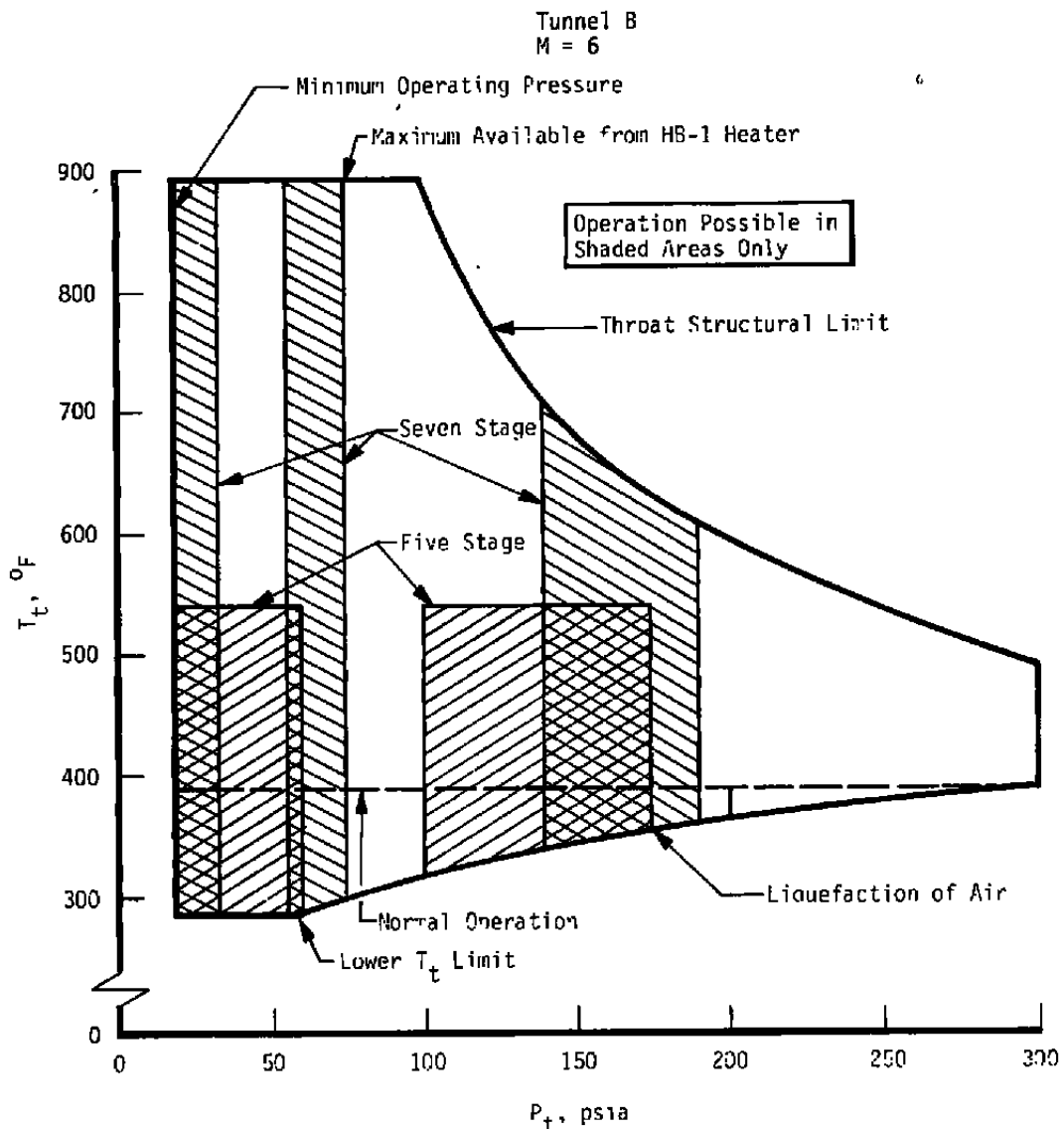
**Figure B-5. Axial pitot pressure distributions,  
Tunnel B — Mach 6.**



**Figure B-6. Vertical pitot pressure profiles, Tunnel B — Mach 6.**

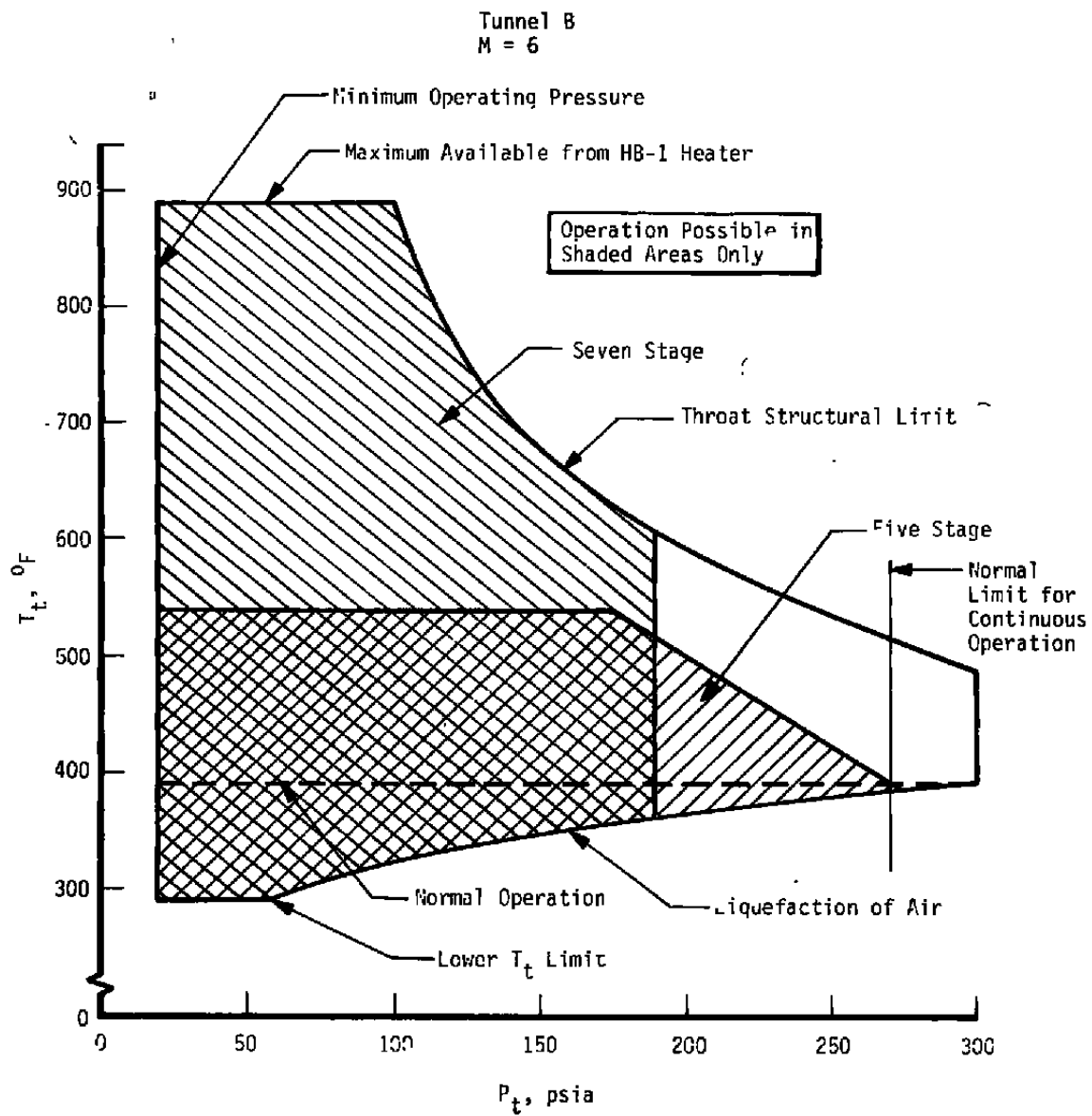


a. Normal operating envelope  
**Figure B-7. Stagnation conditions, Tunnel B — Mach 6.**



b. Open circuit for expanded envelope

Figure B-7. Continued.



c. Closed circuit for expanded envelope  
Figure B-7. Concluded.

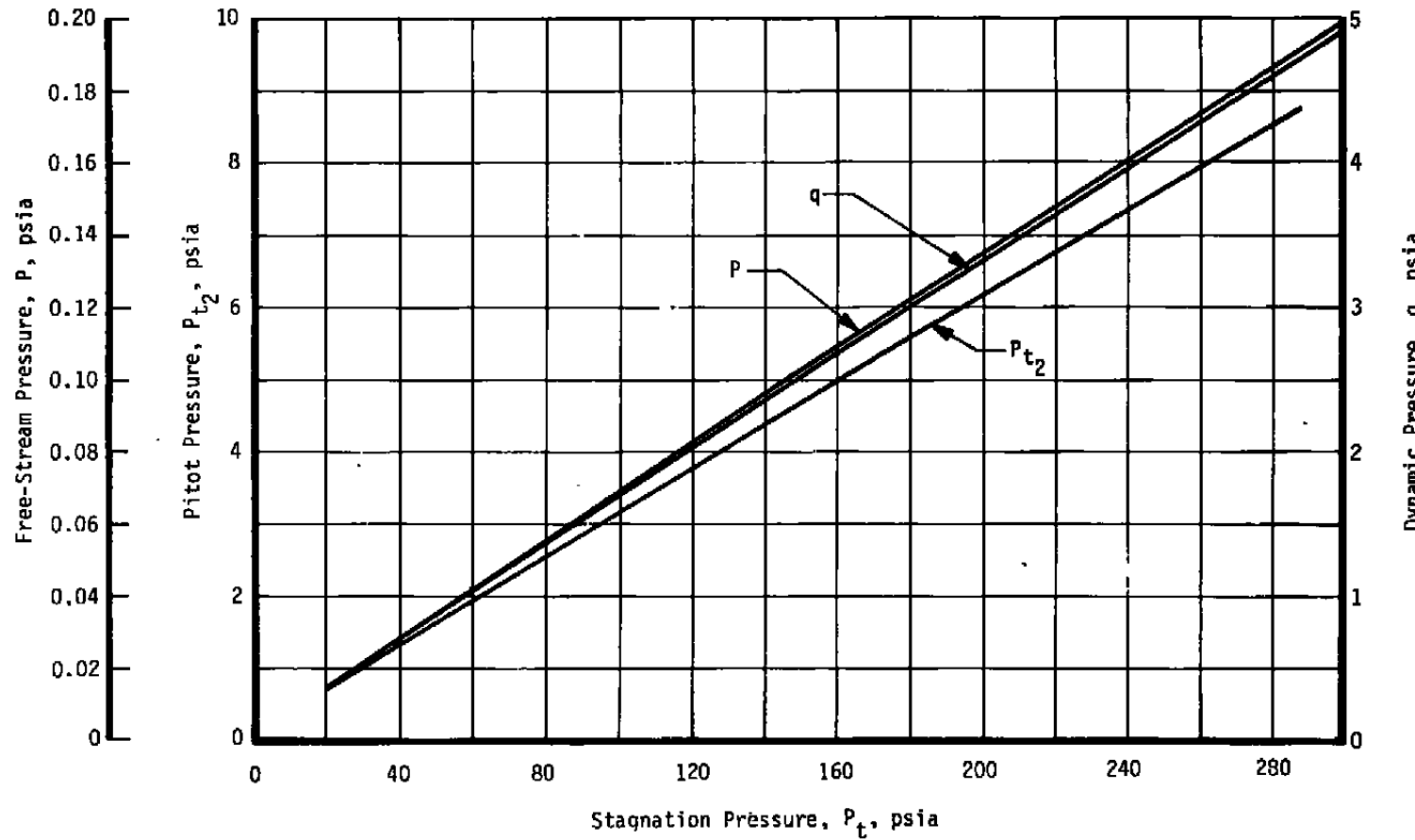


Figure B-8. Free-stream pitot, dynamic, and static pressure,  
Tunnel B — Mach 6.

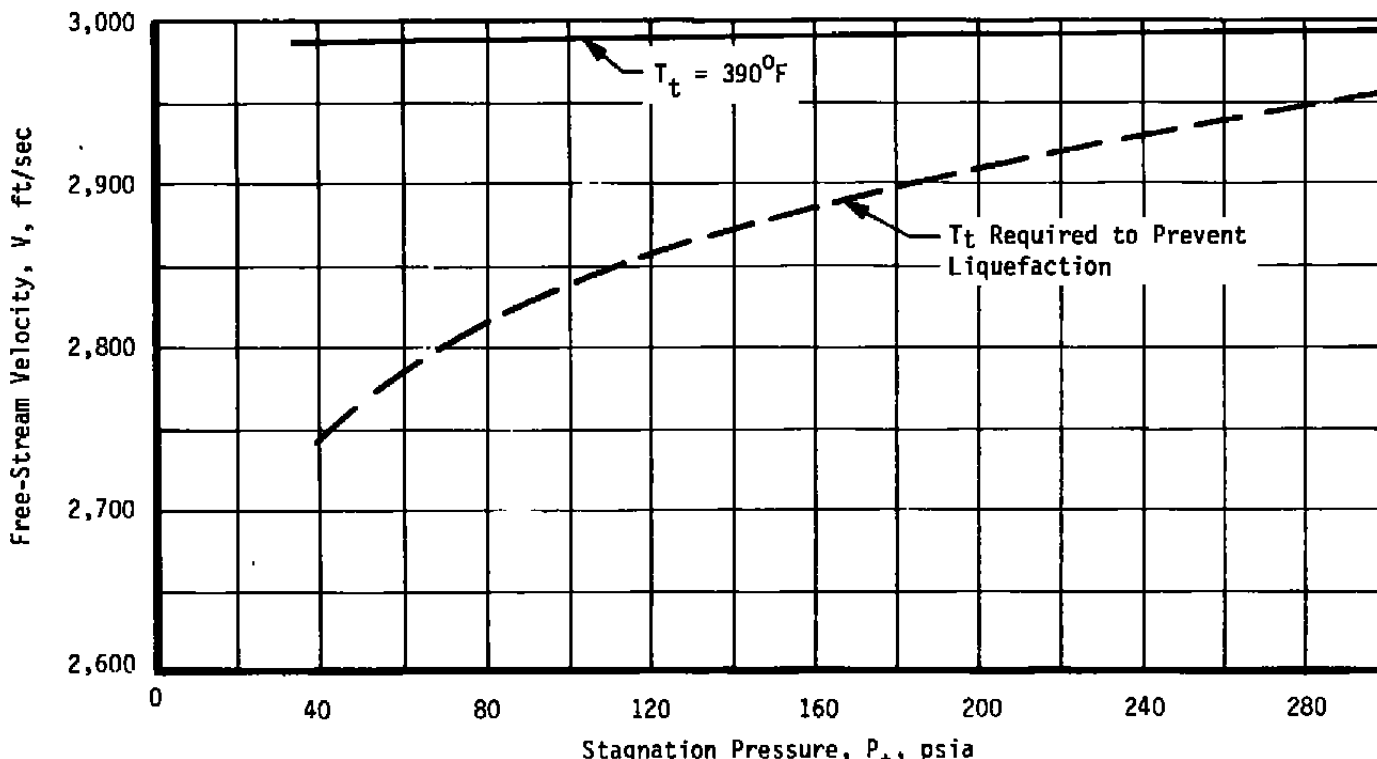


Figure B-9. Free-stream velocity, Tunnel B — Mach 6.

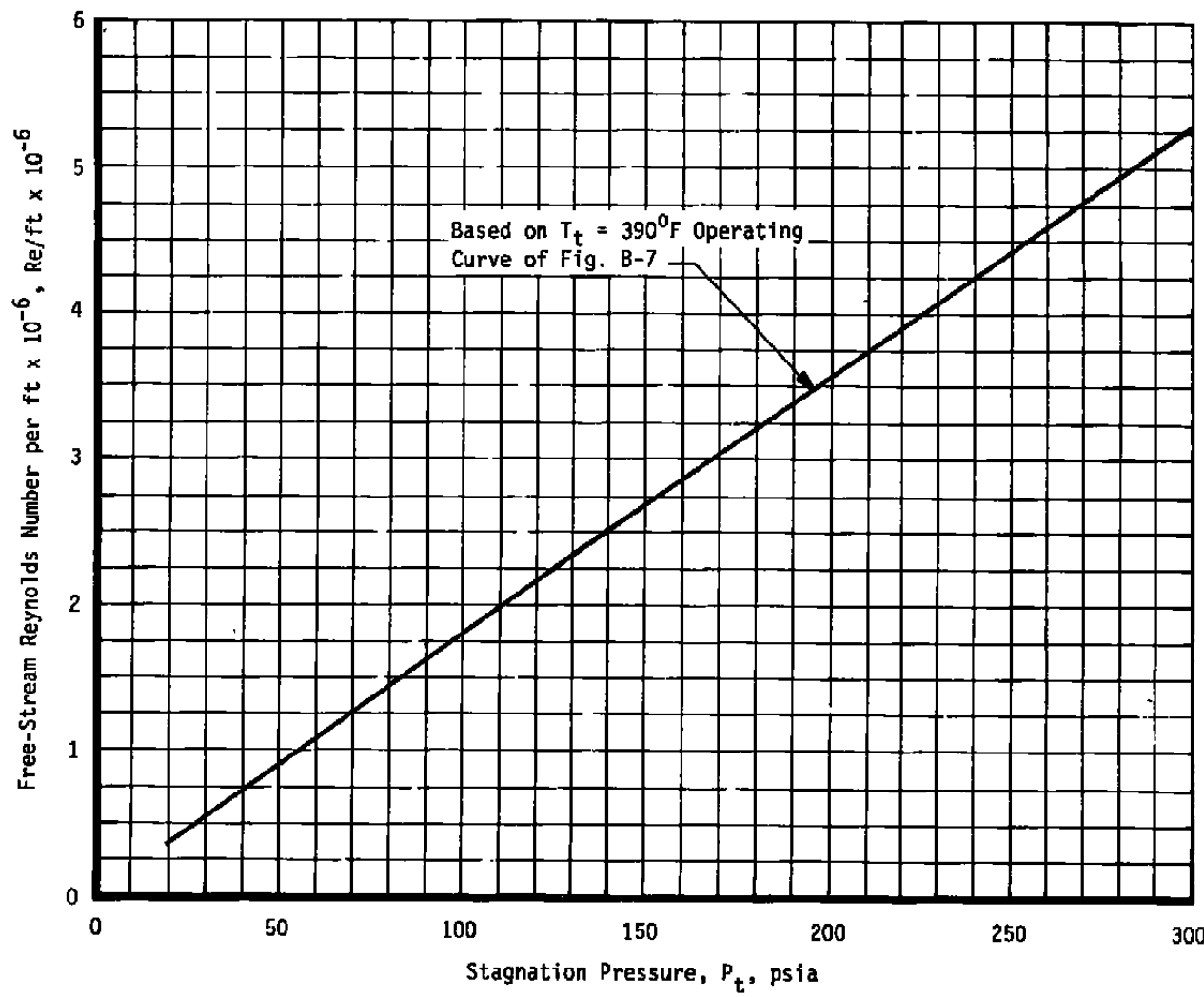


Figure B-10. Free-stream Reynolds number, Tunnel B — Mach 6.

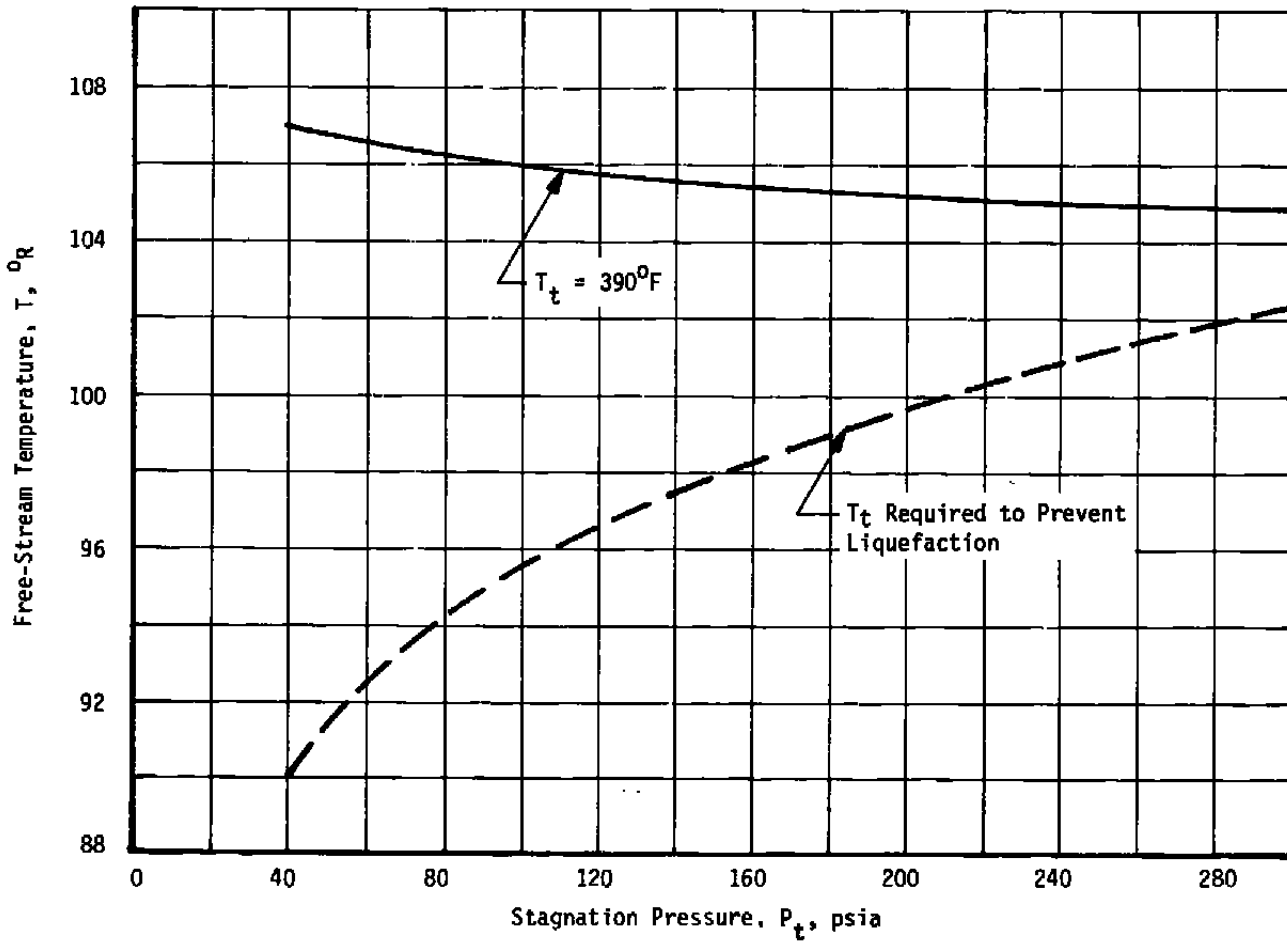


Figure B-11. Free-stream temperature, Tunnel B — Mach 6.

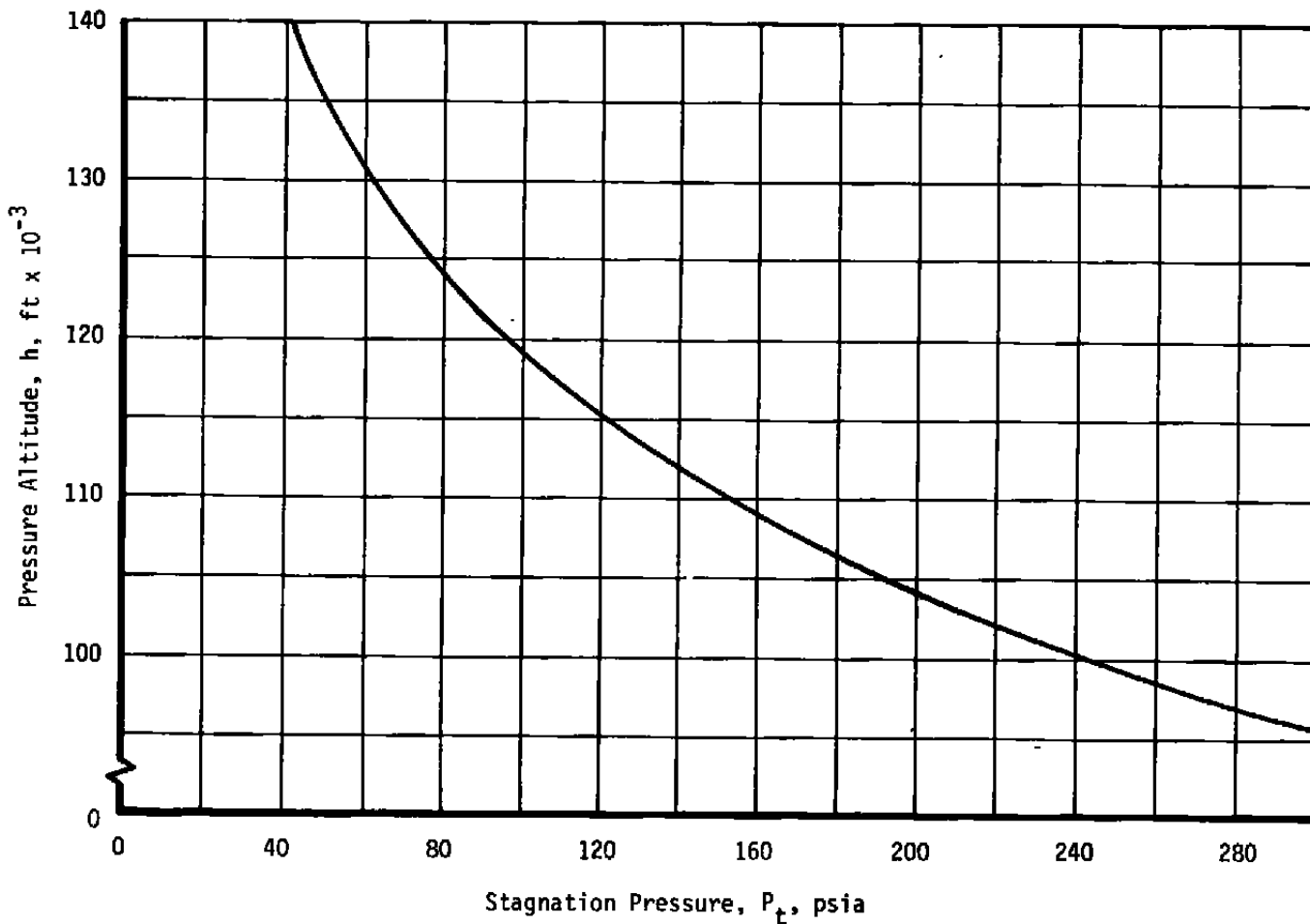


Figure B-12. Simulated altitude, Tunnel B — Mach 6.

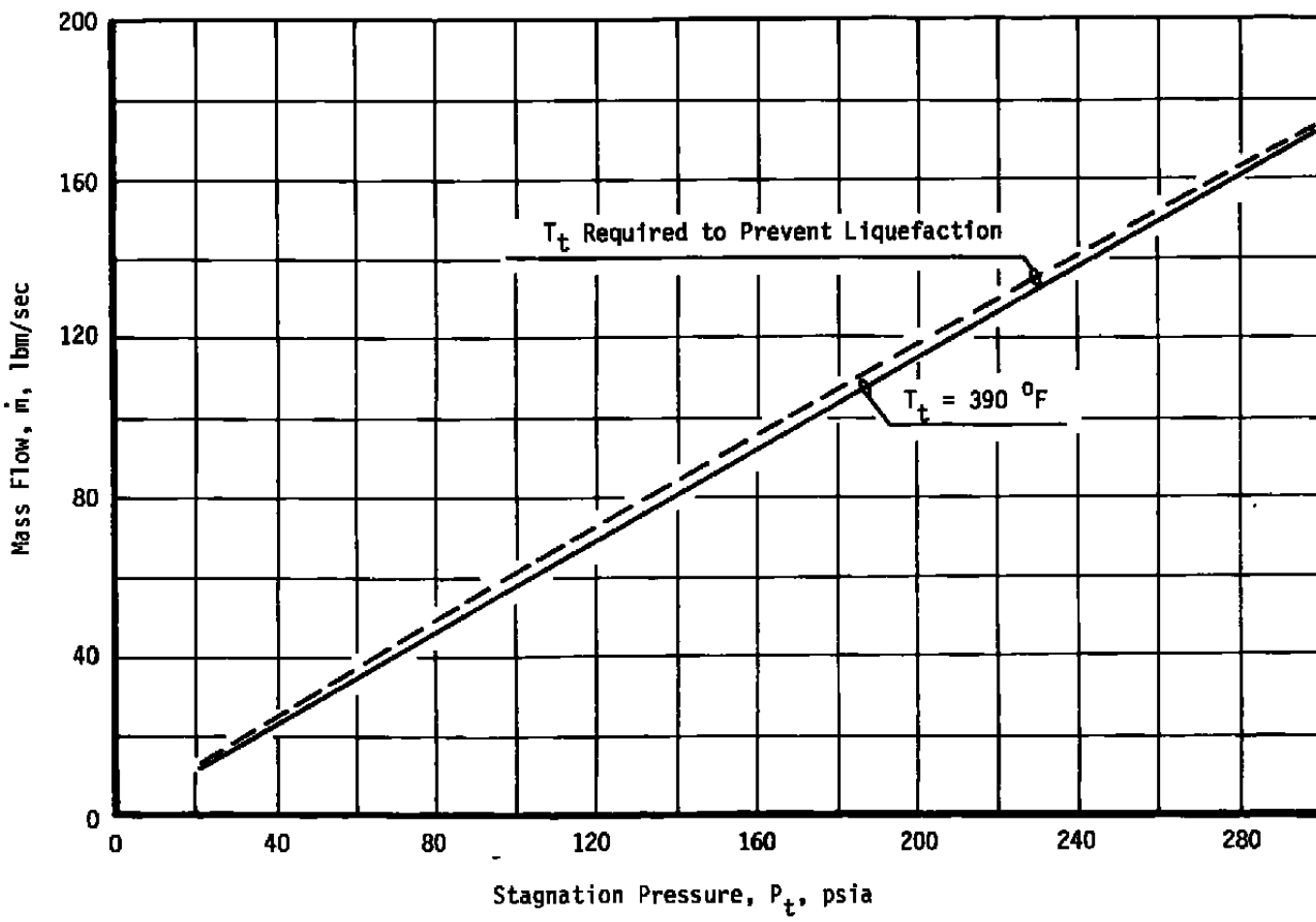
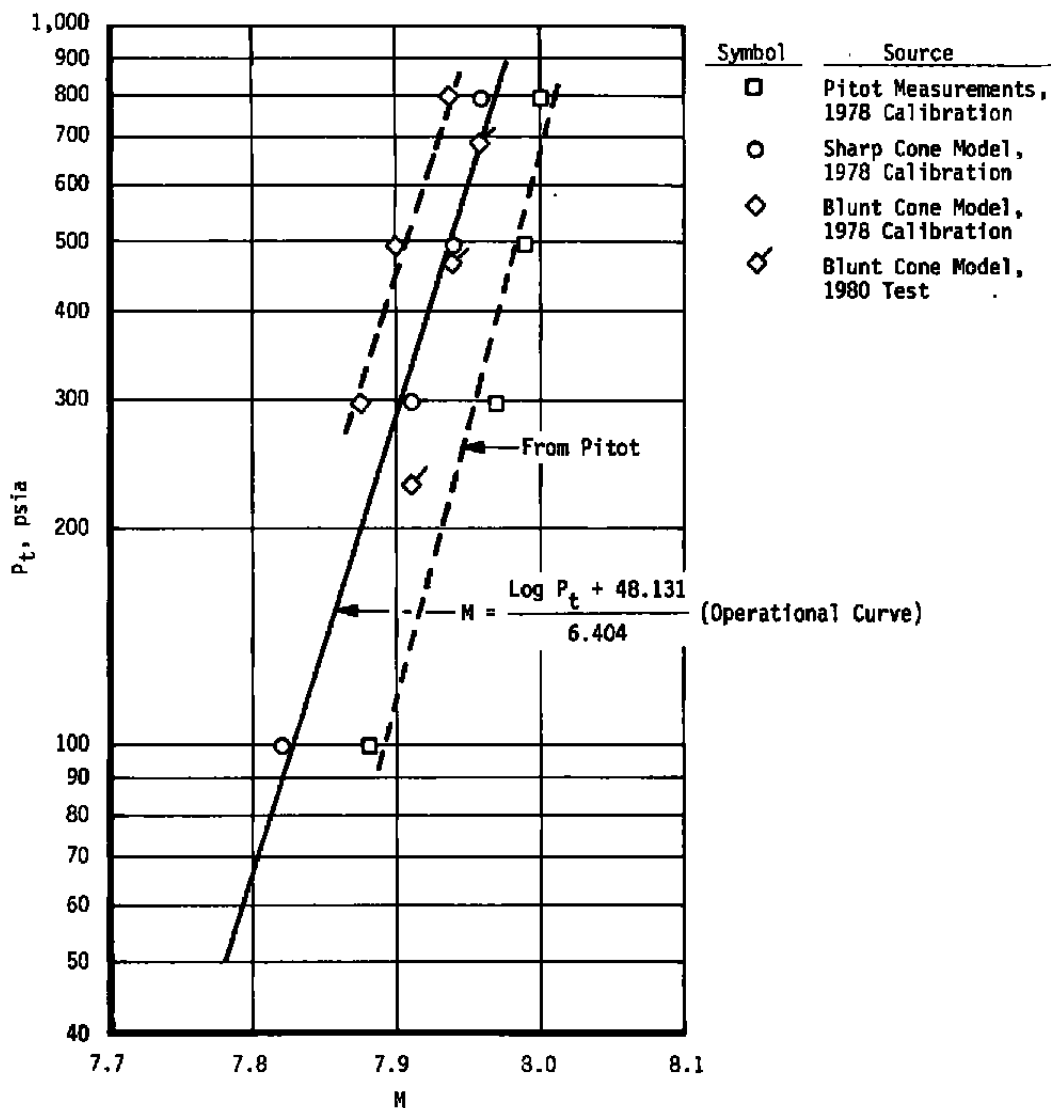
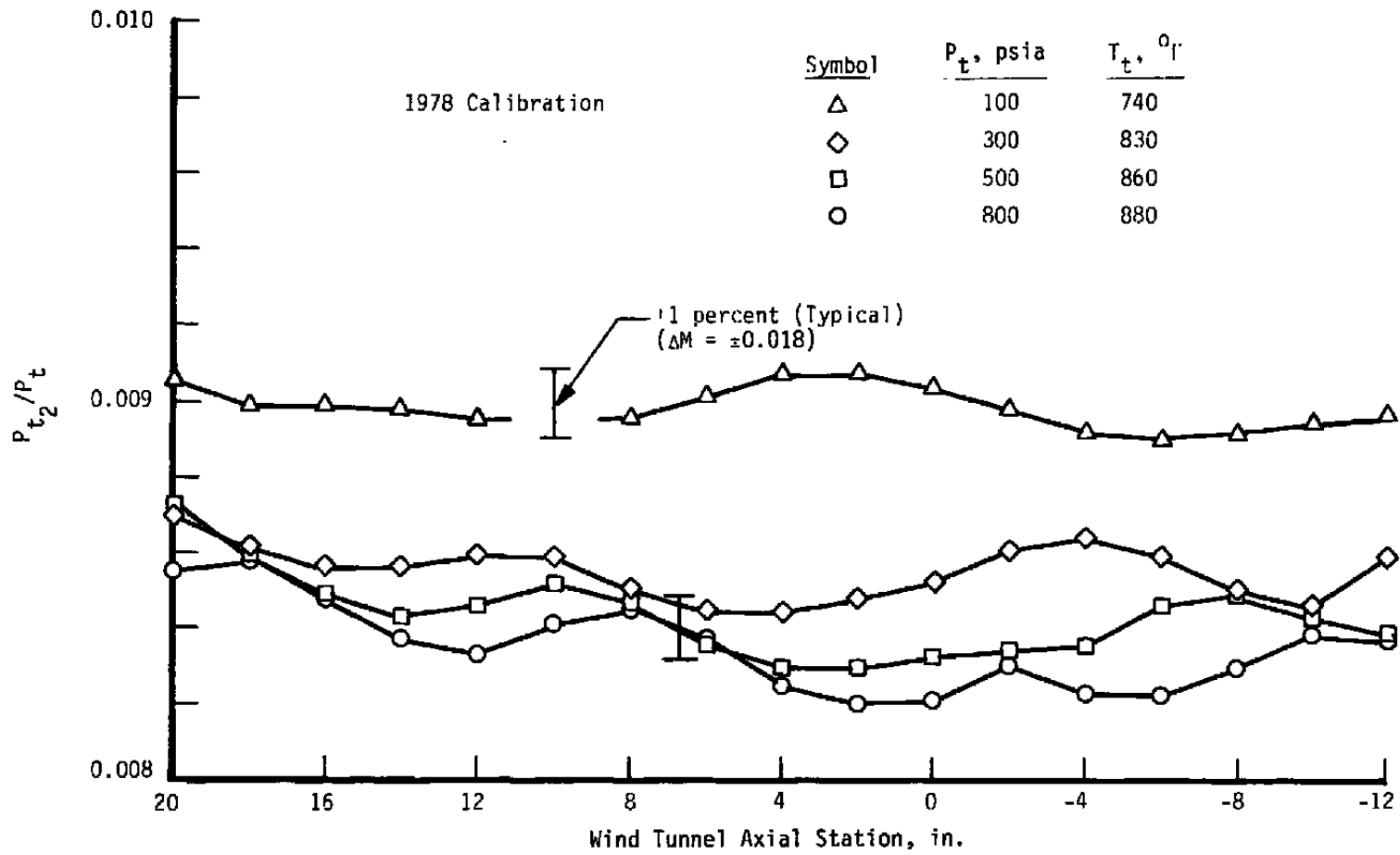


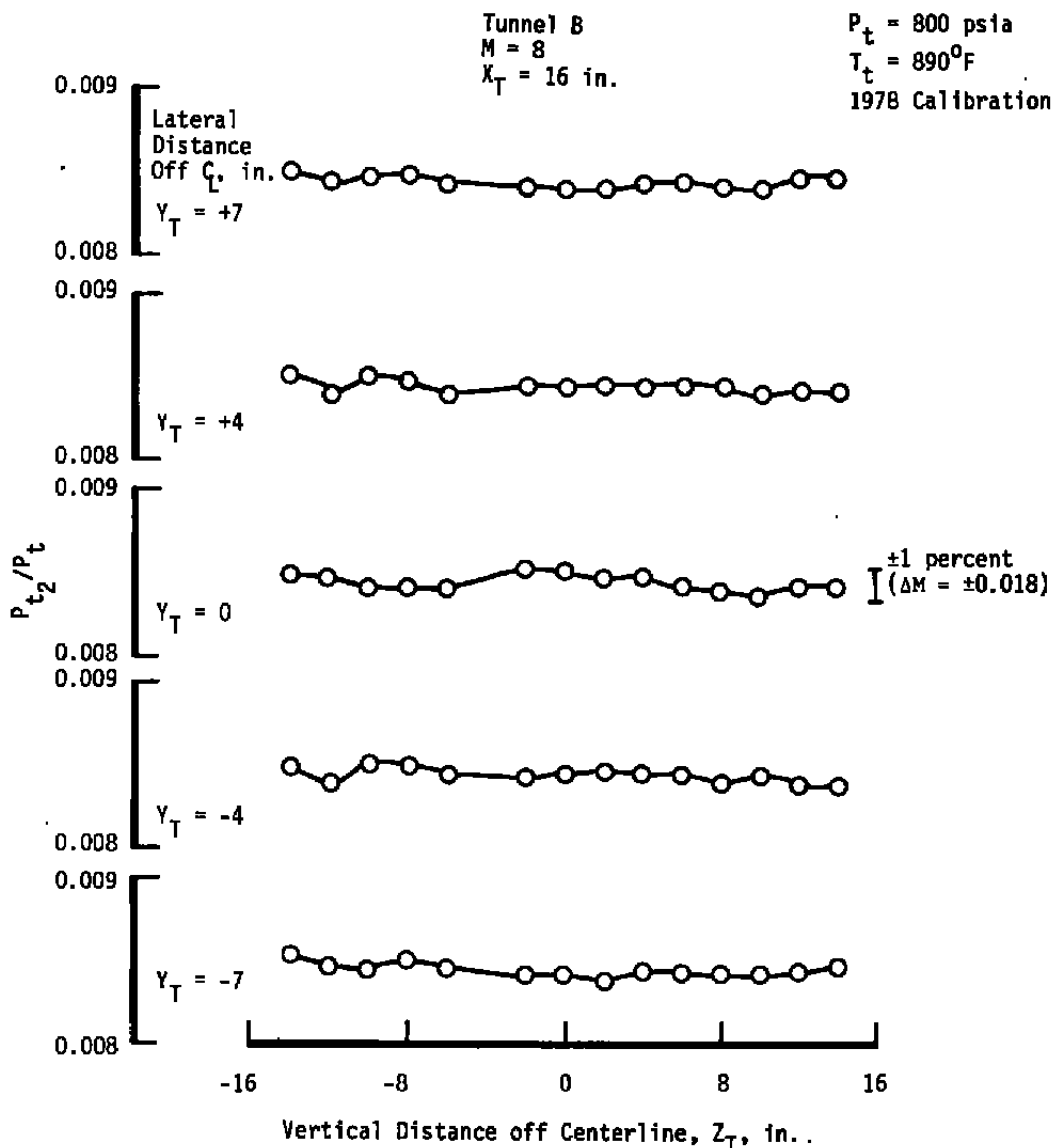
Figure B-13. Mass flow, Tunnel B — Mach 6.



**Figure B-14. Mach number, Tunnel B — Mach 8.**

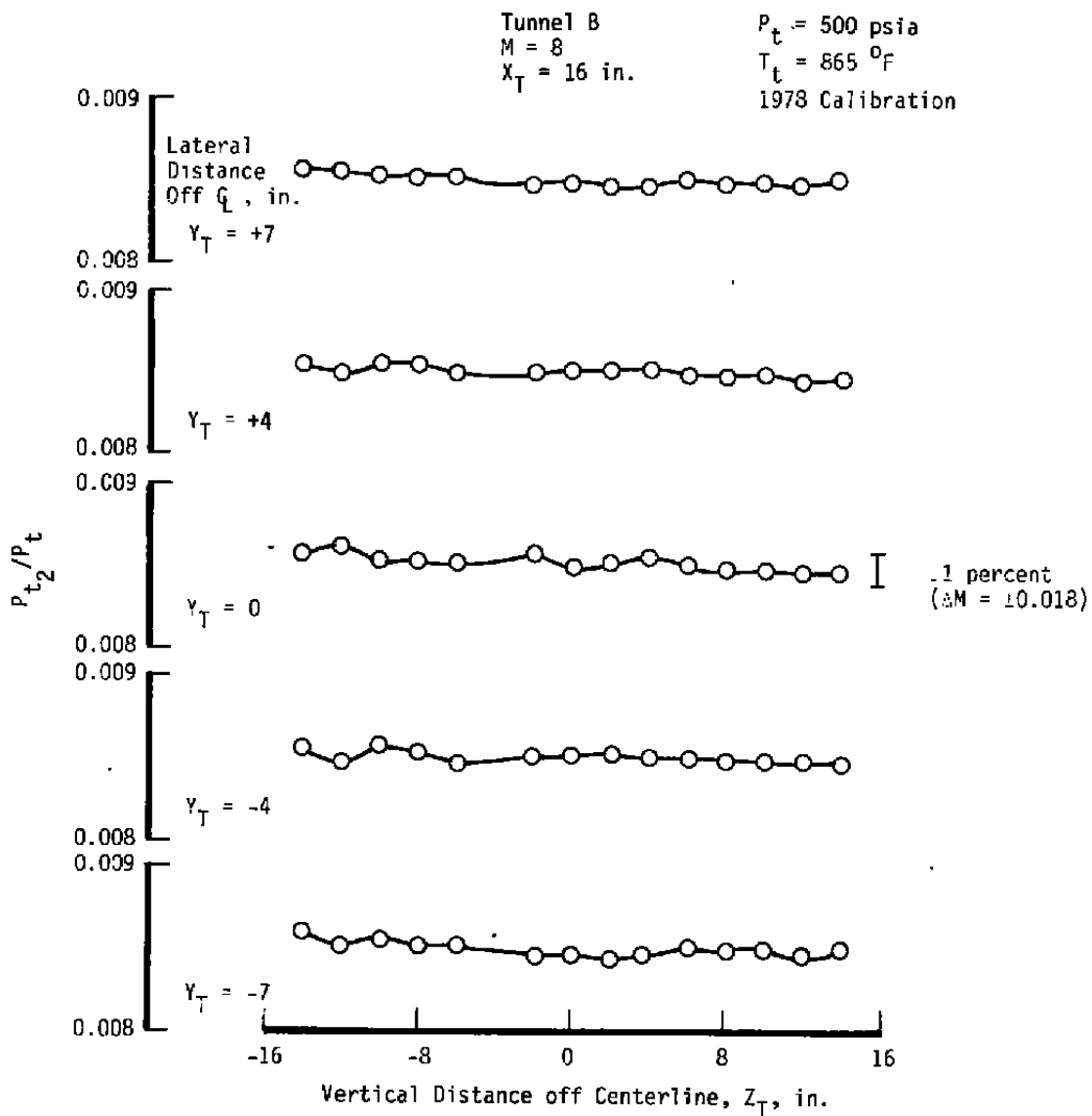


**Figure B-15. Axial centerline pitot pressure distributions,  
Tunnel B — Mach 8.**

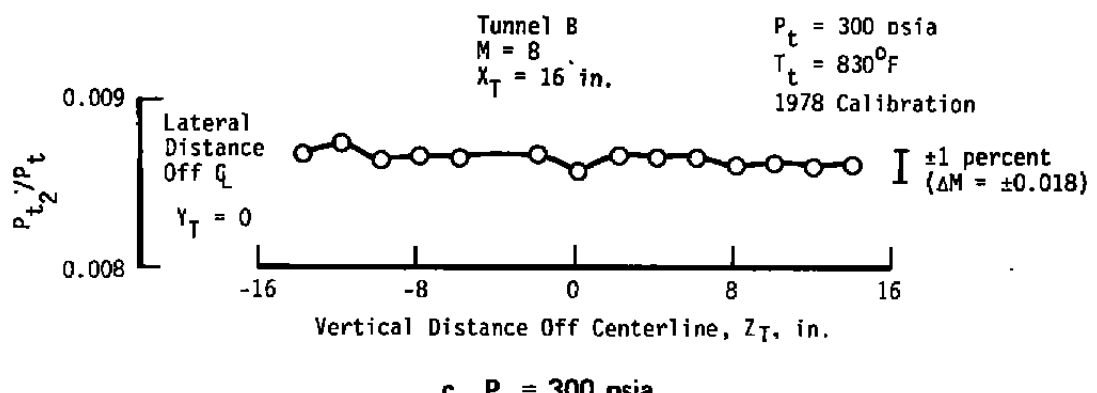


a.  $P_t = 800$  psia

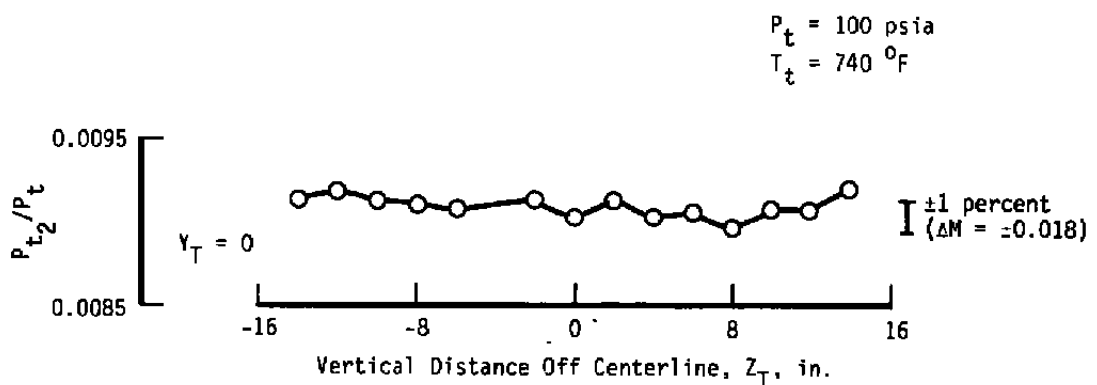
Figure B-16. Vertical pitot pressure profiles, Tunnel B — Mach 8.



b.  $P_t = 500 \text{ psia}$   
**Figure B-16. Continued.**



c.  $P_t = 300$  psia



d.  $P_t = 100$  psia  
Figure B-16. Concluded.

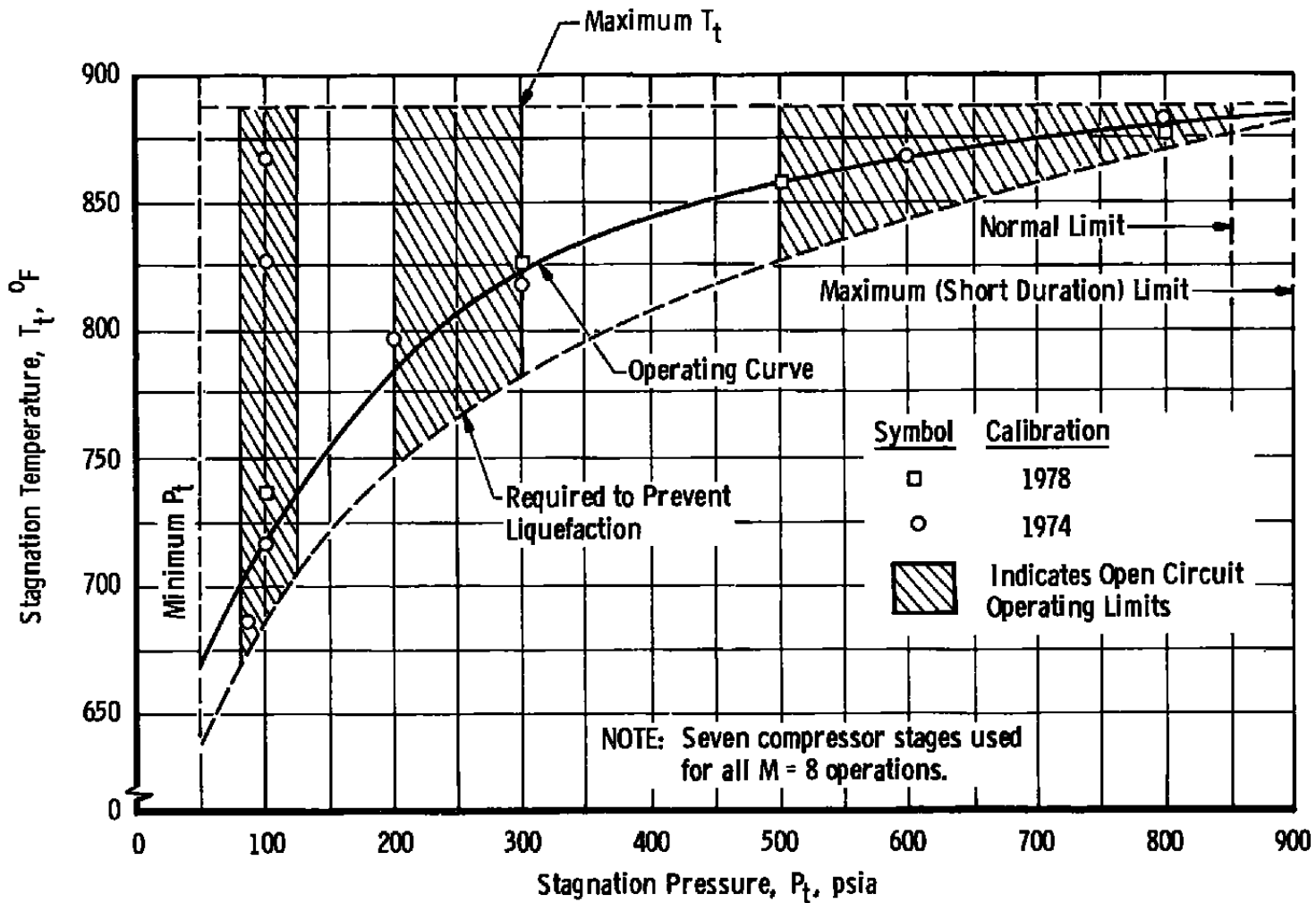


Figure B-17. Stagnation conditions, Tunnel B — Mach 8.

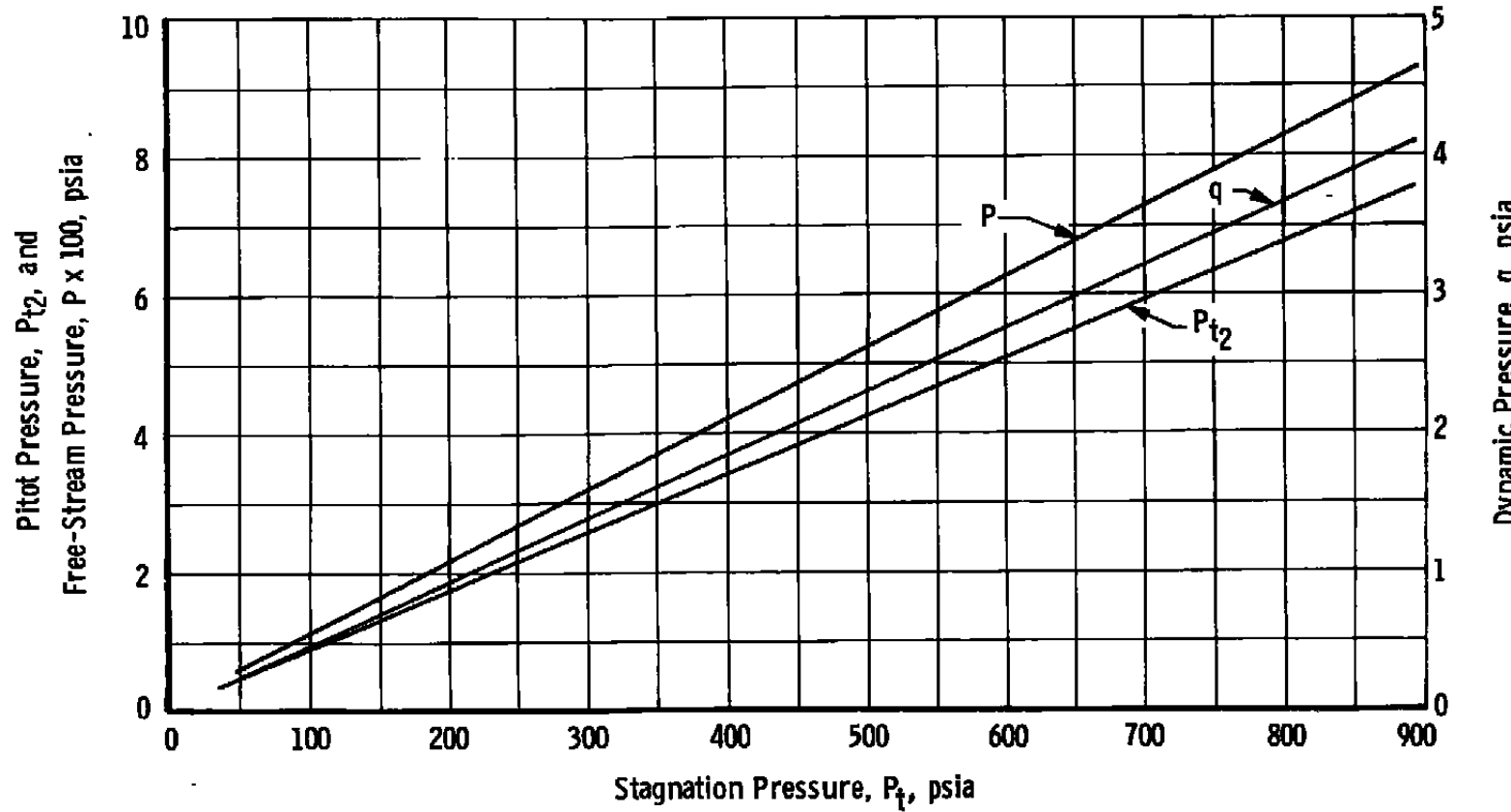


Figure B-18. Free-stream pitot, dynamic, and static pressure,  
Tunnel B — Mach 8.

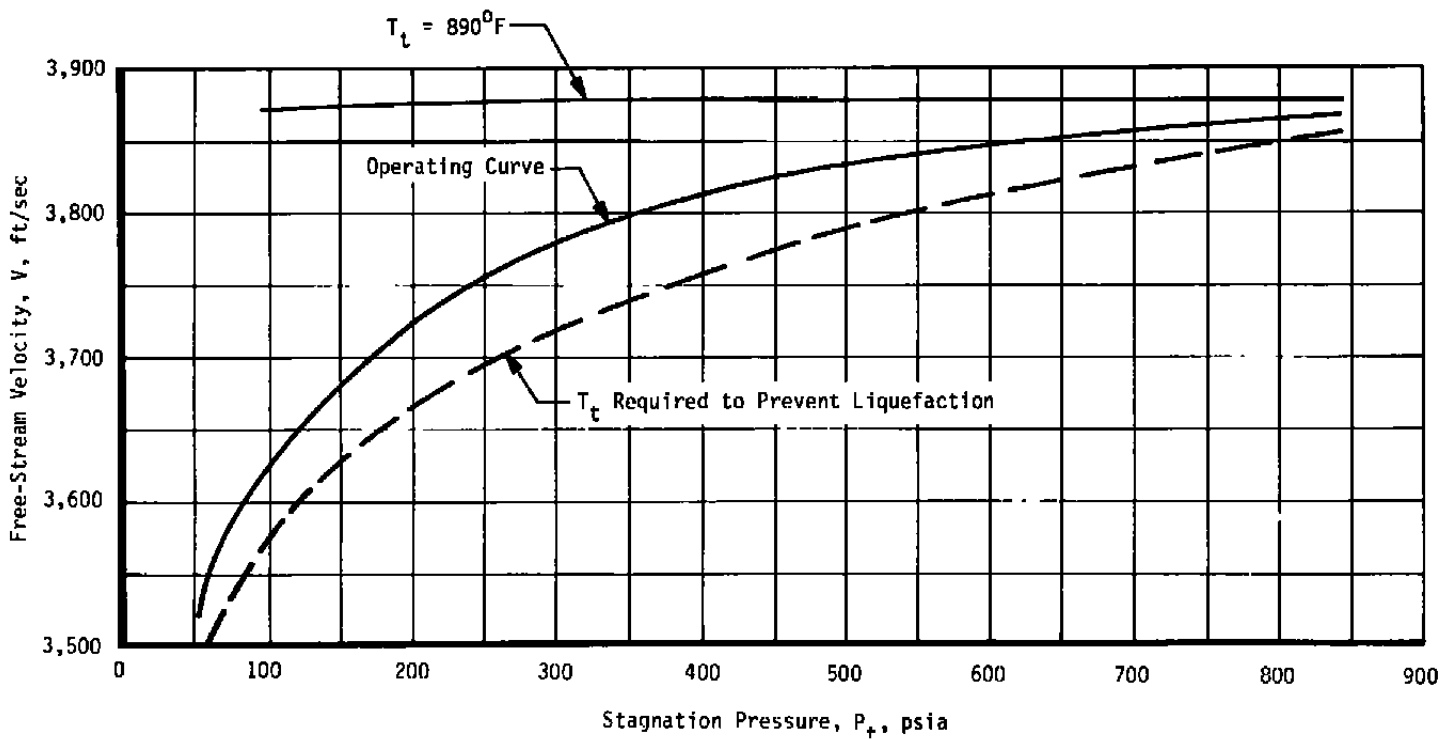


Figure B-19. Free-stream velocity, Tunnel B — Mach 8.

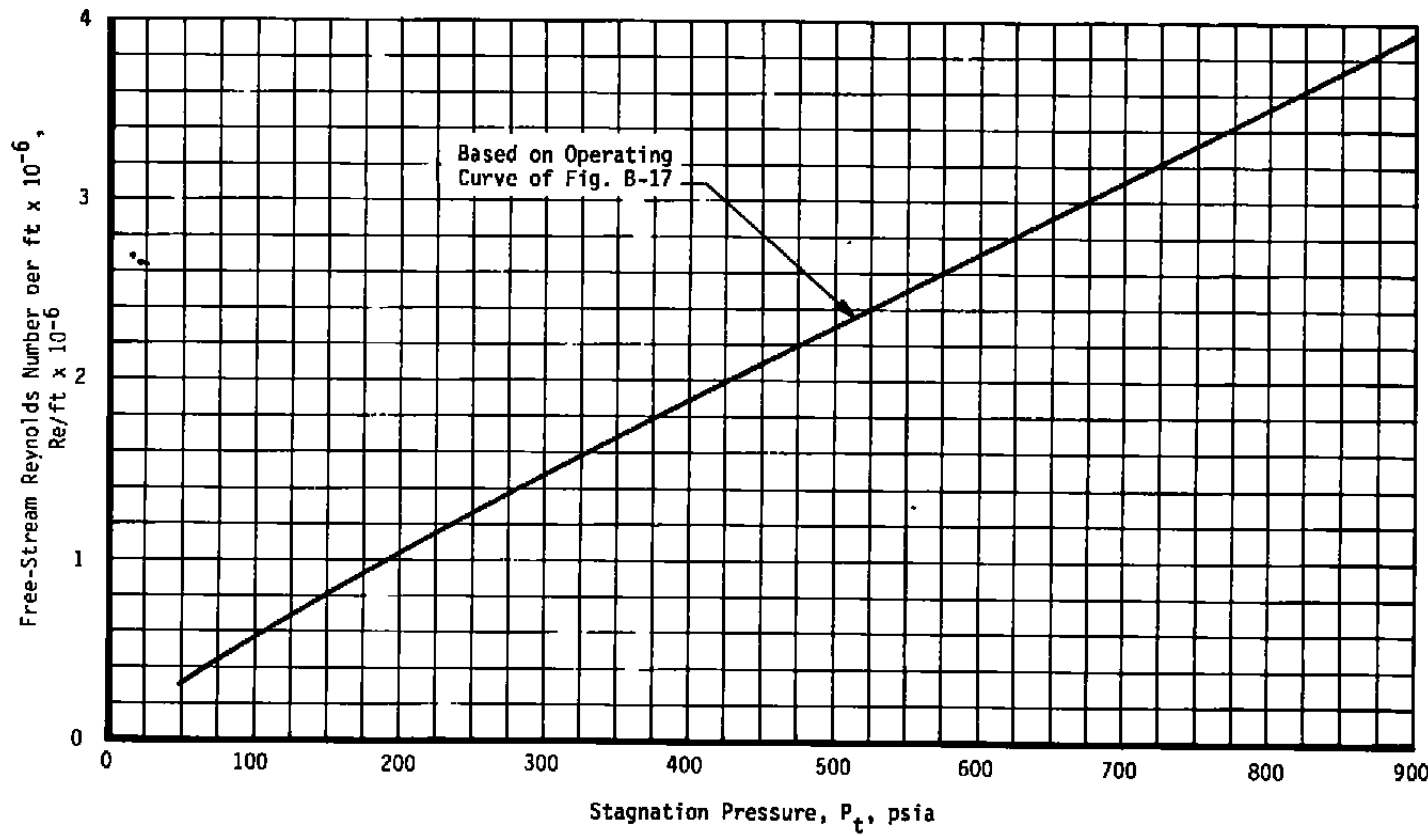


Figure B-20. Free-stream Reynolds number, Tunnel B – Mach 8.

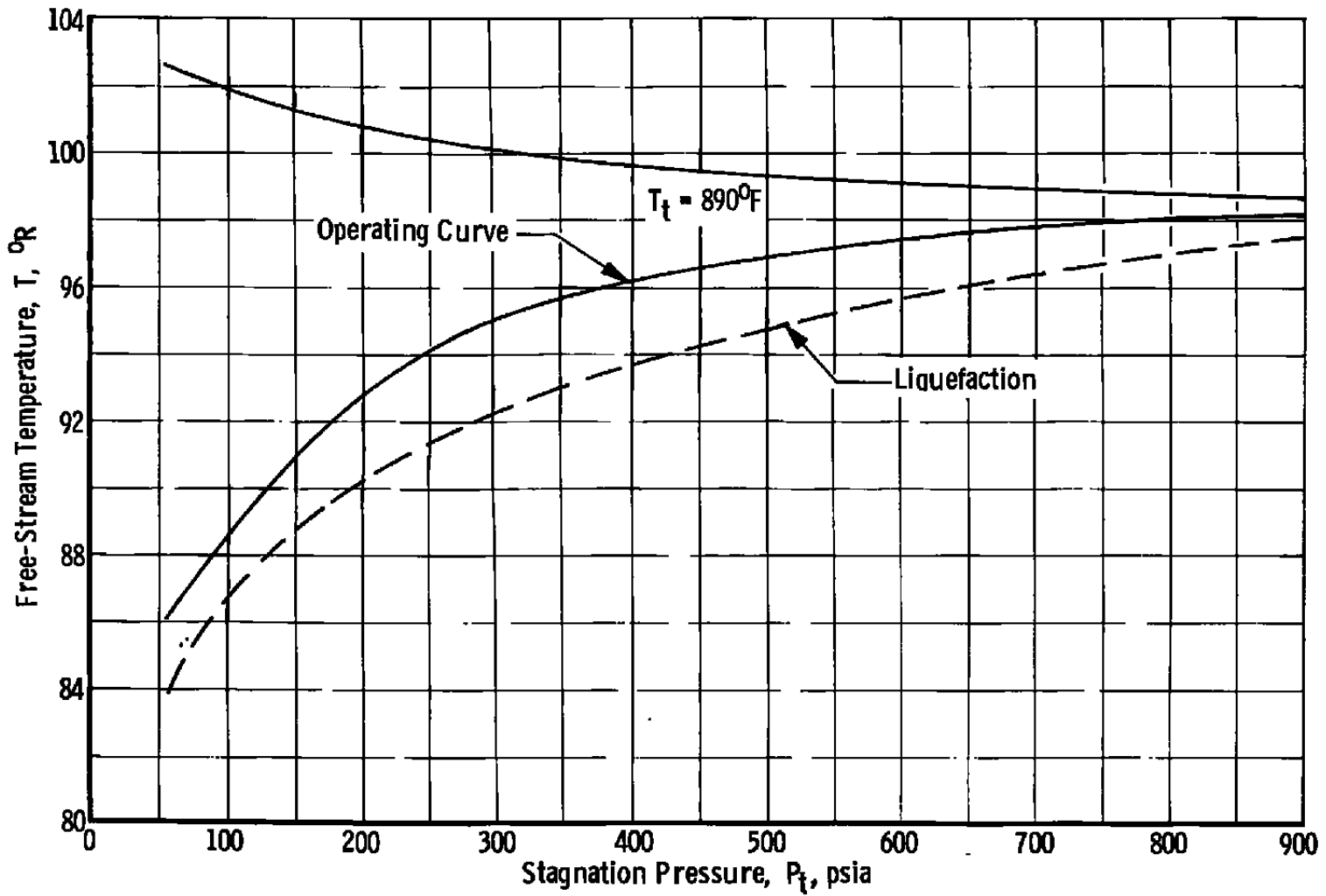


Figure B-21. Free-stream temperature, Tunnel B — Mach 8.

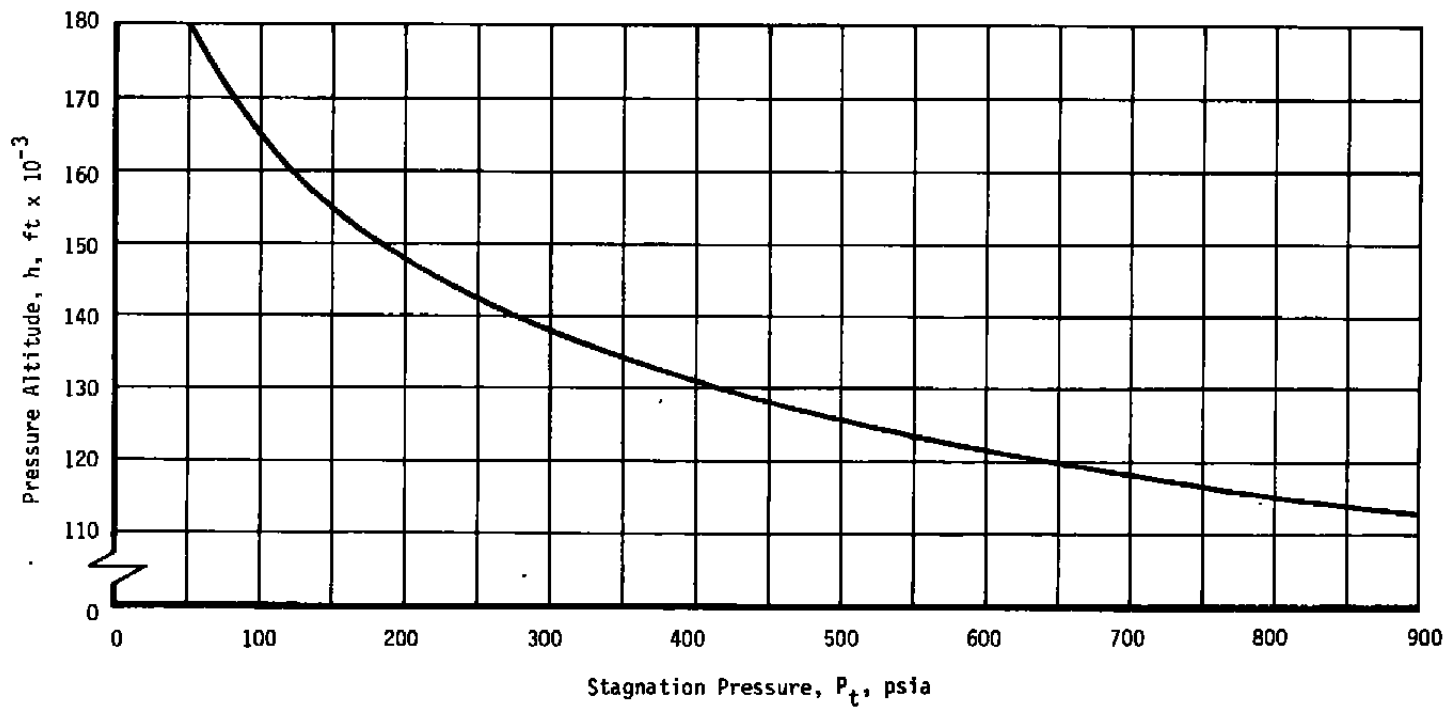


Figure B-22. Simulated altitude, Tunnel B — Mach 8.

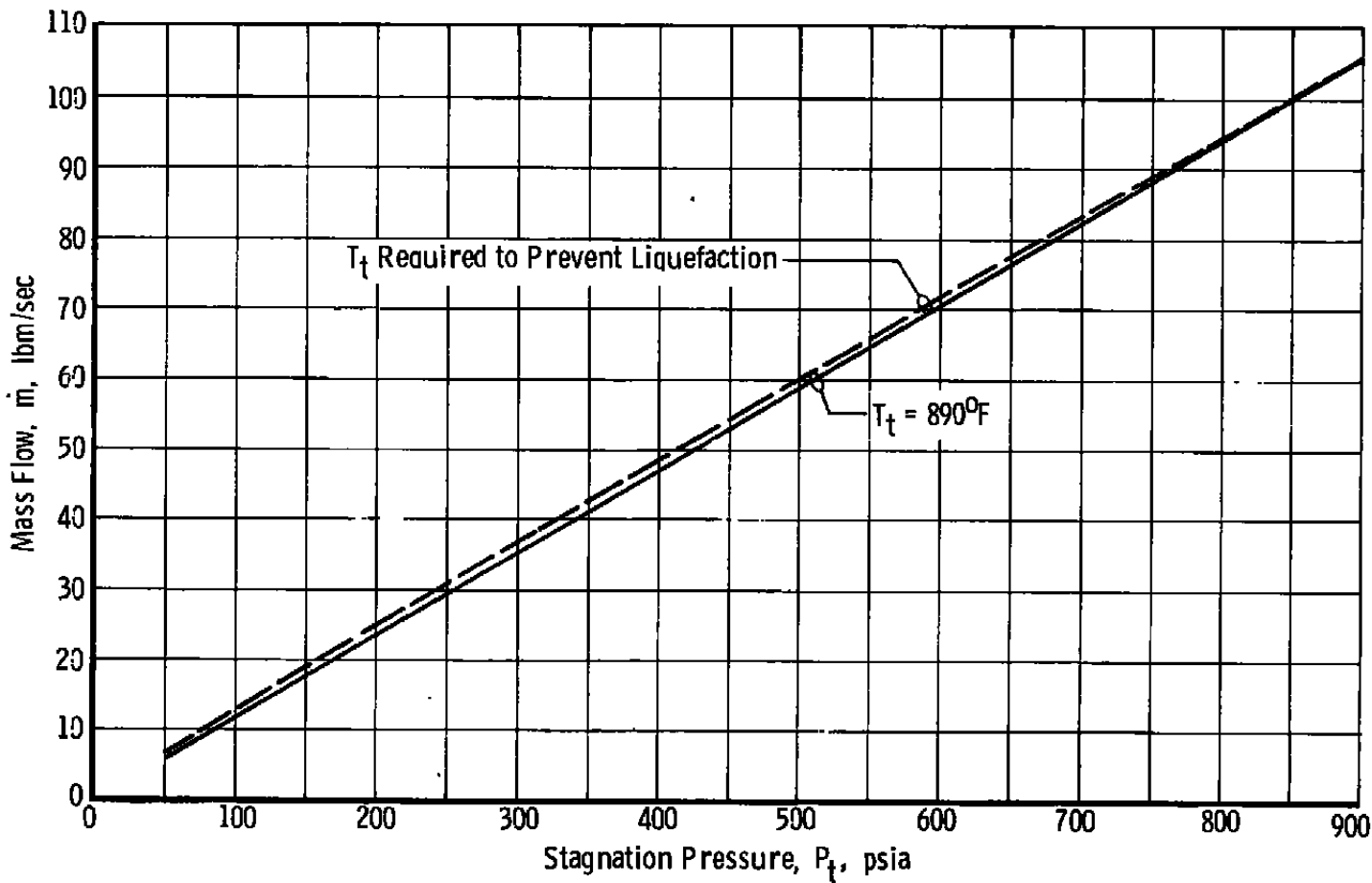


Figure B-23. Mass flow, Tunnel B — Mach 8.

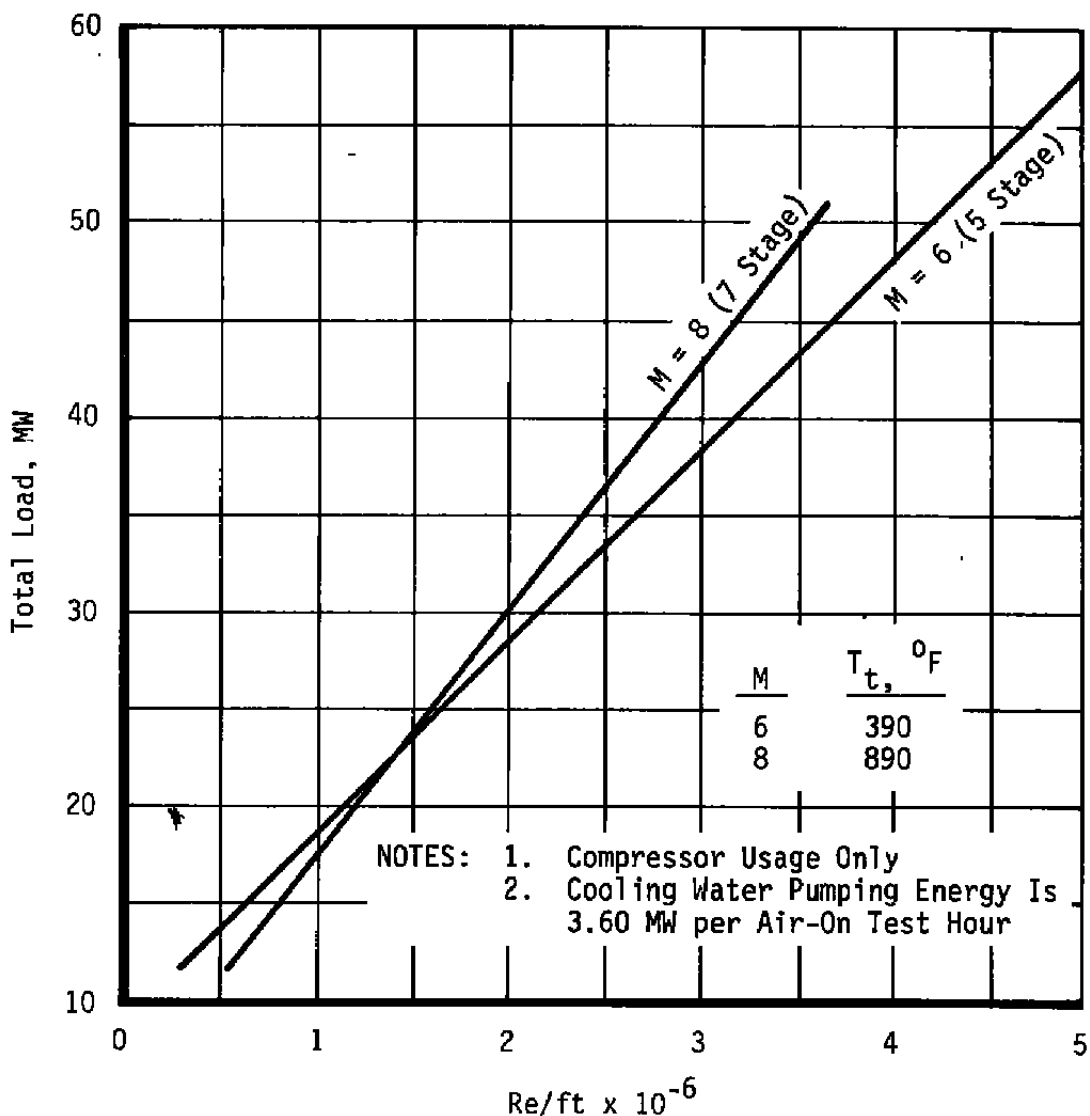


Figure B-24. Electrical usage for Tunnel B.

**Table B-1. Tunnel B Operational Time Considerations**

Operation	Time Increments, min. (Unless Noted)	Notes
Tunnel Start	45	
Stagnation Pressure Changes	15	90 percent of Range
Change Mach Number		
Mach No. 6 to 8	24 hr {	
Mach No. 8 to 6	24 hr }	8 hr Actual Work
Change Reynolds Number	15	
Cool Model	5 to 10	
Model Change*	5	
Tunnel Shutdown**	25	

\* Time increment for actual operation on model must also be added.

\*\* Last operational shift of the week requires an additional 20 min.

**Table B-2. Tunnel B Standard Test Condition Tolerances**

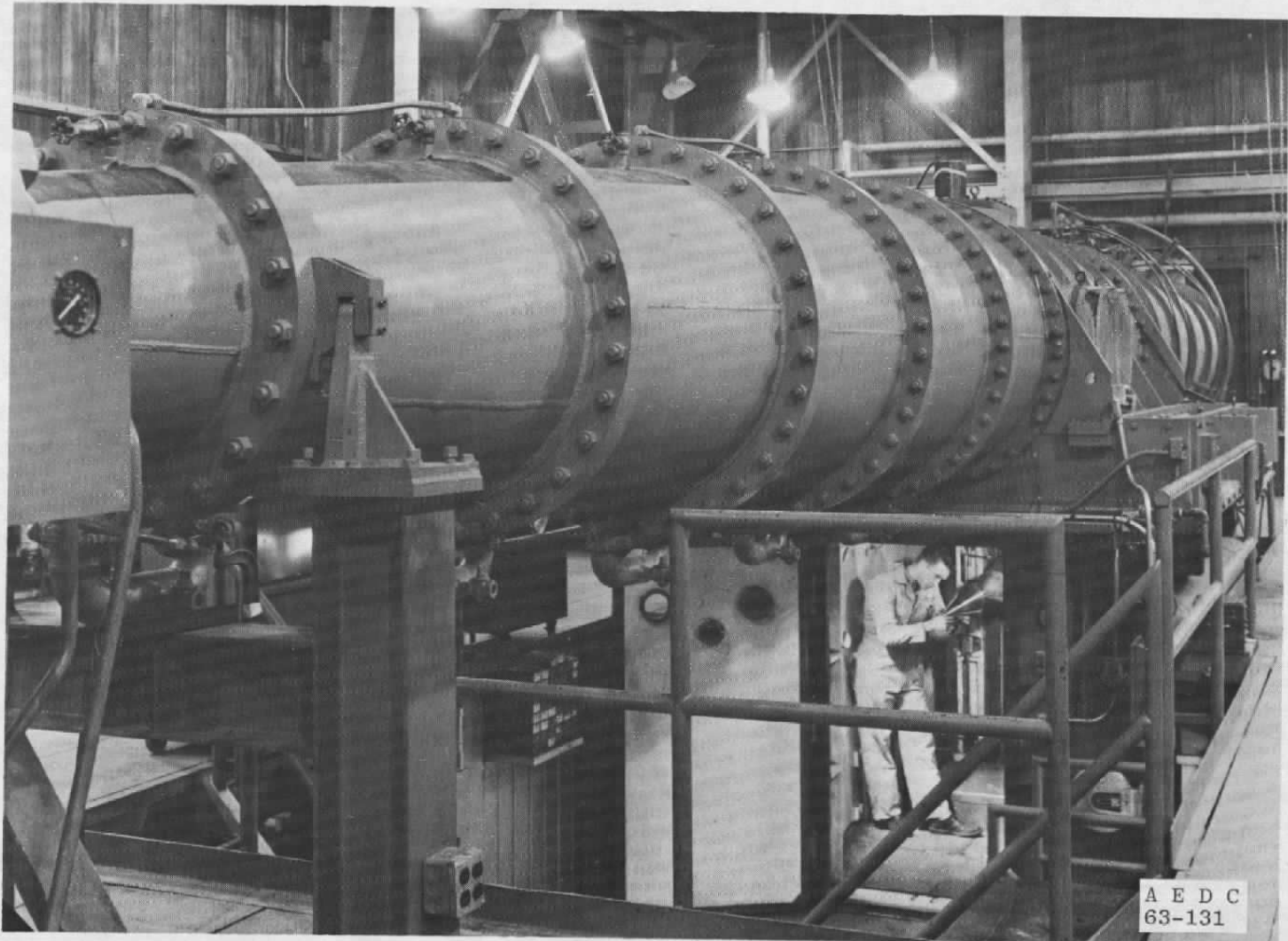
Operational procedures for VKF wind tunnels emphasize efficiency. As a part of this effort, standard tolerances are set that allow the tunnel operator some latitude in setting test conditions.<sup>1</sup> Thus, the following tolerances on stilling chamber pressure and temperature and limits on humidity are recommended.

Mach No.	$P_t$ , psia	$\pm \Delta P_t$ , psia	$T_t$ , °F	$\pm \Delta T_t$ , °F	$T_{DP}^2$ , °F
6	20 to 29	0.2	390	4.0	-10
	30 to 39	0.3			
	40 to 49	0.4			
	50 to 59	0.5			
	60 to 69	0.6			
	70 to 79	0.7			
	80 to 89	0.8			
	90 to 99	0.9			
	100 to 149	1.0			
	150 to 199	1.5			
	200 to 249	2.0			
	250 to 300	2.5			
8	50 to 99	0.5	690	8.0	-18
	100 to 149	1.0			
	150 to 199	1.5			
	200 to 249	2.0			
	250 to 299	2.5			
	300 to 349	3.0			
	350 to 399	3.5			
	400 to 449	4.0			
	450 to 499	4.5			
	500 to 549	5.0			
	550 to 599	5.5			
	600 to 649	6.0			
	650 to 699	6.5			
	700 to 799	7.0			
	800 to 900	8.0			

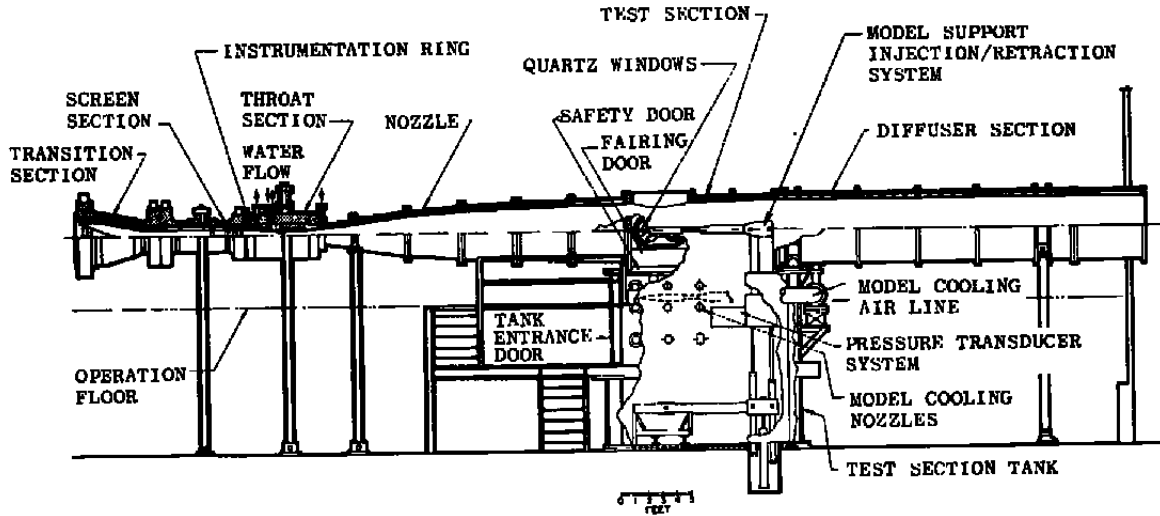
<sup>1</sup> Tolerances are based on Reynolds number set to within  $\pm 1.5$  percent of requested value.

<sup>2</sup> The  $T_{DP}$  values listed are ideal limits. Operation above these values is possible; however, the type of test and test objectives must be considered.

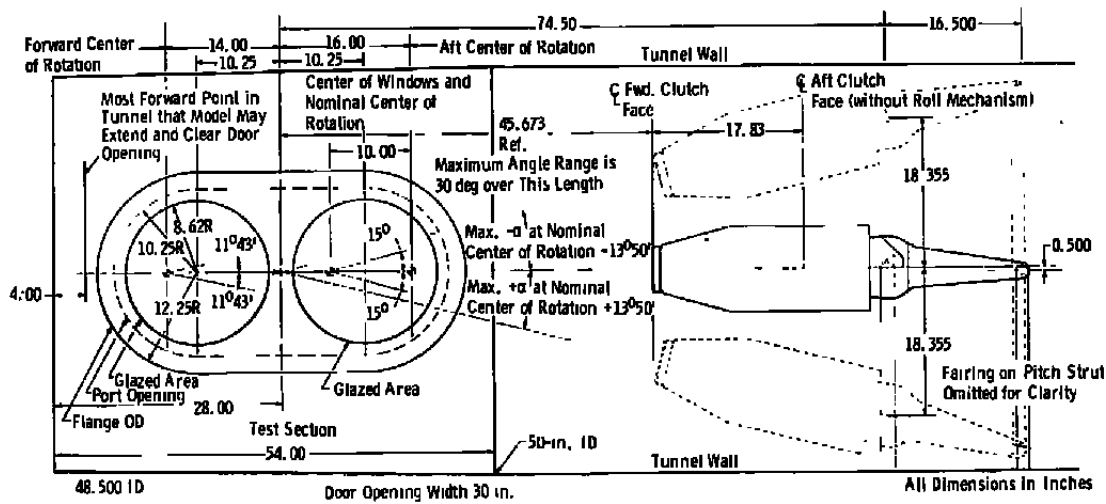
**APPENDIX C  
TUNNEL C**



a. Tunnel C  
Figure C-1. Tunnel C.

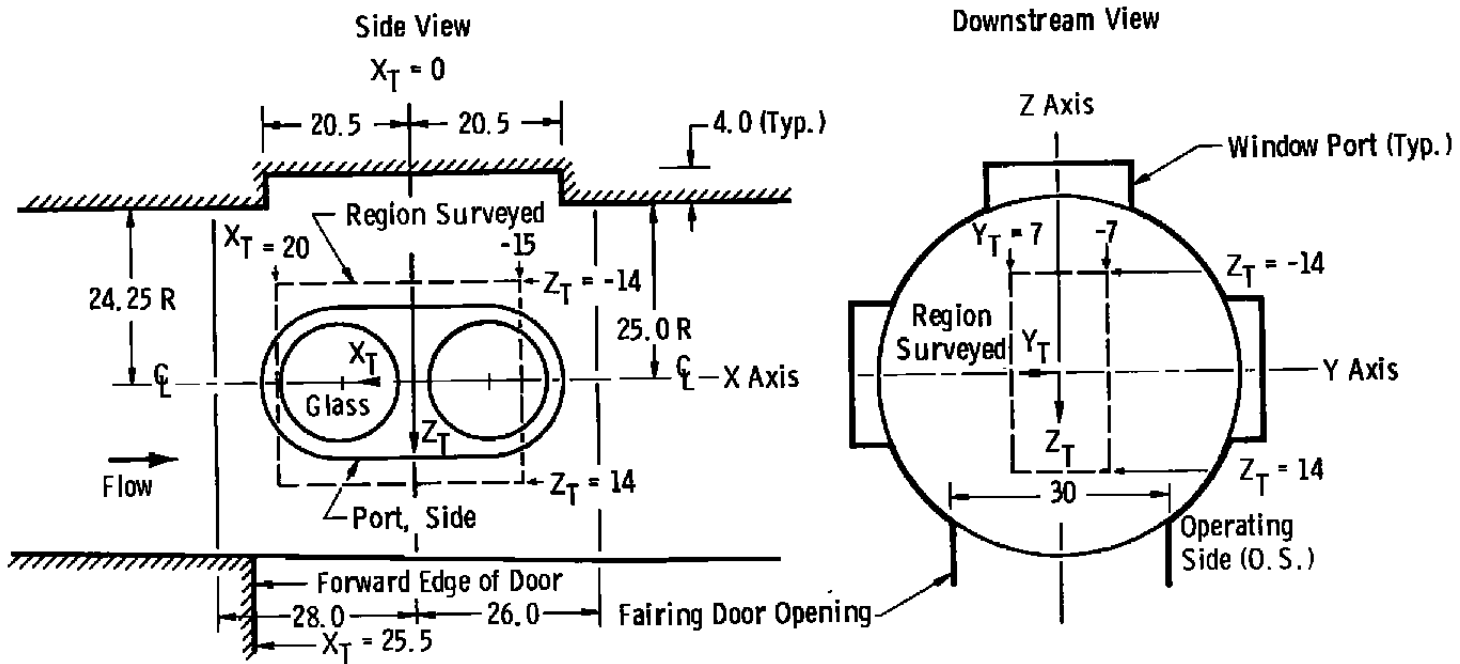


b. Tunnel C assembly  
Figure C-1. Continued.

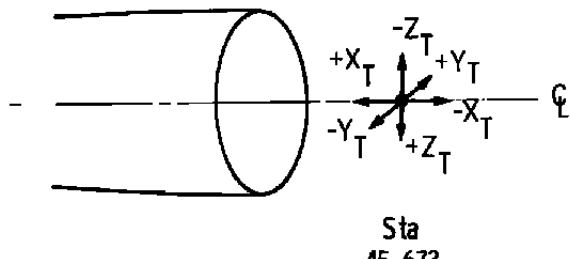


c. Test section (elevation), Tunnel C

Figure C-1. Concluded.

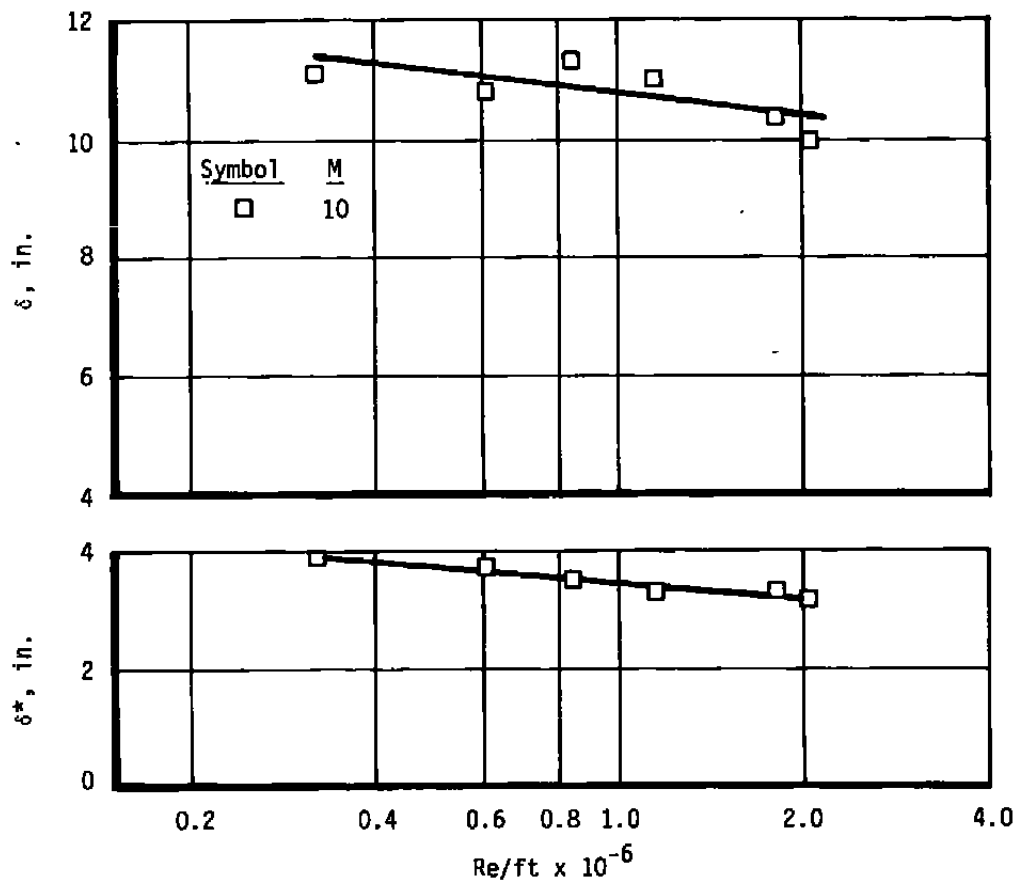


All Dimensions in Inches



a. Surveyed area

Figure C-2. Test section of Tunnel C.



b. Tunnel C boundary-layer and displacement thickness  
Figure C-2. Concluded.

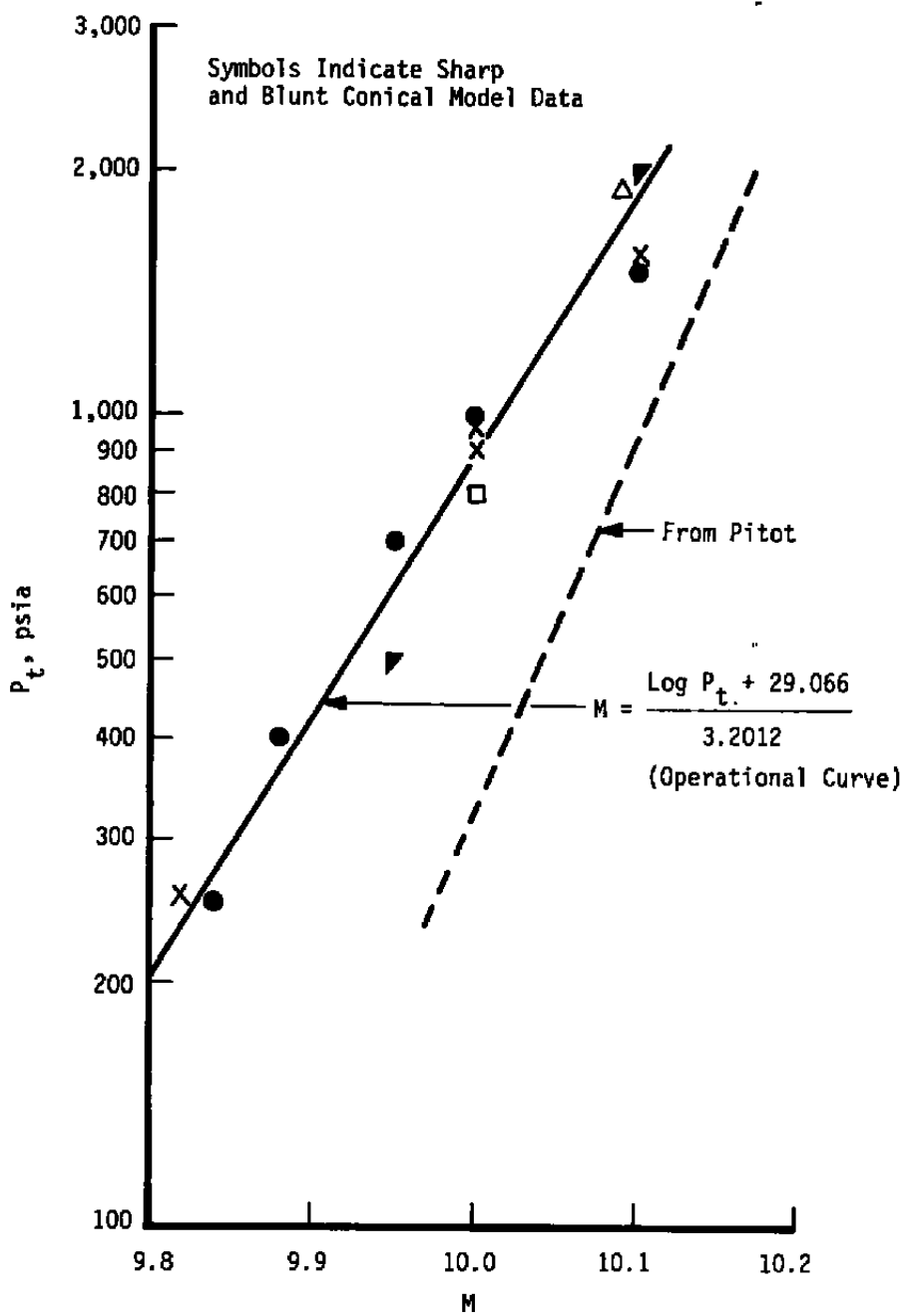


Figure C-3. Tunnel C, Mach 10.

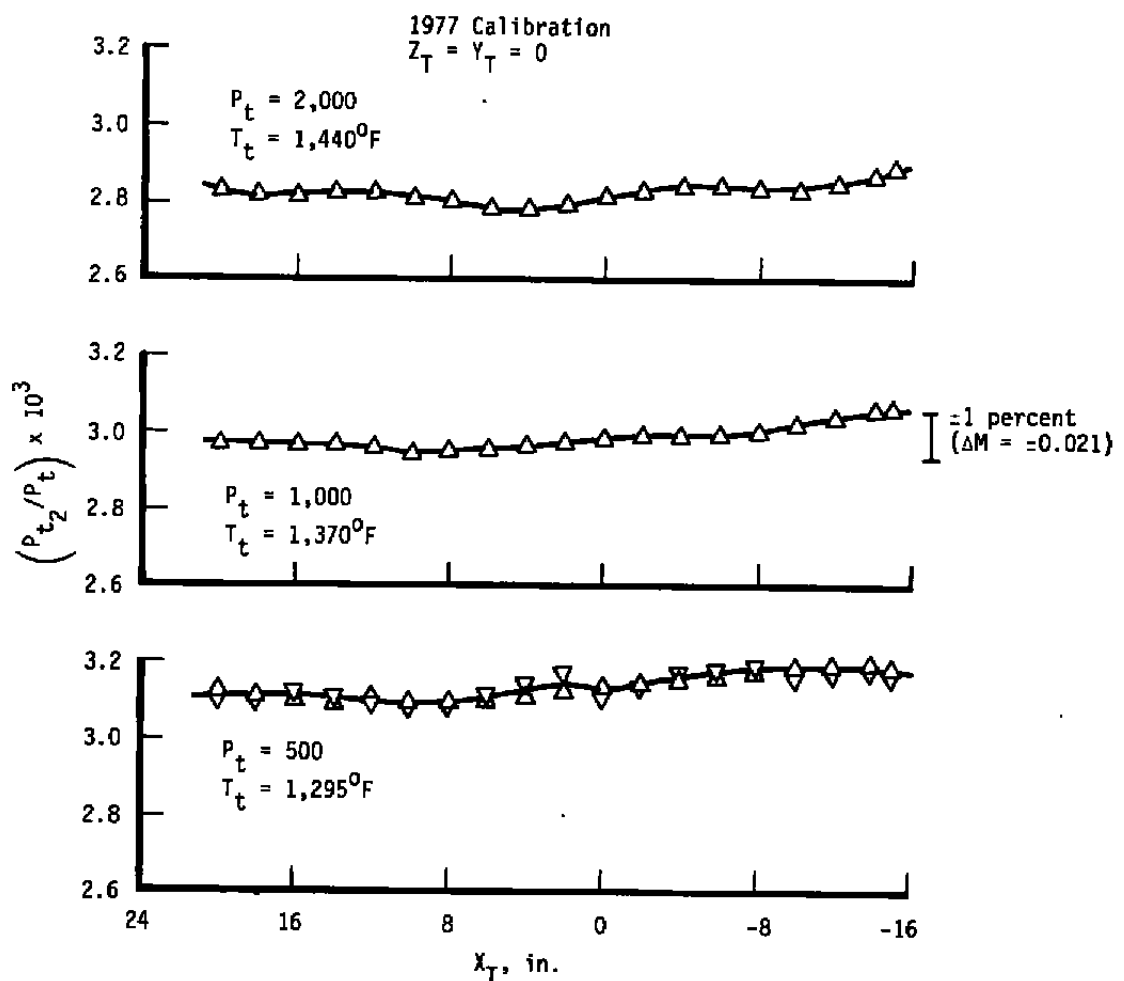


Figure C-4. Axial centerline pitot pressure distributions,  
Tunnel C — Mach 10.

100

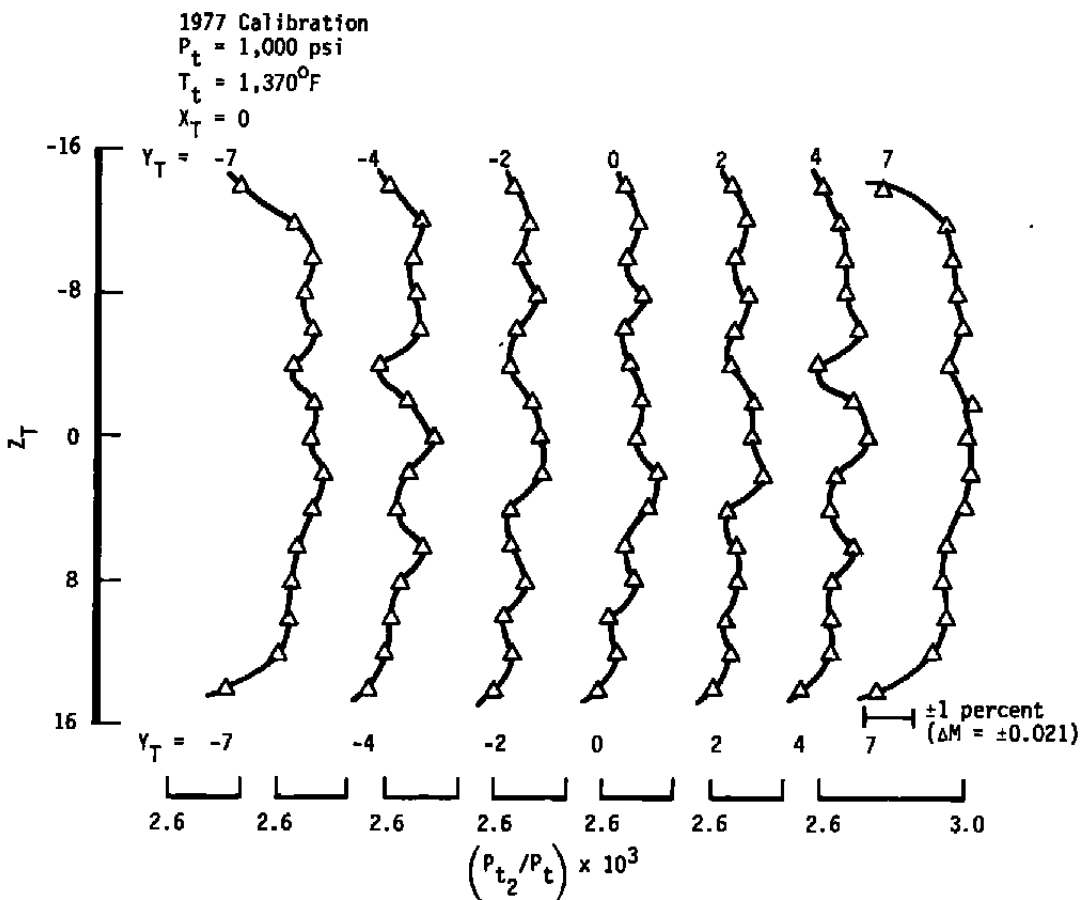


Figure C-5. Vertical pitot pressure profiles, Tunnel C — Mach 10.

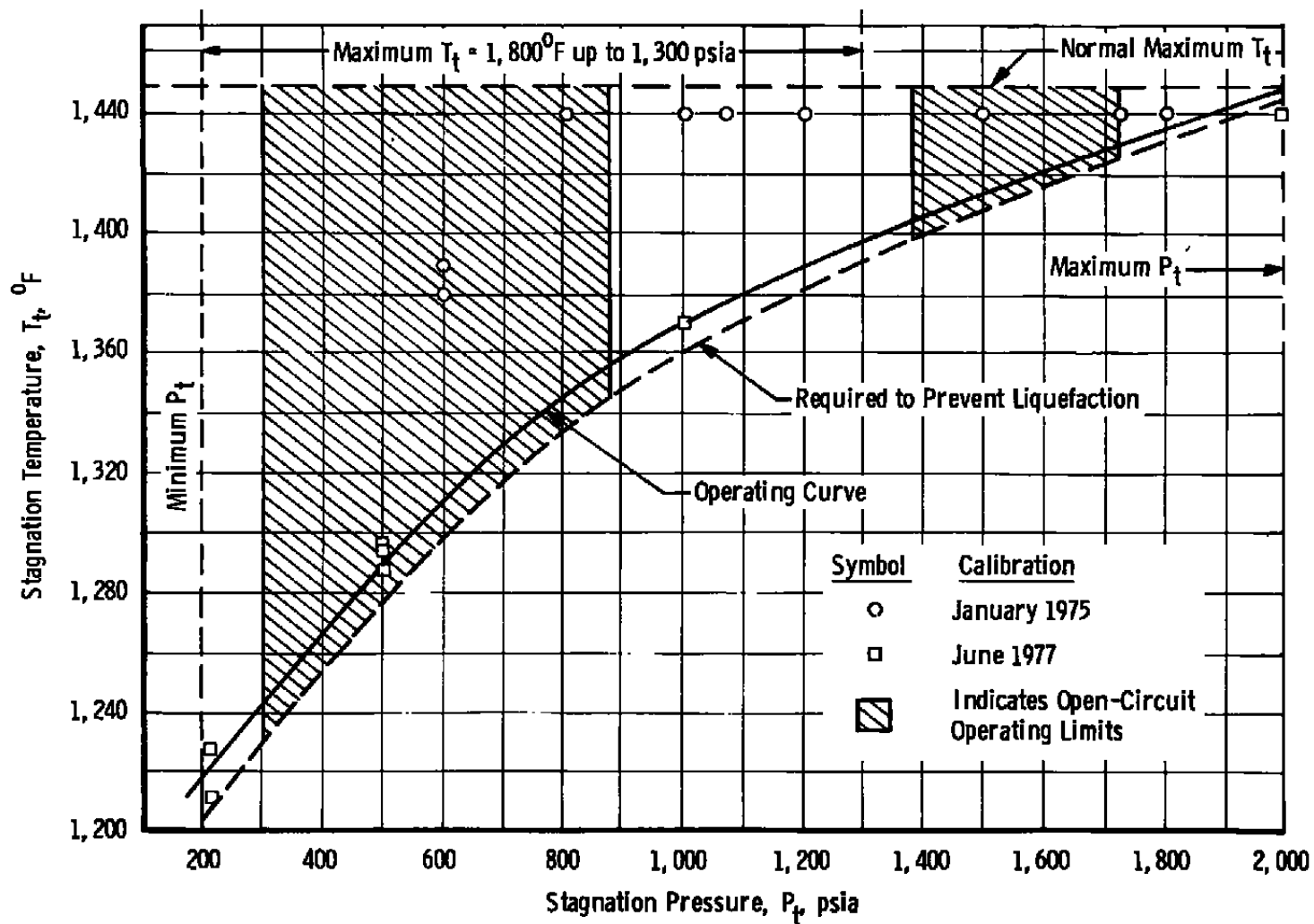


Figure C-6. Stagnation conditions, Tunnel C — Mach 10.

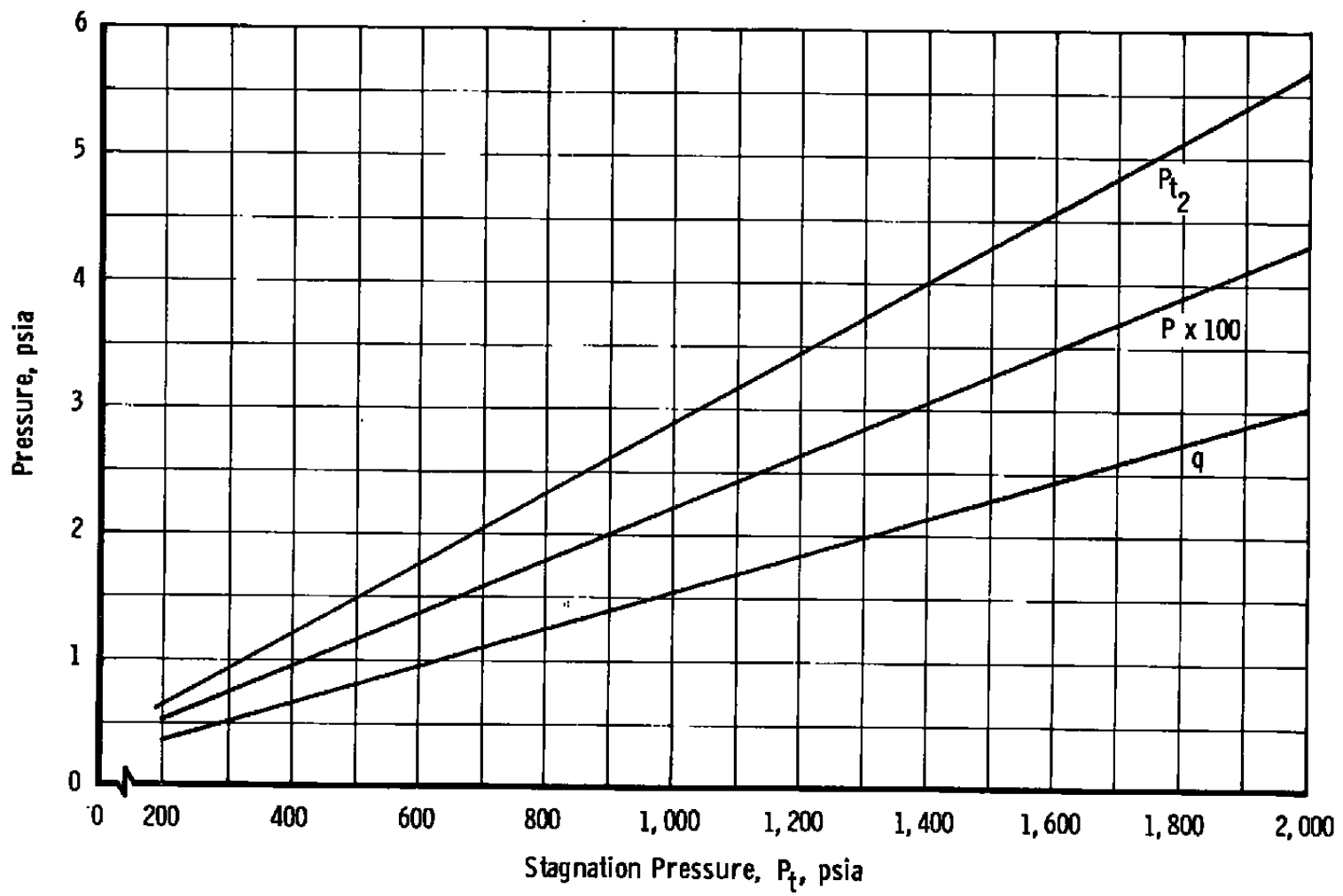


Figure C-7. Free-stream pitot, dynamic, and static pressure,  
Tunnel C — Mach 10.

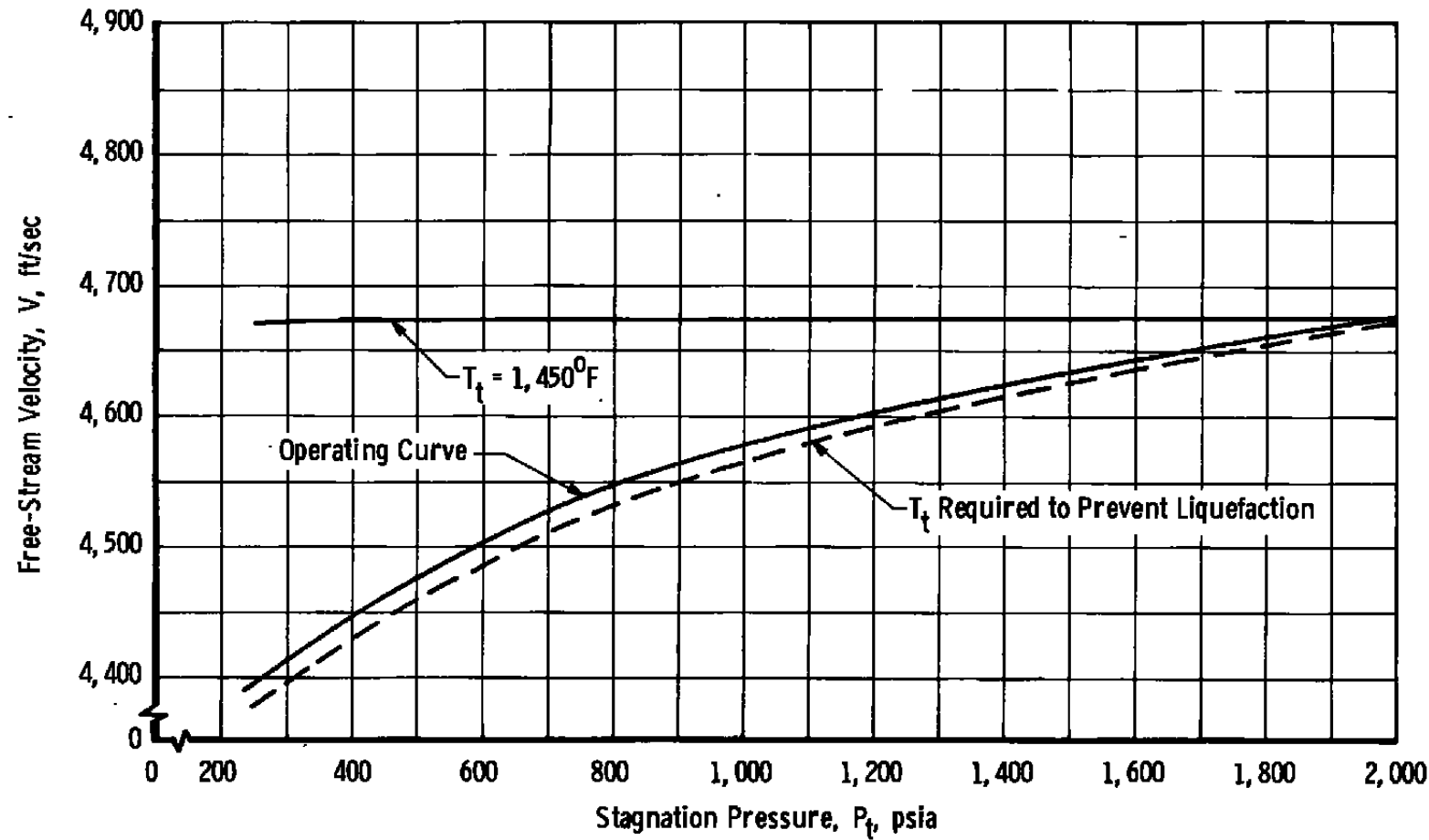


Figure C-8. Free-stream velocity, Tunnel C — Mach 10.

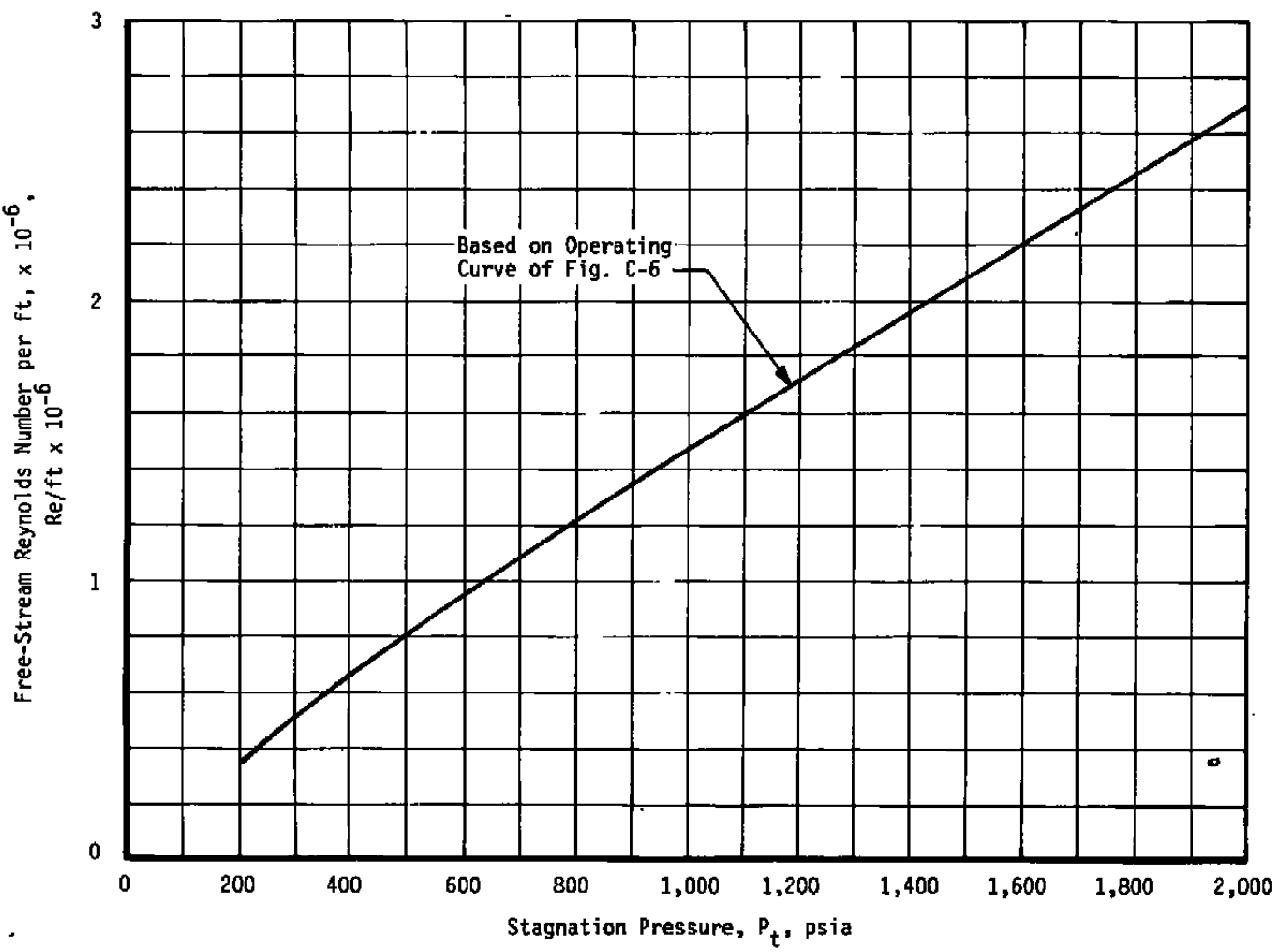


Figure C-9. Free-stream Reynolds number, Tunnel C — Mach 10.

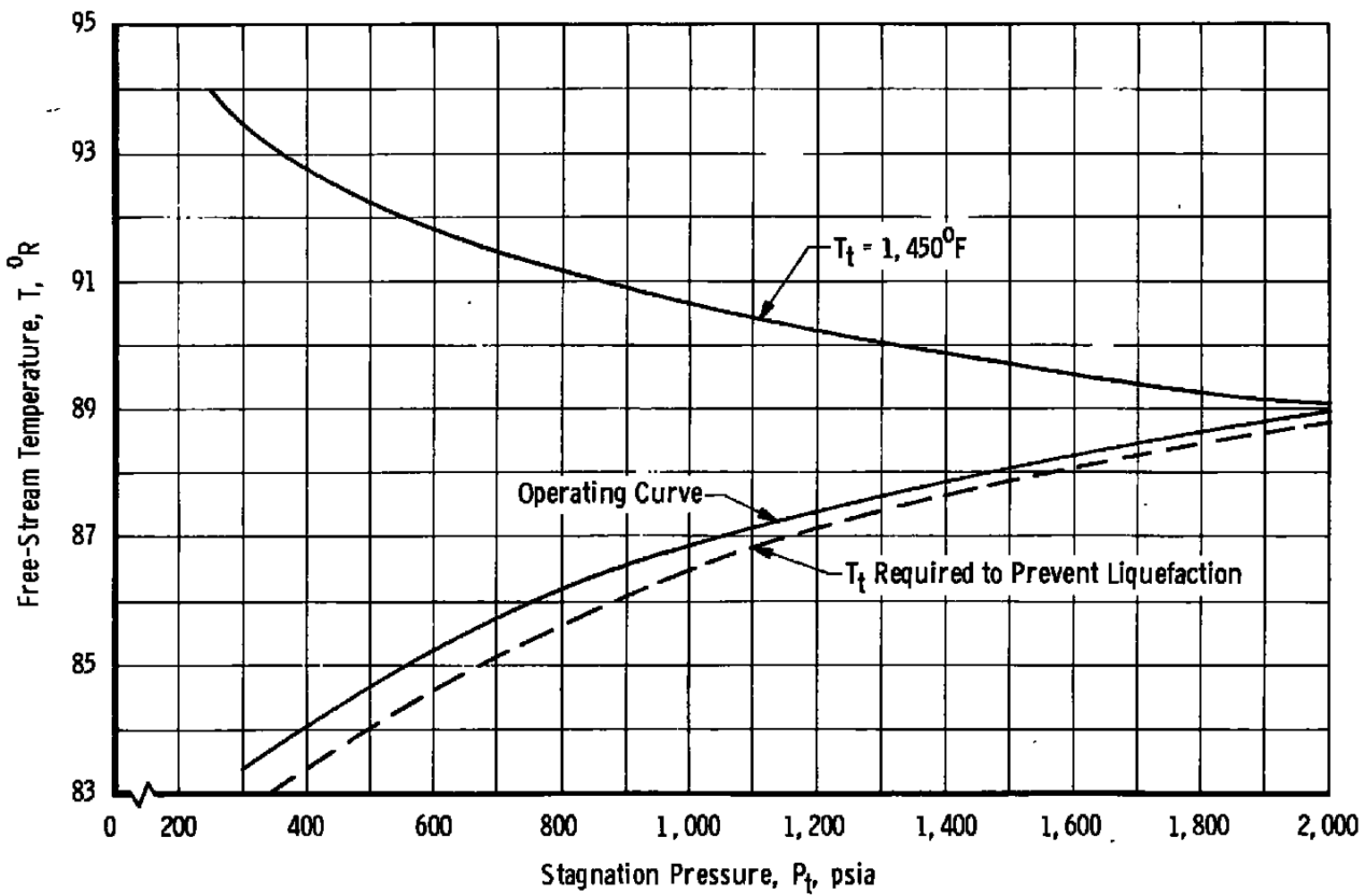


Figure C-10. Free-stream temperature, Tunnel C — Mach 10.

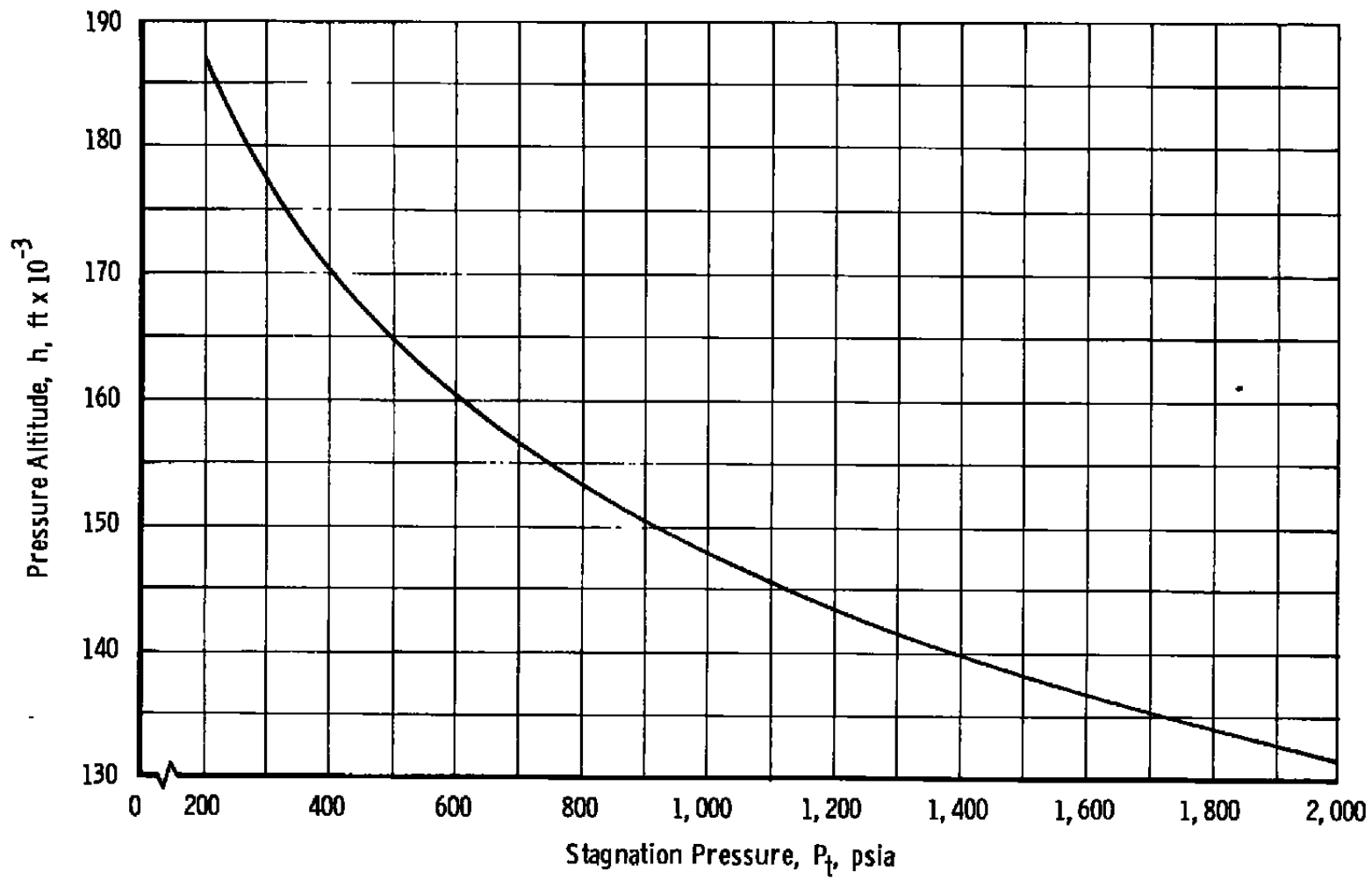


Figure C-11. Simulated altitude, Tunnel C — Mach 10.

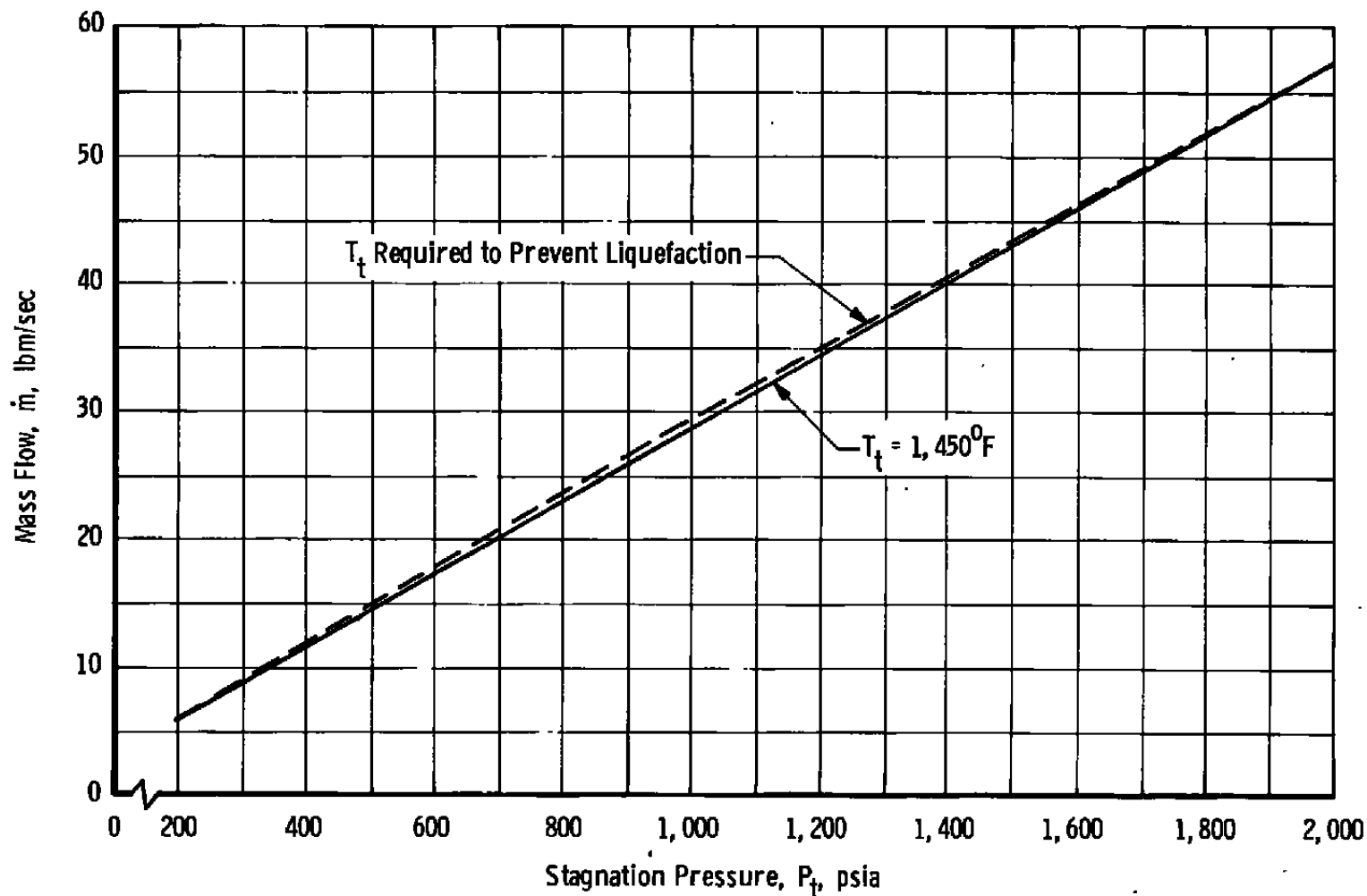


Figure C-12. Mass flow, Tunnel C — Mach 10.

Notes: (1) Compressor Usage plus  
Heater HB-3  
(2) Cooling water pumping energy  
is 3.6 mw per air-on test  
hour.

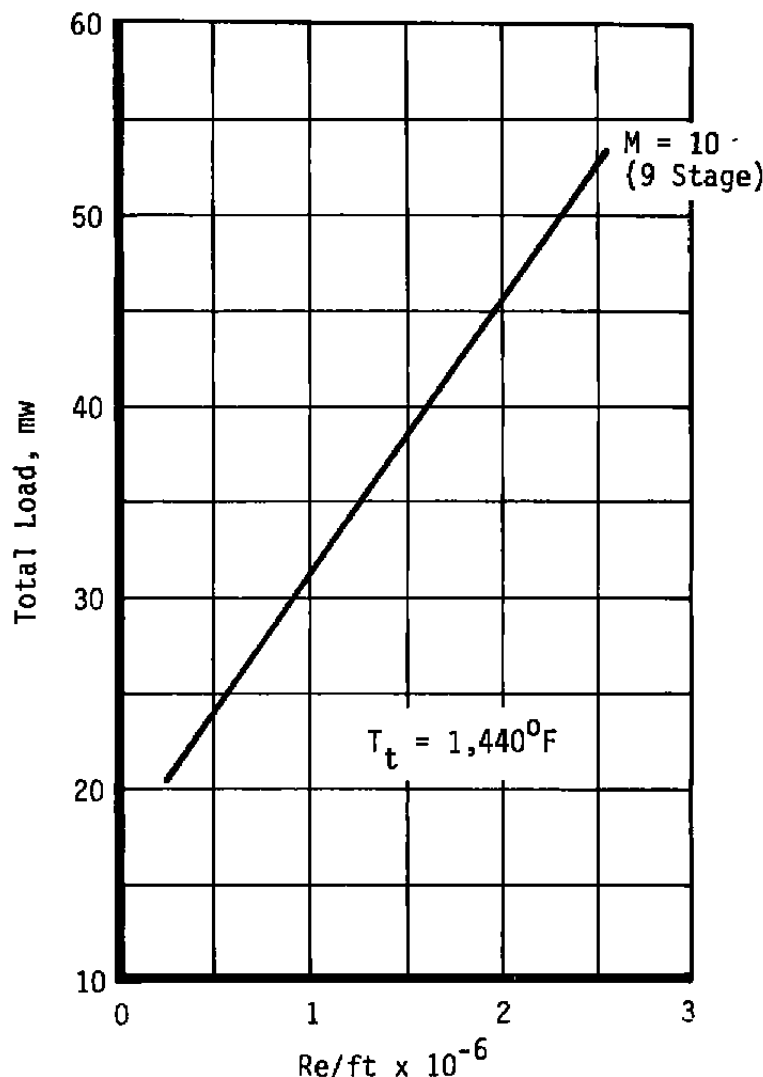


Figure C-13. Electrical usage for Tunnel C.

**Table C-1. Tunnel C Operational Time Considerations**

<b>Operation</b>	<b>Time Increments, min</b>	<b>Notes</b>
Tunnel Start	60	
Stagnation Pressure Changes	30	90 percent of Range (Changes from 90 to 100 percent of range are subject to addi- tional limitations.)
Change Reynolds Number	20	50 percent of Range or Less
Cool Model	5 to 10	
Model Change*	5	
Tunnel Shutdown**	30	

\* Time increment for actual operation on model must also be added.

\*\* Last operational shift of the week requires an additional 20 min.

**Table C-2. Tunnel C Standard Test Condition Tolerances**

Operational procedures for VKF wind tunnels emphasize efficiency. As a part of this effort standard tolerances are set which allow the tunnel operator some latitude in setting test conditions.\* The following tolerances on stilling chamber pressure and temperature and limits on humidity are recommended.

$P_t'$ psia	$\pm \Delta P_t'$ psia	$T_t'$ °F	$\pm \Delta T_t'$ °F	$T_{DP}^{**}$ , °F
200 to 299	2.0	1,210	13	$\leq -70$
300 to 399	3.0	1,240		
400 to 499	4.0	1,270		
500 to 599	5.0	1,300		
600 to 699	6.0	1,320		
700 to 799	7.0	1,340		
800 to 899	8.0	1,350		
900 to 999	9.0	1,360		
1,000 to 1,099	10.0	1,380		
1,100 to 1,199	11.0	1,390		
1,200 to 1,299	12.0	1,400		
1,300 to 1,399	13.0	1,410		
1,400 to 1,499	14.0	1,410		
1,500 to 1,599	15.0	1,420		
1,600 to 1,699	16.0	1,430		
1,700 to 1,799	17.0	1,430		
1,800 to 1,899	18.0	1,440		
1,900 to 2,000	19.0	1,440		

\* Tolerances are based on Reynolds number set to within  $\pm 2$  percent of requested value.

\*\* The  $T_{DP}$  value listed is an ideal limit. Operation above this limit is possible; however, the type of test and the test objectives must be considered.

**APPENDIX D  
TUNNEL C REAL GAS**

## APPENDIX D

### REAL-GAS CORRECTION FACTORS FOR DETERMINING FREE-STREAM CONDITIONS IN TUNNEL C

#### INTRODUCTION

In a hypersonic wind tunnel, free-stream pressures, temperatures, velocities, and so forth are difficult if not impossible to measure directly within an acceptable accuracy. The generally accepted method of obtaining free-stream conditions is to assume an isentropic expansion from the stilling chamber to the test section and calculate the test section conditions directly from the more easily measured stilling chamber pressure and temperature.

Equations and tables contained in NACA Report 1135 (Ref. D-1) are convenient for calculating test section quantities in an isentropic, perfect-gas flow field. Reference D-1 also provides a means of correcting for a calorically imperfect, thermally perfect gas flow field. A similar approach for correcting gas imperfections is presented herein. Correction factors have been calculated based on the Beattie-Bridgeman equation of state (Ref. D-2) in which the thermal and caloric imperfections as well as energy exchanges between various degrees of freedom in gases have been accounted for.

#### DISCUSSION

Test section free-stream conditions are required for data reduction in essentially all wind tunnel tests in VKF. Existing computer programs utilize the compressible perfect-gas equations of Ref. D-1 to calculate test section conditions from measured stilling chamber conditions in Tunnels A and B with only a fraction of a percent error. Tunnel C at Mach 10, however, operates at temperatures and pressures for which the error in using the perfect-gas relations between stilling chamber and test section can amount to as much as 10 percent. To program a real-gas isentropic expansion process for calculating the various test section quantities would be very time consuming. On the other hand, corrective factors of the form given in Ref. D-1 can be inserted into existing computer programs with minimal effort.

Reference D-1 contains corrective factors for a calorically imperfect but thermally perfect gas. At low pressures these corrections are sufficiently accurate, but at anticipated stilling chamber pressures approaching 2,500 psia, the thermal imperfections in the flow are significant. Reference D-3 contains corrective factors of this form based on the National Bureau of Standards data for air (Ref. D-4) calculated to allow for various imperfections

including dissociation and intermolecular force effects. Since the pressure-temperature range of Ref. D-3 was not applicable to Tunnel C operating conditions, it was necessary to calculate corrective factors for determining the free-stream conditions in the tunnel.

The Beattie-Bridgeman equation of state and allowances for vibrational relaxation (Ref. D-2) provided a basis for calculating the corrective factors given in Table D-1. Reference D-2

**Table D-1. Typical Correction Factors for Tunnel C**

Quantity	T Range, °R	P <sub>t</sub> Range, °R	Real/Perfect Ratio
$\frac{P}{P_t}$ and $\frac{q}{P_t}$	1,600 to 1,900	200 to 2,000	0.96 to 0.99
T/T <sub>t</sub>	1,600 to 1,900	200 to 2,000	1.03 to 1.06
P <sub>t2</sub> /P <sub>t</sub>	1,600 to 1,900	100 to 2,000	0.96 to 0.98

$$\frac{(P/P_t)_{\text{real gas}}}{(P/P_t)_{\text{perfect gas}}} = 1.0562 + 49.57 (10^{-6}) P_t$$

$$-(3523 + 1.8300 P_t + 1.3839 T_t - 0.0002196 P_t T_t) (10^{-8}) T_t$$

$$\frac{(q/P_t)_{\text{real gas}}}{(q/P_t)_{\text{perfect gas}}} = 1.0562 + 49.57 (10^{-6}) P_t$$

$$-(3523 + 1.8300 P_t + 1.3839 T_t - 0.0002196 P_t T_t) (10^{-8}) T_t$$

$$\frac{(T/T_t)_{\text{real gas}}}{(T/T_t)_{\text{perfect gas}}} = 0.9378 - 3.900 (10^{-6}) P_t$$

$$+(6533 + 0.6547 P_t - 0.4137 T_t - 0.0001354 P_t T_t) (10^{-8}) T_t$$

$$\frac{(P_{t2}/P_t)_{\text{real gas}}}{(P_{t2}/P_t)_{\text{perfect gas}}} = 1.0419 + 38.31 (10^{-6}) P_t$$

$$-(1968 + 0.7925 P_t + 1.6905 T_t) (10^{-8}) T_t$$

gives a procedure for calculating real-gas isentropic and normal shock flow processes. Numerous calculations were performed with this procedure over the range of Tunnel C conditions, and least-squares curve fits were applied.

These equations are independent of Mach number when the Mach number is high enough to provide a perfect gas in the test section. The lower limit is arbitrarily set at  $M = 10$  as in Ref. D-3. The perfect gas in the test section free stream allows one to compute free-stream velocities, densities, Reynolds numbers, and so forth from the corrected P and T with use of perfect-gas equations.

## REFERENCES

- D-1. NACA Report 1135. "Equations, Tables, and Charts for Compressible Flow." 1953.
- D-2. Randall, R. E. "Thermodynamic Properties of Air: Tables and Graphs Derived from the Beattie-Bridgeman Equation of State Assuming Variable Specific Heats." AEDC-TR-57-8 (AD135331), August 1957.
- D-3. Erickson, W. D. and Creekmore, H. S. "A Study of Equilibrium Real-Gas Effects in Hypersonic Air Nozzles, Including Charts of Thermodynamic Properties for Equilibrium Air." NASA-TN-D-231, April 1960.
- D-4. Hilsenrath, J., Beckett, C. W., et al. "Tables of Thermal Properties of Gases." NBS Ar. 564, U. S. Dept. Commerce, Washington, D.C., 1955.

## NOMENCLATURE

$A^*$	Throat area, in. <sup>2</sup>
$h$	Pressure altitude, ft
$M$	Mach number
$\dot{m}$	Mass flow, lbm/sec
$P$	Free-stream pressure, psia
$P_t$	Stagnation (reservoir) pressure, psia
$P_{t2}$	Free-stream pitot pressure, psia
$q$	Free-stream dynamic pressure, psia
$Re$	Free-stream Reynolds number, ft <sup>-1</sup>
$T$	Free-stream temperature, °R
$T_{DP}$	Dewpoint temperature, °F
$T_t$	Stagnation (reservoir) temperature, °F
$V$	Free-stream velocity, ft/sec
$X$	Axial distance measured from the center of the test section, in.
$Y$	Lateral distance measured from the tunnel centerline, in.
$Z$	Vertical distance measured from the tunnel centerline, in.
$Z^*$	Vertical distance from nozzle centerline to inside edge of throat, in.
$\delta$	Boundary-layer thickness, in.
$\delta^*$	Boundary-layer displacement thickness, in.

## SUBSCRIPTS

$T$	Test section
$t$	Total